Approval Sheet

Title of Dissertation: NOVEL INHIBITORS OF THE HEPATITIS C VIRUS

Name of Candidate: Daniel C. Talley

Doctor of Philosophy, 2016

Dissertation Approved by: _____

Dr. Paul J. Smith

Associate Professor

Department of Chemistry and Biochemistry

Date Approved: ___/___/_____

Abstract

Several analogs of the natural product UK-1 have been identified as potent inhibitors of hepatitis C virus (HCV) replication in a replicon assay. One set of inhibitors has been shown to inhibit the HCV non-structural protein 3 helicase (NS3h), while another acts via an unknown cellular target. Efforts have been focused on (1) identifying the inhibitor binding pocket within the NS3 helicase and (2) exploring the possible role zinc binding may play in the inhibitory mode of action of the latter.

Lead HCV replication inhibitors, inactive against NS3h, have been shown to bind zinc. Within the HCV genome, at least three non-structural proteins (NS2, NS3, and NS5A) contain/require a structural zinc ion and all three proteins are required for viral replication. Disruption of zinc binding within any of the three proteins severely hinders or eliminates protein function, thus inhibiting viral proliferation. It is therefore hypothesized that the activity of lead compounds is related to the coordination of one or more protein-bound structural zinc ions, causing a perturbation of protein structure that diminishes protein activity and thereby inhibits viral replication. To investigate whether or not zinc binding plays a role in the activity of lead HCV replication inhibitors, a series of analogs have been synthesized with structural modifications expected to increase zinc affinity. In addition, a structure activity relationship (SAR) study was performed to explore the effects of hydrogen bonding and sterics/hydrophobicity on inhibitor efficacy. Lead modification has led to a potent inhibitor of HCV replication (EC_{50}= 0.6 μM) that shows minimal toxicity to host-cells (SI> 160). The SAR study, syntheses, zinc binding experiments, and biological data will be presented.

Two lead compounds inhibit HCV NS3 helicase activity with low to sub-micromolar EC_{50} values. Identification of the binding pocket within NS3h would allow for structure-based drug design, facilitating the development of increasingly potent inhibitors. As such, a photoactivatable analog of a lead helicase inhibitor has been designed to be used in a photoaffinity labeling experiment; this analog has been shown to be similarly effective against the NS3 helicase. The design, syntheses, photolysis data, and results of NS3h photolabeling experiments will be presented herein.

Novel Inhibitors of the Hepatitis C Virus

Submitted by:

Daniel C. Talley

Dissertation Submitted to the Faculty of the Graduate School of the
University of Maryland, Baltimore County in Partial Fulfillment
of the Requirements for the Degree of
Doctor of Philosophy
2016

Dedication

To my parents, Rita and Ken Talley.

Acknowledgements

I would like to sincerely thank my advisor, Dr. Paul J. Smith, for his guidance throughout my graduate career. His depth of knowledge in organic theory, synthetic technique, spectroscopy, and scientific writing (among other topics) has paved the path to my doctorate.

I would like to express my gratitude to the entire faculty and staff in the Department of Chemistry and Biochemistry at the University of Maryland Baltimore County for their assistance and for making this school a great place to work. In particular, I would like to thank Dr. Katherine Seley-Radtke for her useful discussions. I would like to thank Dr. Marcin Ptaszek and Dr. Steven Fletcher for their synthetic advice and also Dr. Elsa Garcin for her biochemical tips. Lastly, Sandy Wilkens and Patty Gagne for their extensive assistance in organization and ensuring I am fulfilling the proper requirements over the years.

I would also like to thank our collaborators at the REGA Institute for Medical Research for their work with the HCV replicon assays and Dr. Andrea Baier at John Paul II Catholic University of Lublin for her work with the HCV NS3 helicase.

The most integral part of my success can be directly attributed to my parents, Rita and Ken Talley. Their love and support has forever picked me up when I'm knocked down and pushed me to succeed far beyond my dreams. Although cliché, I never would have achieved this degree without them on my side. Thank you!

Table of Contents

List of Figures

List of Tables

List of Schemes

Chapter 1: The Hepatitis C Virus and Therapeutic Development

A. Overview

The Hepatitis C Virus (HCV), the causative agent of the Hepatitis C infection, has been declared a worldwide health concern by the World Health Organization (WHO).[1,2] Estimates suggest that 150-180 million people are currently infected with HCV and as many as 500,000 die each year from viral related ailments.[3] In 70-80% of cases, HCV cannot be suppressed by the body's immune system and a chronic liver infection develops.[4] This acute infection of the hepatocytes leads to liver cirrhosis, hepatocellular carcinoma, and liver failure.[5] HCV infection is currently the leading cause of liver transplantation in the United States.[6]

HCV is a positive sense single-stranded RNA virus that, following entry into a host hepatocyte, encodes for a single polyprotein of approximately 3000 amino acids.[7] The polyprotein is processed co- and post-translationally by both host and viral proteases, to yield ten viral proteins (**Figure 1**). The amino terminal third of the peptide contains the four structural proteins core, E1, E2, and p7. The remaining two-thirds of the protein is composed of the non-structural (NS) proteins NS2, NS3, NS4A, NS4B, NS5A, and NS5B.[7] Although each NS protein possesses a unique function (or functions), as a whole they are responsible for the synthesis of viral RNA, and thus viral replication.[8]

Figure 1. HCV RNA translation and processing of the resulting polypeptide.[8]

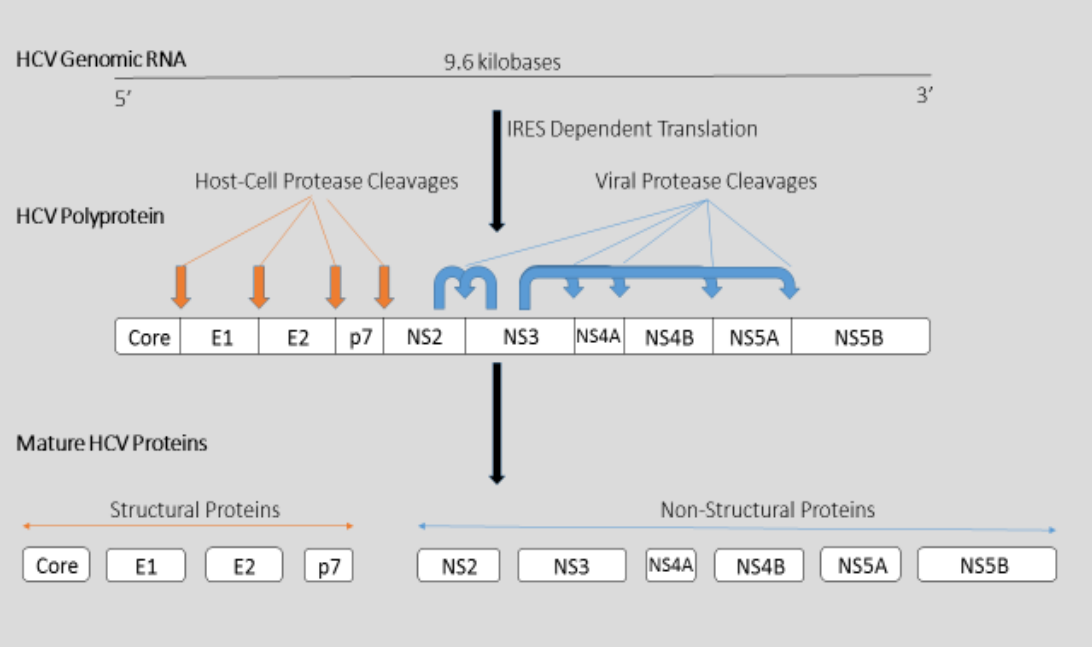

B. The HCV Non-Structural Proteins: Structure and Function

Nonstructural-protein 2 (NS2) is a transmembrane protein with protease activity and is located at the 5' end of the NS proteins. This novel dimeric cysteine protease contains a composite active site, where two of the three residues in the catalytic triad come from one monomer, and the third comes from the other.[9] NS2 is responsible for the intramolecular cleavage of itself from adjacent NS3, which remains attached to the remaining downstream NS proteins.[10] The role of this cleavage event as it pertains to HCV RNA replication is not fully understood, but it is required for viral RNA replication *in vivo*.[10] The N-terminal domain of NS3, which acts as a cofactor for NS2, contains a zinc-binding region and increases NS2 protease activity. It has been hypothesized that the NS3 zinc-binding domain promotes the correct positioning of the NS2/NS3 scissile bond.[11]

NS3 is a protein exhibiting multiple functions and is well characterized both structurally and functionally. NS3 and the adjacent NS4A function as a complex, with NS4A serving as both a cofactor for NS3 and as a membrane anchor.[12] The amino terminal domain of NS3 and NS4A form a dimeric serine protease that is responsible for the intramolecular cleavage of NS3 from NS4A, as well as the intermolecular cleavage between all downstream non-structural proteins.[13] Without an active NS3 protease, the remainder of the polypeptide encoded by the RNA genome remains unprocessed, and is thus nonfunctional.[14] In addition, the carboxy-terminus of NS3 functions as an ATP-dependent helicase; this activity is facilitated by NS4A.[15] The exact relevance of the helicase activity as it pertains to HCV viral replication is not known, nor is the enzyme's natural substrate. However, a functional helicase is required for *in vivo* HCV replication.[8, 16,17] Several functions for the helicase activity have been proposed which include, but are not limited to, aiding in the polymerase processivity, assistance in RNA folding, modulating host gene expression, and involvement in genome encapsidation.[18-20] Although its specific function in viral proliferation is currently unknown, it has been shown that helicase activity is required for *in vivo* HCV replication.[16,17]

Non-structural protein 4B is an integral membrane protein that associates with the endoplasmic reticulum (ER) of the host cell.[21] Like the other NS proteins, NS4B is essential for viral RNA replication.[22] The most important and widely accepted role of NS4B is the rearrangement of host cell membranes. During the HCV lifecycle, RNA replicative structures, including all non-structural proteins, assemble in a rearranged host-cell ER or the 'membranous web'. It has been shown that expression of NS4B alone is

capable of generating these membranous structures, strongly suggesting this as a critical role in the viral life-cycle.[23]

NS5A is a large protein that exists in two phosphorylated forms (56 kD and 58 kD) and has been proven crucial to the replication of HCV.[24,25] It has been shown that NS5A associates post-translationally with the cytoplasmic membranes and is capable of binding RNA, however the exact role that NS5A plays in viral replication remains unclear.[24,26] It has been proposed that NS5A plays a role in virion assembly, RNA replication, host cell protein modification, and overall lifecycle regulation.[27,28] NS5A also contributes to viral propagation by binding to host-cell protein kinases, that would otherwise impede viral replication.[29] This gives rise to viral persistence by downgrading the production of host interferons (IFNs). It has also been shown that expression of NS5A alone can promote hepatocellular carcinoma.[25]

NS5B is a 68kDa RNA dependent RNA polymerase and is therefore essential for viral replication both *in vitro* and *in vivo*.[28] Importantly, this polymerase is prone to error when synthesizing viral RNA. This leads to extremely high mutation rates in all genotypes of HCV, which results in the development of viral resistance to various HCV therapeutic options.[30]

C. HCV Treatment

Prior to 2011, the standard of care for an acute HCV infection was a combination of the broad spectrum antivirals pegylated interferon alfa (PEG-IFN) and ribavirin. PEG-IFN is a signaling protein that induces the production of host-cell genes with antiviral

functions.[31] Ribavirin, a nucleoside analog, acts synergistically with PEG-IFN through an unknown mechanism. This treatment had moderate to poor efficacy, depending upon the genotype of the causative virus. Sustained virological response (SVR), defined as no detectable HCV RNA six months after completing treatment, was achieved in approximately 40% of infections caused by the viral genotype (genotype 1) common to North America and Europe.[32] Throughout the 48-72 weeks of required therapy, severe side effects including fatigue, depression, flu-like symptoms, and hemolytic anemia were reported for these antivirals. It was common for patients to discontinue the drugs prior to the advised treatment period.[33] Detailed discovery and analysis of the HCV life cycle through the development of cell culture systems, has paved the road to a new age of drug development.[34,35] Direct acting antivirals (DAAs), targeting specific HCV proteins essential for viral replication, has been a promising area of HCV research. Numerous DAAs for HCV treatment have been released from 2011-2015. All of the currently FDA approved therapies are combination treatments, targeting two or more of the HCV non-structural proteins.

The first two DAAs for HCV treatment, boceprevir and telaprevir, were approved in 2011 (**Figure 2**). Both of these compounds target the NS3/4A protease. During early phases of development it was found that monotherapy, administering either of these drugs alone, resulted in the rapid development of resistant strains.[36,37] As a result, these drugs were only FDA approved when given in combination therapy with ribavirin and PEG-IFN.[38,39] This new treatment regime had increased overall response rates, but the severe side effects and extremely high cost associated with PEG-IFN and ribavirin remained a problem.[40] Both of these drugs were discontinued by 2015.[41]

Figure 2. (left) Boceprevir and (right) telaprevir. First direct acting antivirals (NS3 protease inhibitors) approved for HCV treatment, in combination with PEG-IFN and ribavirin.

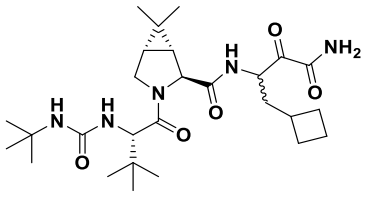

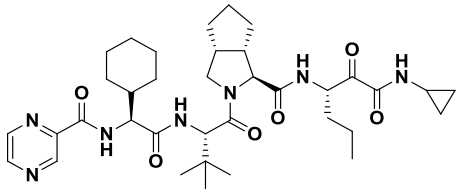

From 2011 to 2015, a plethora of DAAs were approved by the FDA. This began with sofosbuvir and simeprevir (**Figure 3**).[41,42] In late 2011, simeprevir, an NS3/4A protease inhibitor, was approved only in combination with both PEG-IFN and ribavirin. In 2013, sofosbuvir, a nucleoside analog that targets the HCV NS5B RNA polymerase, was approved in combination with ribavirin and/or PEG-IFN, depending on the genotype of the infection.[41,42]. As such, both of these treatment regimens were associated with the severe side effects of previously approved therapy.

Figure 3. (Left) Sofosbuvir, an NS5B polymerase inhibitor. (Right) Simeprevir, an NS3/4A protease inhibitor.

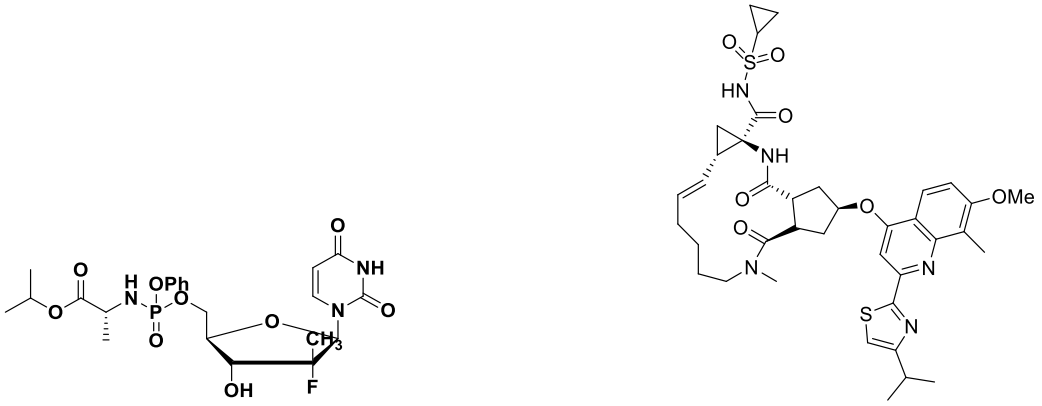

Then in 2014, sofosbuvir was approved for treatment of genotype 1 infections in combination with simeprevir.[41,42] This marked the first all-oral interferon-free HCV therapy for genotype 1 infections; a breakthrough in the HCV treatment field.[43] Shortly after, Harvoni®, a combination of sofosbuvir and the NS5A targeting drug ledipasvir (**Figure 4**), was approved for treatment of HCV genotype 1,4,5 or 6.[44] In December of 2014, Abbvie's four drug combination therapy Viekira Pak® received FDA approval for treatment of genotype 1 infections.[41,42] This treatment consists of the NS5A inhibitor ombitasvir, the NS3/4A protease inhibitor paritaprevir, the non-nucleoside NS5B RNA polymerase inhibitor dasabuvir and ritonavir, a previously approved cytochrome P450-3A inhibitor shown to increase the bioavailability of paritaprevir (**Figure 4**). Depending on the HCV subtype and the state of the patient's liver, ribavirin may still be required with Viekira Pak®.[41,42] In 2015, Technivie® was approved for genotype 4 infections in combination with ribavirin.[41,42] This all-oral treatment consists of ombitasvir, paritaprevir, and ritonavir. Later that year, Daklinza® was approved for treatment of

genotype 3 infections; this therapy contains an NS5A targeting compound, daclatasvir and previously approved sofosbuvir (**Figure 4**).[41,42]

Figure 4. Direct acting HCV antivirals approved from 2013-2015.[41,42]

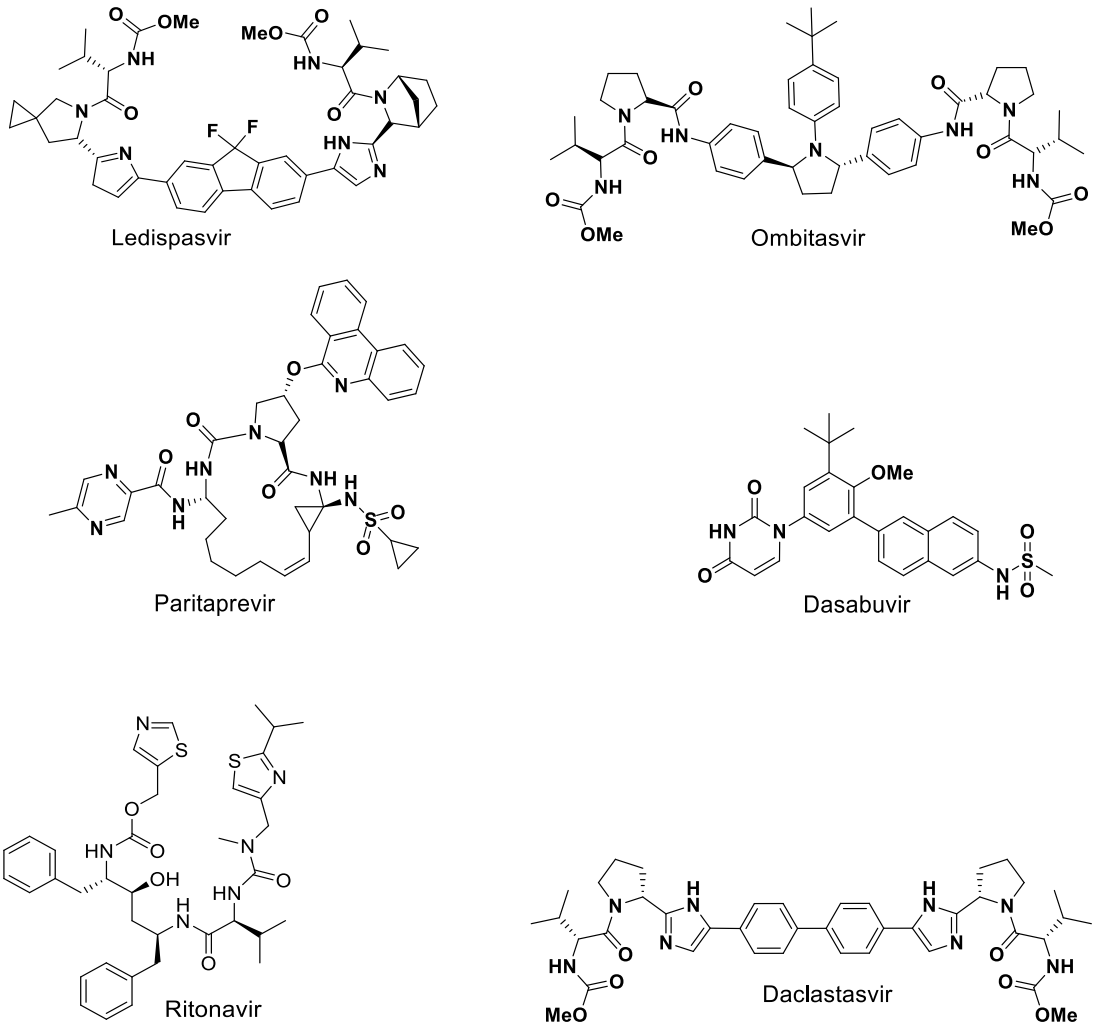

Early results for all-oral treatment regimens have been promising, but the estimated treatment costs range from approximately $84,000 to $189,000, depending on the drug and the required treatment time (12-24 weeks).[45,46] Early cases of resistant strains have

already been reported for many of the individual DAAs.[47-51] The elusive nature of the error-prone NS5B polymerase and the extremely high viral replication rate are sufficient to generate skepticism that the HCV problem has been solved. Research towards additional HCV therapeutics will hopefully decrease the cost and length of treatment, while providing additional modes of action in halting viral replication thus decreasing resistance.

Chapter 2: Natural Product UK-1 and Structural Analogs Are Potent Inhibitors of Hepatitis C Virus Replication

A. Natural Product UK-1: A Lead for Drug Discovery

UK-1, a secondary *Streptomyces* metabolite, exhibits broad spectrum anticancer activity and also inhibits human topoisomerase II (topo II) (**Figure 5**, left).[53-55] Importantly, UK-1 has been shown to bind various divalent metal ions (Mg^{2+}, Zn^{2+}, Co^{2+}, and Ni^{2+}) and DNA, in a magnesium ion-dependent manner.[53,55]

Figure 5. (left) Bacterial natural product UK-1. (right) An HIV-I integrase inhibitor, L-708.906, that binds to a magnesium ion in the enzyme's active site.

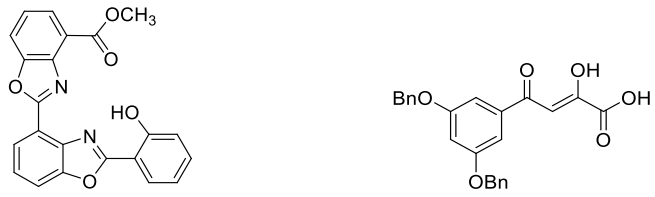

A key step in the replication of human immunodeficiency virus type-1 (HIV-I), is the integration of viral DNA into host-cell chromosomes; HIV-I integrase is the enzyme responsible for carrying out this crucial step. A catalytic magnesium ion is found in the active site of integrase. It has been shown that various compounds capable of coordinating this ion, are potent inhibitors of integrase activity and thus, HIV-I replication.[56] One such integrase inhibitor is L-708.906 (**Figure 5**, right).[57,58]

In an effort to discover potential inhibitors of HIV-I integrase, the unique magnesium binding scaffold of UK-1 and the hydrophobicity of L-708.906 were incorporated in the design of lead compounds, **1** and **2** (**Figure 6**). Following synthesis, **1** and **2** were screened against HIV-I integrase. Unfortunately, no notable activity against integrase was observed. Both compounds, as well as UK-1, were then sent for a broad screen against a panel of viruses. Quite interestingly, all three compounds inhibit replication of hepatitis C virus type 1b in a replicon assay with low to sub-micromolar EC_{50} values.[59] From leads **1** and **2**, a third analog **3** (**Figure 6**, right) was designed, which retains the Mg^{2+} binding scaffold of UK-1, but lacks the additional hydrophobicity of L-708.906. Following synthesis, **3** was also screened against HCV replication and was similarly active with a low micromolar EC_{50}.[59] These findings marked the beginning of our interest in the development of novel HCV inhibitors.

Figure 6. Lead compounds **1-3**.

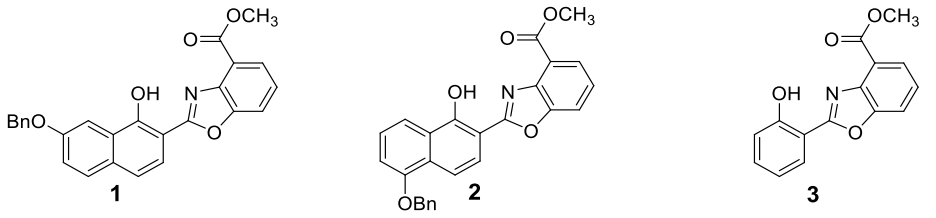

B. Exploring the Importance of Zinc Binding and Steric/Hydrophobic Factors in Novel HCV Inhibitors

In an effort to identify the inhibitory mode of action for leads **1-3** and UK-1, all compounds were screened against three enzymes within the HCV non-structural proteins: the NS3 helicase, NS3 NTPase, and the NS5B RNA polymerase. Lead compounds **1**, **2**,

and also UK-1 (although less effective) were active against the NS3 helicase; these compounds will be discussed in further detail in Chapter 3.[59] Surprisingly, **3** was ineffective as an NS3 helicase inhibitor, although similarly active against viral replication. This prompted our attempt to determine how **3** is inhibiting viral replication, without affecting the NS3 helicase/NTPase or NS5B polymerase.

Similar to UK-1, truncated analog **3** has been shown to bind divalent zinc, presumably *via* the Lewis-basic carbonyl oxygen, phenolic hydroxyl group, and heterocyclic nitrogen (**Figure 7**).[60] Within the HCV genome, at least three non-structural proteins (NS2, NS3, and NS5A) contain/require a structural zinc ion and all three proteins are required for viral replication.[11,26,61-65] Disruption of zinc binding within any of these three proteins severely hinders or eliminates protein function, thus inhibiting viral proliferation.[11,63,65] It is therefore hypothesized that the activity of UK-1 and **3** is related to the coordination of one or more protein-bound structural zinc ions, causing a perturbation of protein structure that diminishes protein activity, thereby inhibiting viral replication.[60]

Figure 7. Triangular arrangement of Lewis-basic groups in **3** bind divalent zinc.

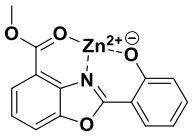

The N-terminal domain of NS3, which acts as a cofactor for NS2, contains a zinc-binding region and increases NS2 protease activity. It has been hypothesized that the NS3 zinc-binding domain promotes the correct positioning of the NS2/NS3 scissile bond.[61]

Consistent with these predictions, NS2 protease activity is inhibited by the zinc chelator 1,10-phenanthroline, albeit weakly (**Figure 8**).[62]

Figure 8. Zinc chelator, 1,10-phenanthroline, inhibits the HCV NS2/3 and NS3/4A proteases.

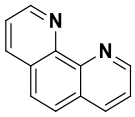

Furthermore, point mutations to residues involved in zinc binding completely eliminate NS2 activity.[62] Prior to NS2 cleavage from NS3, it has been suggested that the structural zinc ion is coordinated by four cysteine residues, three within NS3 and one in the C-terminus of NS2. Following NS2 cleavage, a change in coordination occurs and the zinc ion becomes bound completely within the N-terminus of NS3. This change in conformation has been hypothesized to activate the NS3 protease.[61]

An active NS3 protease is required for viral replication and it has been shown that the structural zinc bound in the N-terminus of NS3 is required for protease activity.[62-64,66,67] The amino-terminal domain of NS3 and adjacent NS4A function as a dimeric serine protease that is responsible for the intramolecular cleavage of NS3 from NS4A, as well as the intermolecular cleavage between all downstream NS proteins.[13] Similar to NS2, NS3 protease activity is weakly inhibited by 1,10-phenanthroline and point mutations to zinc binding residues significantly diminish NS3 protease activity.[62,63,67]

NS5A is yet another protein required for viral replication that relies on a structural zinc ion for proper function.[25,26] This protein has three domains. Domain one, which is the most conserved among genotypes, contains a novel fold coordinating a structural zinc ion.[26,65] The zinc ion likely plays a structural role in the stabilization of this fold. It has

been shown *via* mutational analysis that the structural zinc is required for viral replication.[26]

To investigate whether or not zinc binding plays a role in the activity of HCV replication inhibitors such as **3**, a series of analogs have been synthesized with structural modifications expected to increase zinc affinity (**Figure 9**).[60]

Figure 9. Modifications expected to increase zinc affinity.

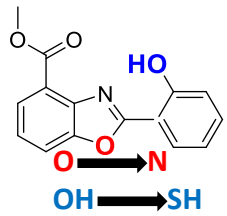

First, the benzoxazole heterocycle has been replaced with a benzimidazole. It has been shown in UK-1 that replacement of one benzoxazole with a benzimidazole, increases zinc affinity by approximately a factor of two (**Figure 10**, top).[54]

Figure 10. Previously reported compounds provide support for the hypothesis that benzimidazoles will have a higher affinity for zinc than analogous benzoxazoles. (top) Zinc dissociation constants for UK-1 and an analog with one benzoxazole replaced with a benzimidazole. (middle) pKa values for of *N*-protonated heterocycles of related compounds. (bottom) Zinc dissociation constants for structurally related compounds.

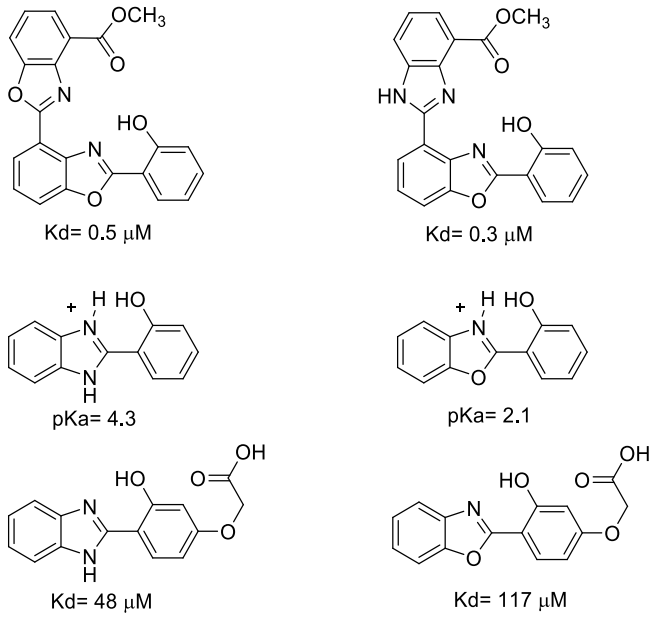

This is likely due to the decreased electronegativity of the 1-position heterocyclic nitrogen versus the oxygen of the benzoxazole, which should increase the Lewis-basicity of the nitrogen involved in zinc binding. In addition, acid-dissociation constants have been determined for 2-(2-hydroxyphenyl)benzimidazole and 2-(2-hydroxyphenyl)benzoxazole, the latter of which is structurally identical to **3**, but lacking a 4-position substituent on the heterocycle (**Figure 10**, middle).[68] It was shown that the nitrogen involved in zinc binding has a pKa of 4.3 for the structurally related benzimidazole, and only 2.1 for the analogous benzoxazole. Assuming Bronsted-basicity provides insight into Lewis-basicity, this suggests the lone-pair of electrons on the nitrogen in the benzimidazole scaffold are more available for donation than in the analogous benzoxazole. Precedent for the hypothesis that benzimidazoles bind zinc better than benzoxazoles has been demonstrated in an additional set of structurally related

compounds (**Figure 10,** bottom). The benzimidazole (**Figure 10**, bottom left) has a greater affinity for zinc (Kd=48) than the analogous benzoxazole (Kd=117) (**Figure 10**, bottom right).[69]

Secondly, the 2-position phenolic hydroxyl of **3** has been replaced with a sulfhydryl group (**Figure 9**). Cysteine is by far the most common zinc coordinating residue in all human zinc containing proteins.[70] Of zinc containing proteins whereby the metal is coordinated by four ligands, 96% contain at least one cysteine residue.[70] The relationship between sulfur and zinc has been extensively studied, and it is widely accepted that thiols have a high affinity for divalent zinc.[70,71]

In addition to modifications expected to increase zinc affinity, a structure-activity relationship (SAR) study was performed to explore the effects of sterics/hydrophobicity and hydrogen bonding on inhibitor efficacy (**Figure 11**). These modifications include variation of the 4-position of the heterocycle, *N*-benzylation of the benzimidazole nitrogen, and addition of steric/hydrophobic bulk about the phenolic ring *via* various naphthylene- and quinoline- containing analogs. If these inhibitors are disrupting protein function *via* structural zinc ion coordination, additional steric bulk could further perturb protein structure, increasing inhibitor efficacy.

Figure 11. Modifications to explore the effects of sterics/hydrophobicity and hydrogen bonding.

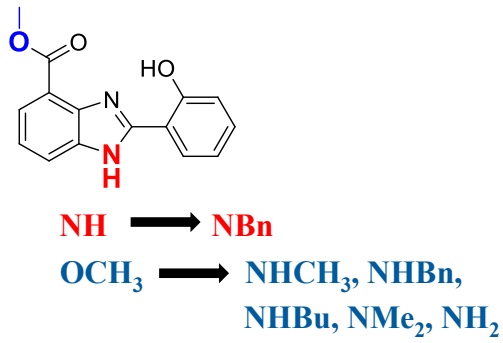

C. Synthesis and Zinc Binding Studies

The syntheses of lead compound **3** and analogous acid **8** are shown in **Scheme 1**. Dibenzylation of salicylic acid followed by ester hydrolysis gave hydroxyl protected acid **5**. Acid activation with dichlorotriphenylphosphorane and subsequent amide formation with methyl 3-hydroxyanthranilate gave **6**.[72] The resulting amide was refluxed in toluene in the presence of pyridinium *p*-toluene sulfonate (PPTS) to give benzoxazole **7**. Hydroxyl deprotection *via* hydrogenation with catalytic Pd/C gave lead ester **3**. Hydrolysis of **3** with NaOH in THF gave acid **8**.

Scheme 1. Synthesis of lead compound **3** and acid analog **8**.[a]

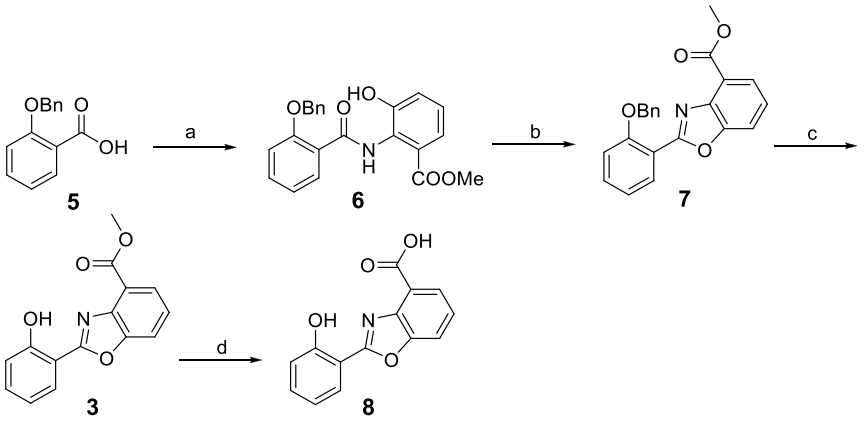

[a] Reagents, conditions, and yields: **(a)** Methyl-3-hydroxyanthranilate, Cl_2PPh_3, $CHCl_3$, reflux, 76%; **(b)** PPTS, toluene, reflux, 91%; **(c)** H_2, 45 PSI, Pd/C (10%), MeOH, 99%; **(d)** NaOH, THF, reflux, 87%.

Benzimidazoles were prepared as shown in **Scheme 2**, using modified previously reported methodology.[73] Methyl 2-amino-3-nitrobenzoate was reduced *via* hydrogenation with catalytic Pd/C to give diamine **9**. Hydroxyl protected acid **5** was activated with 1,1'-carbonyldiimidazole and coupled to diamine **9** to give **10**. The amide was refluxed in glacial acetic acid to give the cyclization-dehydration product **11**. Debenzylation of **11**

via hydrogenation with catalytic Pd/C gave target ester **12**. Alternatively, hydroxyl protected ester **11** was hydrolyzed with NaOH in THF to give acid **13**, which was subsequently debenzylated *via* hydrogenation to give target acid **15**. The benzyl protected amide **14** was obtained *via* activation of **13** with dichlorotriphenylphosphorane and subsequent reflux with a solution of methylamine in THF. Debenzylation *via* hydrogenation gave target amide **16**.

Scheme 2. Synthesis of benzimidazole analogs **12, 15,** and **16**.[a]

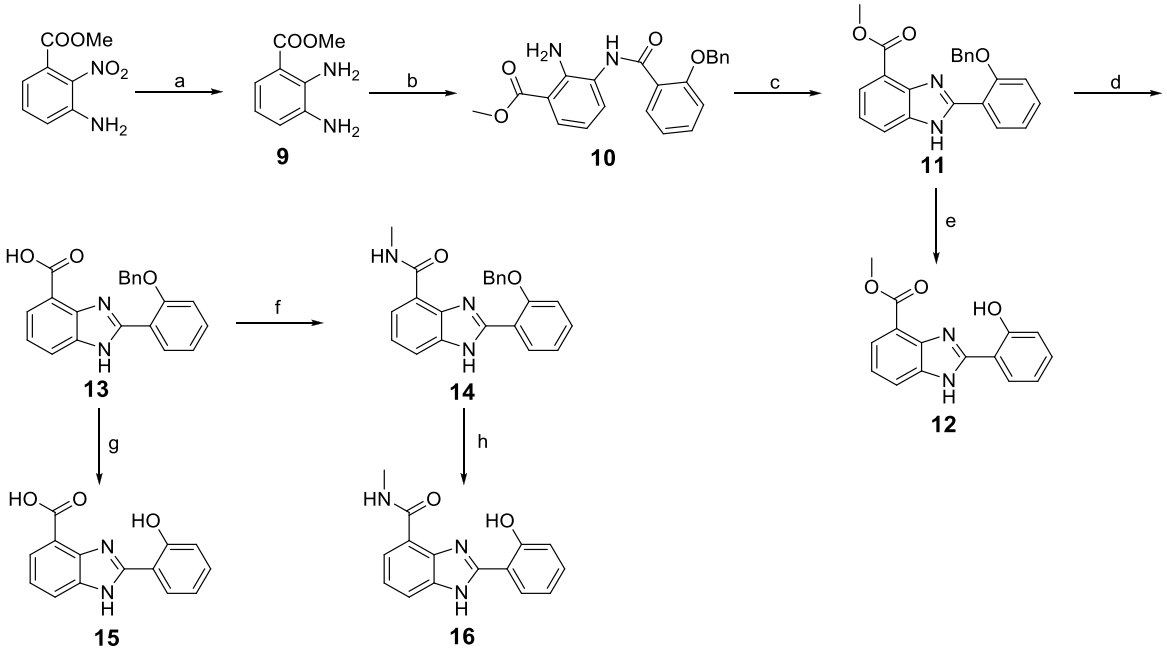

[a] Reagents, conditions, and yields: **(a)** H_2, 45 PSI, Pd/C (10%), MeOH, 99%; **(b)** i. CDI, **5**, THF; ii. **9**, reflux, 59%; **(c)** AcOH, reflux, 99%; **(d)** NaOH, THF, reflux, 65%; **(e)** H_2, 45 PSI, Pd/C (10%), MeOH, 99%; **(f)** H_2NCH_3, Cl_2PPh_3, $CHCl_3$, reflux, 23%; **(g)** H_2, 45 PSI, Pd/C (10%), 57%; **(h)** H_2, 45 PSI, Pd/C (10%), 84%.

Thiobenzoxazole analog **19** was prepared from commercially available 2,2'-dithiodibenzoic acid as shown in **Scheme 3**, whereby protection of the potentially reactive thiol was achieved via a symmetrical disulfide. Activation of 2,2'-

dithiodibenzoic acid with 1,1'-carbonyldiimidazole and subsequent coupling to methyl 3-hydroxyanthranilate, gave diamide **17**. Refluxing **17** in toluene in the presence of pyridinium *p*-toluene sulfonic acid (PPTS) gave disulfide **18**. Reduction of the disulfide using triphenylphosphine in acidic aqueous methanol gave target thiol **19**.[74]

Scheme 3. Synthesis of thiobenzoxazole analog **19**.[a]

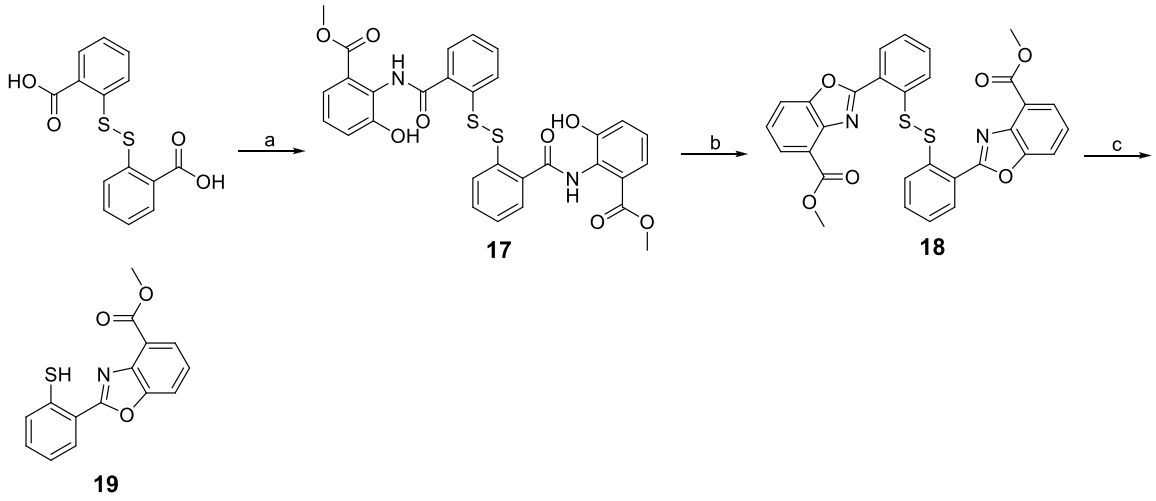

[a] Reagents, conditions, and yields: **(a)** i. CDI, THF; ii. Methyl-3-hydroxyanthranilate, reflux, 33%; **(b)** PPTS, toluene, reflux, 37%; **(c)** Ph_3P, HCl, MeOH, 57%.

The synthesis of thiobenzimidazole **22** began with activation of 2,2'-dithiodibenzoic acid with 2-chloro-4,6-dimethoxy-1,3,5-triazine and *N*-methylmorpholine, and subsequent coupling to diamine **9** giving diamide **20** (both CDI and the dichlorotriphenylphosphorane were unsuccessful in obtaining **22**).[75] Refluxing **20** in glacial acetic acid gave disulfide **21**, which was subsequently reduced with sodium borohydride in a mixture of THF and ethanol to give target thiol **22**. It was found that during purification of **22**, rapid oxidation back to **21** took place. This oxidation also occurred in neat samples stored under inert atmosphere. For this reason, the biological

activity against HCV replication and zinc binding properties were not measured for **22**, as interpretation of the results would be difficult.

Scheme 4. Synthesis of benzimidazole thiol **22**.[a]

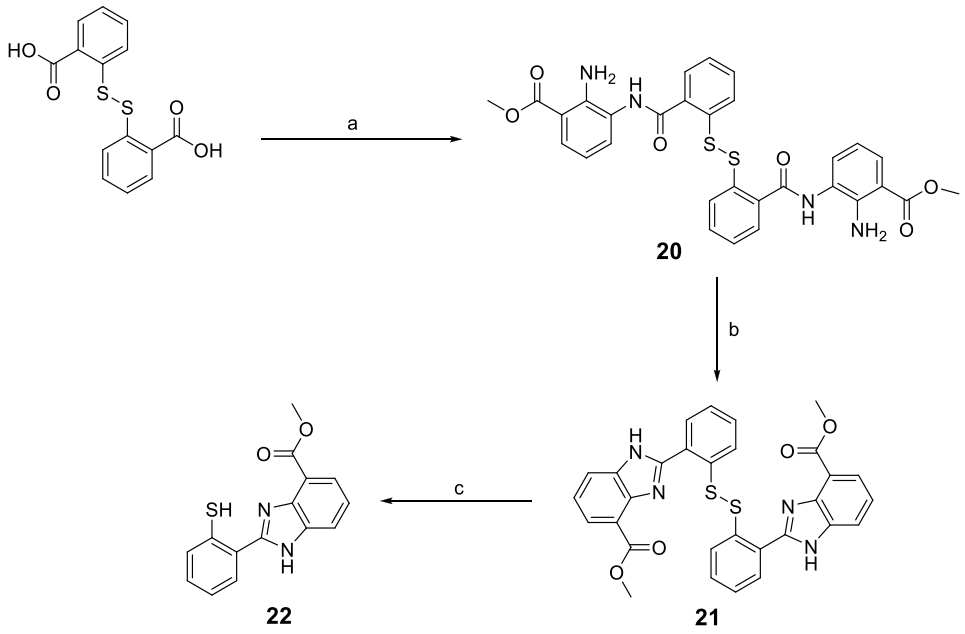

[a] Reagents, conditions, and yields: **(a)** i. 2-chloro-4,6-dimethoxy-1,3,5-triazine, *N*-Methylmorpholine, THF, -5°C-RT, 25%. ii. **9**. **(b)** AcOH, reflux, 68%. **(c)** $NaBH_4$, MeOH:THF (1:1), 90%.

The synthesis of benzoxazole amides **29**-**33** is shown in **Scheme 5**. The hydroxyl protected ester **7** was hydrolyzed with NaOH in THF to give the benzyl protected acid **23**. The general protocol for amide formation using dichlorotriphenylphosphorane was used, along with the appropriate amine to provide the corresponding amides **24, 25,** and **27** in 72%, 80%, and 73% yield, respectively. Primary amide intermediate **28** was prepared *via* activation of **23** with 1-1'-carbonyldiimidazole and subsequent reflux with a solution of ammonia in THF; dichlorotriphenylphosphorane could not be utilized for primary amide formation, which may be due to complex formation between starting amine and/or the product primary amide and the phosphorane reagent, as previously described.[72]

Debenzylation *via* hydrogenation afforded target amides **29, 30, 32,** and **33** in 99%, 90%, 94%, and 96% yield, respectively.[†]

Scheme 5. Synthesis of benzoxazole amides **29-33**.[a]

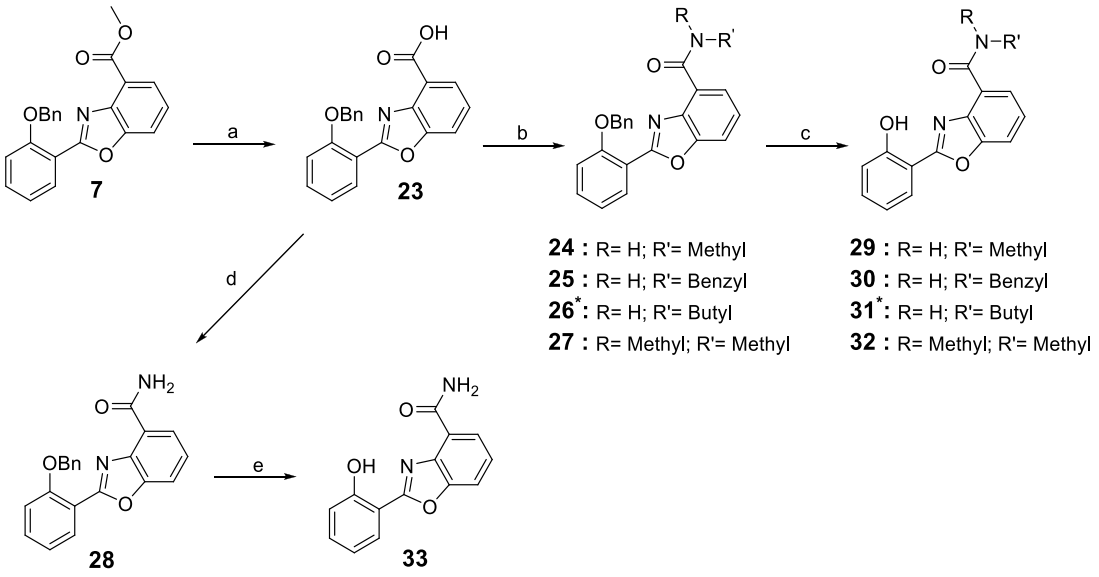

[a] Reagents, conditions, and yields: **(a)** NaOH, THF, reflux, 92%; **(b)** HNRR', Cl_2PPh_3, $CHCl_3$, reflux, (see text for yields); **(c)** H_2, 45 PSI, Pd/C (10%), MeOH; **(d)** i. CDI, THF; ii. NH_3 (0.5M in THF), reflux, 66%; **(e)** H_2, 45 PSI, Pd/C (10%), MeOH, 96%.

N-Benzylated benzimidazole analogs were prepared as shown in **Scheme 6**, starting from the hydroxyl protected ester **11**. *N*-Benzylation of **11** as previously described using Cs_2CO_3 and benzyl bromide in DMF provided **34**.[76] Selective debenzylation *via* hydrogenation gave target ester **35**. When sodium hydride was used to deprotonate the benzimidazole nitrogen for subsequent alkylation, quantitative hydrolysis of the methyl

[†] It should be noted that target amide **31** was synthesized using different methodology. The amide was introduced early in the synthesis, rather than late. This approach provided enough of the target amide for biological testing, but proved less efficient and was thus abandoned. The protected intermediate **26** and final compound **31** were included in **Scheme 4** for ease of interpretation.

ester occurred along with the desired benzylation. Although unexpected, the reaction yielded *N*-benzylated acid **36,** a synthetic intermediate required for the synthesis of targets **38** and **39**. Activation of **36** with 2-chloro-4,6-dimethoxy-1,3,5-triazine and *N*-methylmorpholine in dichloromethane, and coupled to methylamine gave amide **37**.[75] Debenzylation, *via* slightly less harsh hydrogenation conditions, selectively removed the *O*-benzyl group to give target compound **38**. Analogous *O*-debenzylation of **36**, provided acid **39**.

Scheme 6. Synthesis of *N*-benzylated benzimidazoles **35, 38,** and **39**.[a]

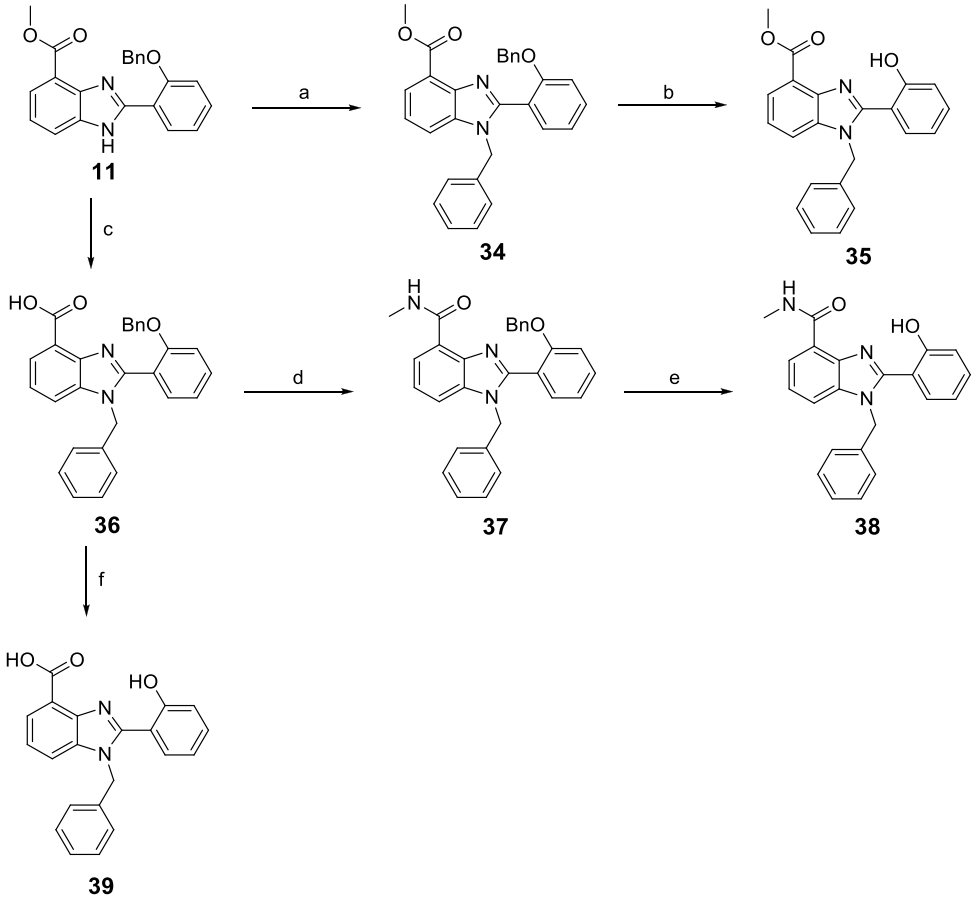

[a]Reagents, conditions, and yields: **(a)** BnBr, Cs_2CO_3, DMF, reflux, 61%; **(b)** H_2 30PSI, Pd/C (5%), MeOH, 77%; **(c)** BnBr, NaH, THF, 55%; **(d)** i. 2-Chloro-4,6-dimethoxy-1,3,5-triazine, N-methylmorpholine, CH_2Cl_2; ii. H_2NCH_3 (2M in THF), 60%; **(e)** H_2, 30 PSI, Pd/C (5%), MeOH, 98%; **(f)** H_2, 30 PSI, Pd/C 5%, MeOH, 57%.

To confirm the desired benzimidazole nitrogen had been benzylated, total correlation spectroscopy (TOCSY) followed by a nuclear Overhauser effect (NOE) experiment were conducted on a representative compound (**38**). TOCSY was first used to identify the signals for the three aromatic protons on the benzimidazole ring, as this was not initially clear using 1D experiments (**Figure 12**). The three spin-coupled aromatic signals were clearly identified in the TOCSY spectrum (**Figures 13** and **14**).

Figure 12. Zoomed in ^{1}H NMR of **38** to show the aromatic and benzylic methylene signals.

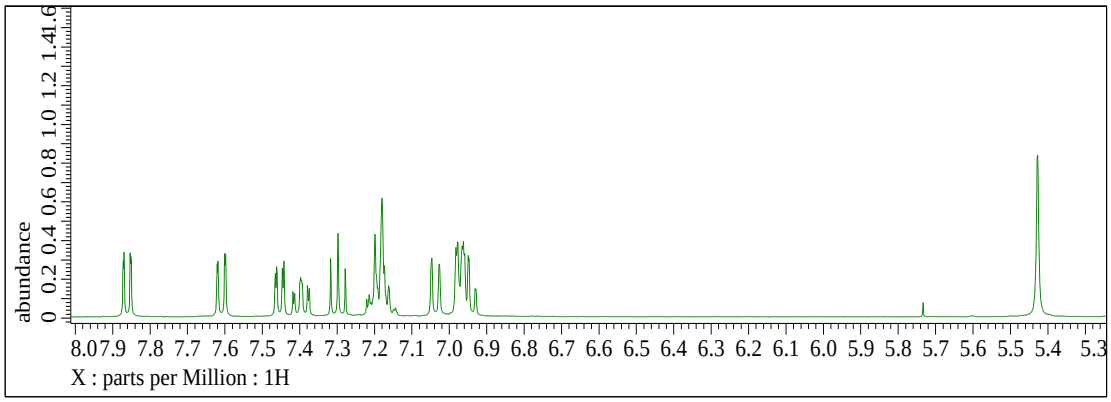

Figure 13. TOCSY spectrum of **38** showing the three spin-coupled aromatic protons of the benzimidazole ring.

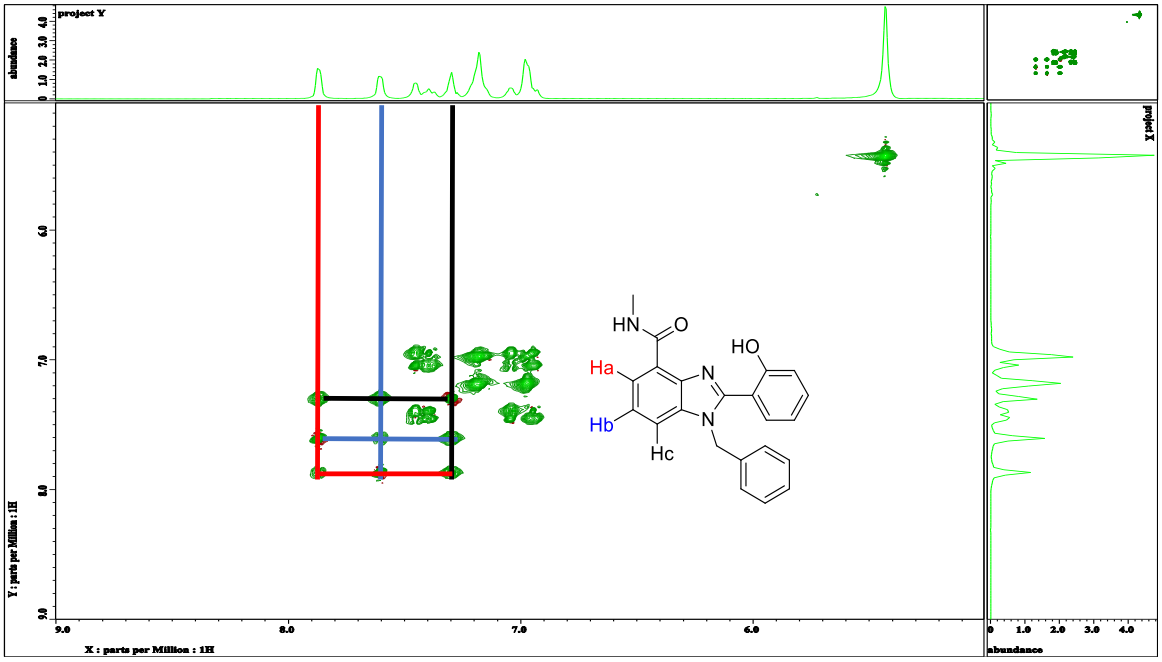

Figure 14. Overlay of **38** on the corresponding ^{1}H NMR identifying the signals of the three spin-coupled signals of the benzimidazole protons.

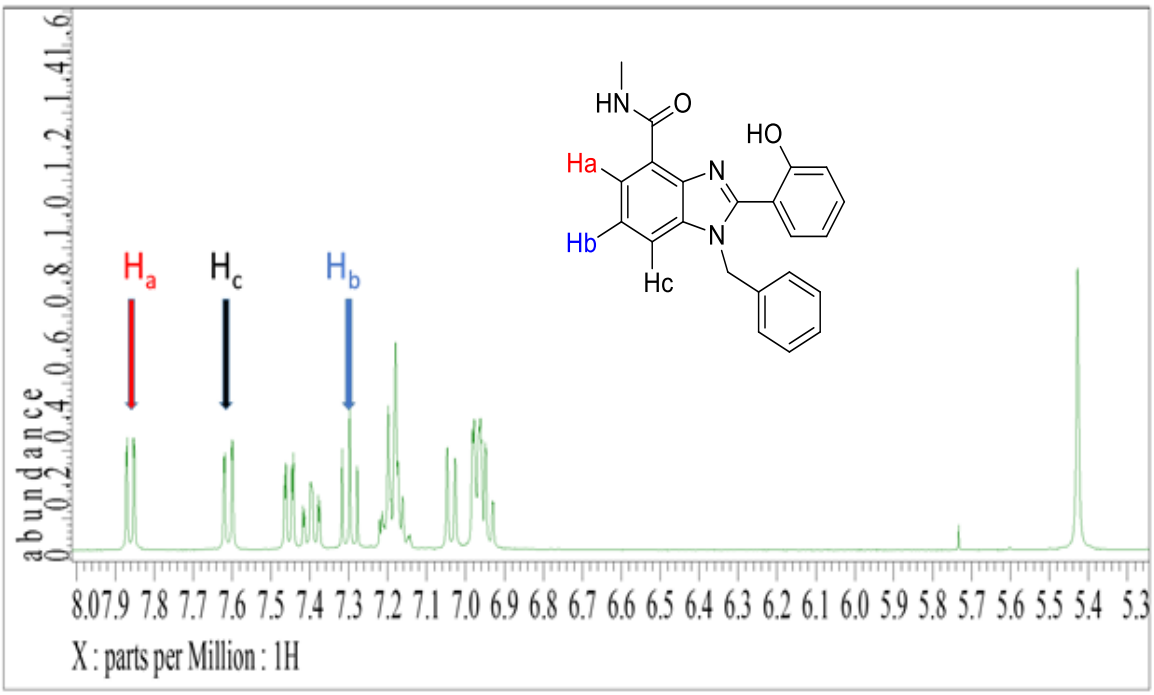

For the desired isomer, it was hypothesized that an NOE would be observed between the methylene protons of the benzyl group and H_c (**Figure 14**) of the benzimidazole ring due to their close proximity. When selectively irradiated at the resonance frequency of the benzylic-methylene protons (5.4ppm), as expected, there was a positive NOE to H_c (~7.6ppm) (**Figure 15**) The other positive NOE arises from aromatic protons on the benzyl-ring. Similarly, when selectively irradiated at the resonance frequency of H_c (7.6ppm), a positive NOE was observed to the benzylic methylene (5.4ppm) (and also to H_a, H_b, and protons of the benzylic ring), thus confirming the structure as the desired isomer (**Figure 16**).

Figure 15. ^{1}H NMR spectrum of **38**, showing a positive NOE to H_c (7.6ppm) of the benzimidazole ring when irradiated at the benzylic methylene resonance frequency (5.4ppm).

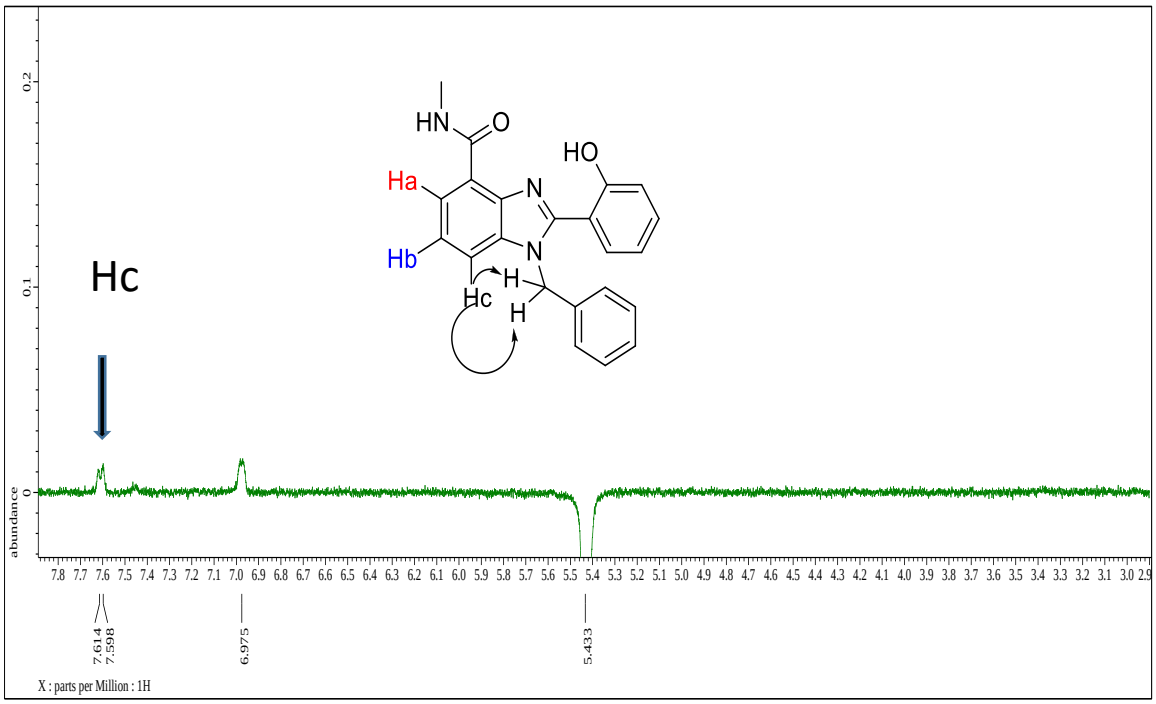

Figure 16. ^{1}H NMR spectrum of **38** showing a positive NOE to the benzylic methylene protons (5.4ppm) when irradiated at the resonance frequency of H_c on the benzimidazole ring (7.6ppm).

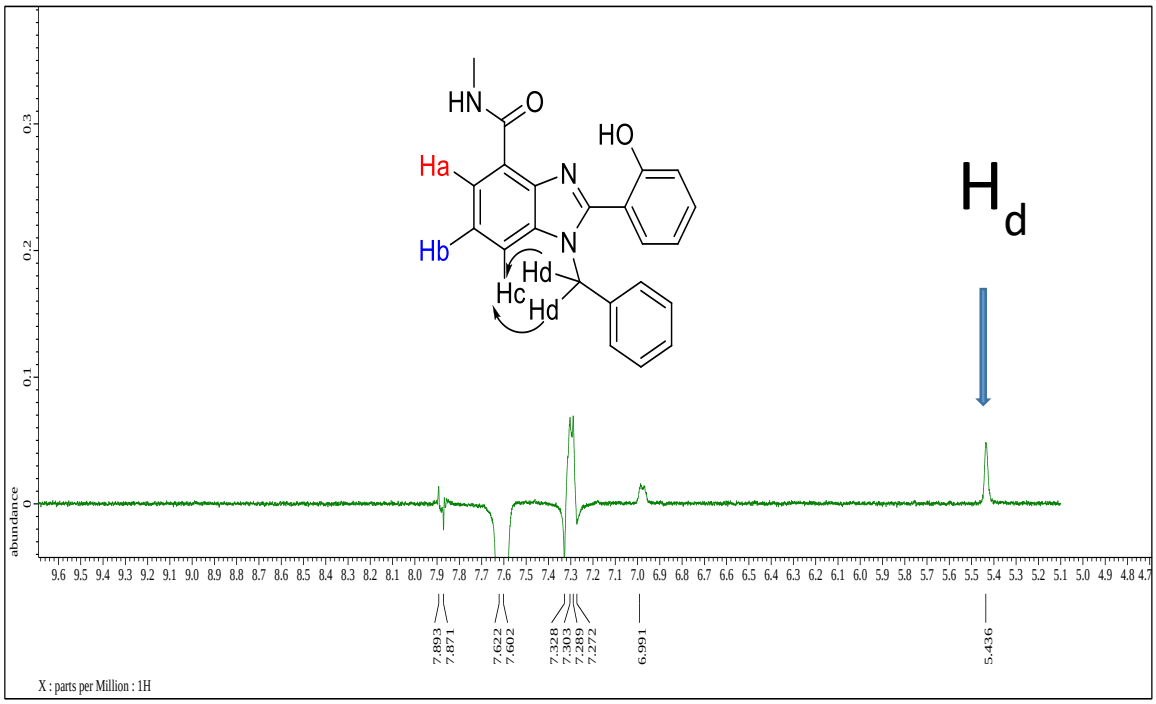

Naphthol analogs **41**-**43** were synthesized analogously, starting from the appropriate naphthoic acid isomer; a representative scheme in shown in **Scheme 7**. Activation of 1-hydroxy-2-napthoic acid with 1,1'-carbonydiimidazole and coupling to methyl 3-hydroxyanthranilate gave amide **40**, which was used without purification due to poor solubility. The crude amide was refluxed in *m*-xylene in the presence of PPTS to give the target analog **41** in 28% yield (two steps).

Scheme 7. Representative synthesis of a naphthol analog

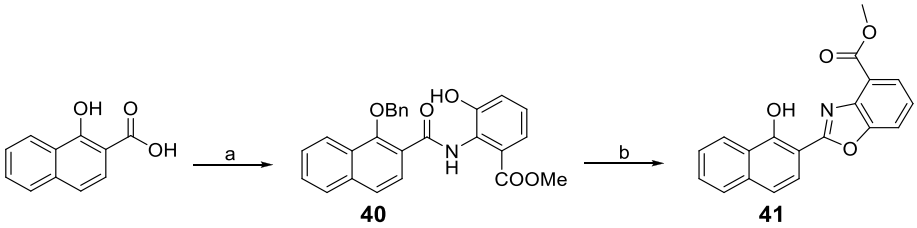

[a] Reagents, conditions, and yields. **(a)** i. CDI, THF; ii. Methyl 3-hydroxyanthranilate; **(b)** PPTS, *m*-xylene, reflux, 28% (two steps).

The quinoline derivative **45** was prepared as shown in **Scheme 8**, starting with acid activation of commercially available quinoline-8-carboxylic acid using oxalyl chloride and DMF. Addition of methyl 3-hydroxyanthranilate gave **44**. The amide was refluxed in *m*-xylene to give target quinoline **45**.

Scheme 8. Synthesis of quinoline analog **45**.[a]

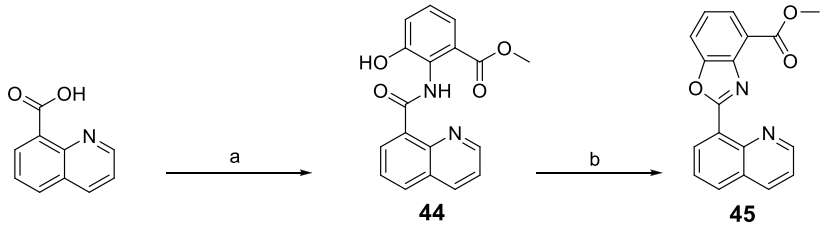

[a]Reagents, conditions, and yields: **(a)** Oxalyl chloride, DMF, DCM, 59%. **(b)** PPTS, *m*-xylene, reflux, 84%.

To investigate a correlation between zinc binding and inhibitor efficacy, Zn^{2+} dissociation constants were measured *via* equilibrium titration experiments monitored by UV-VIS spectroscopy, for five representative analogs: **3, 8, 29** (lead ester, and analogous acid and *N*-methyl amide)**, 12** (benzimidazole ester)**,** and **19** (thiobenzoxazole). Representative (one trial for each compound) UV-VIS spectra can be found in **Figures 17-21**.

Figure 17. Representative UV-VIS spectra for the titration of lead compound **3** with $Zn(OAc)_2$ in 50:50 methanol:H_2O. $[Zn]^{2+}$ range from 0-125μM.

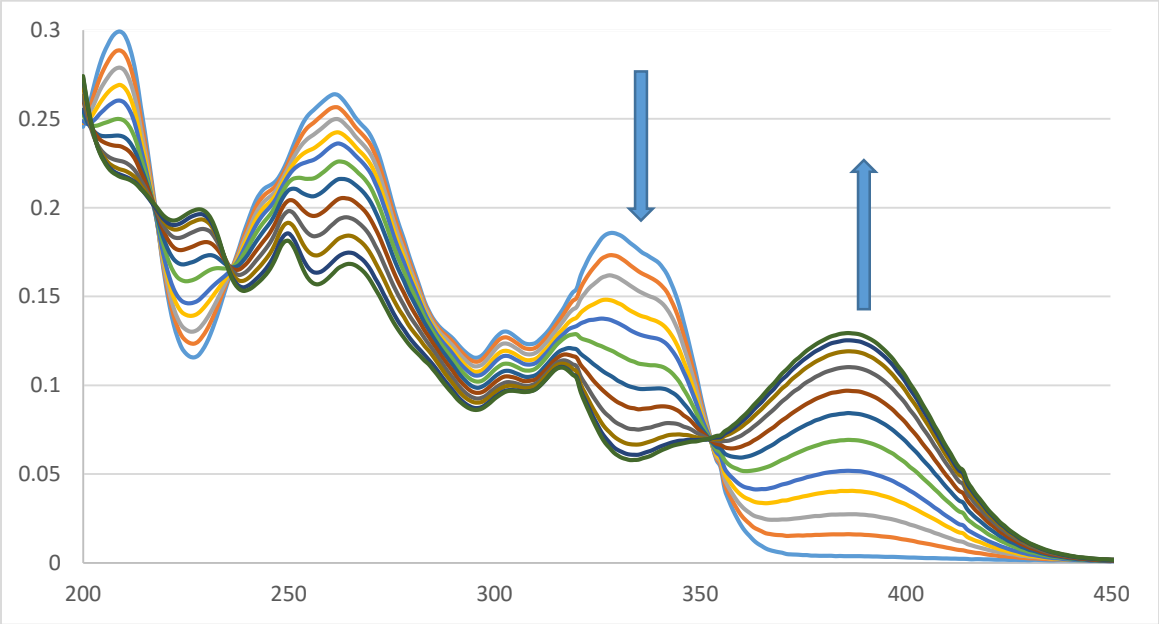

Figure 18. Representative UV-VIS spectra for the titration of acid **8** with $Zn(OAc)_2$ in 50:50 methanol:H_2O. $[Zn]^{2+}$ range from 0-25μM.

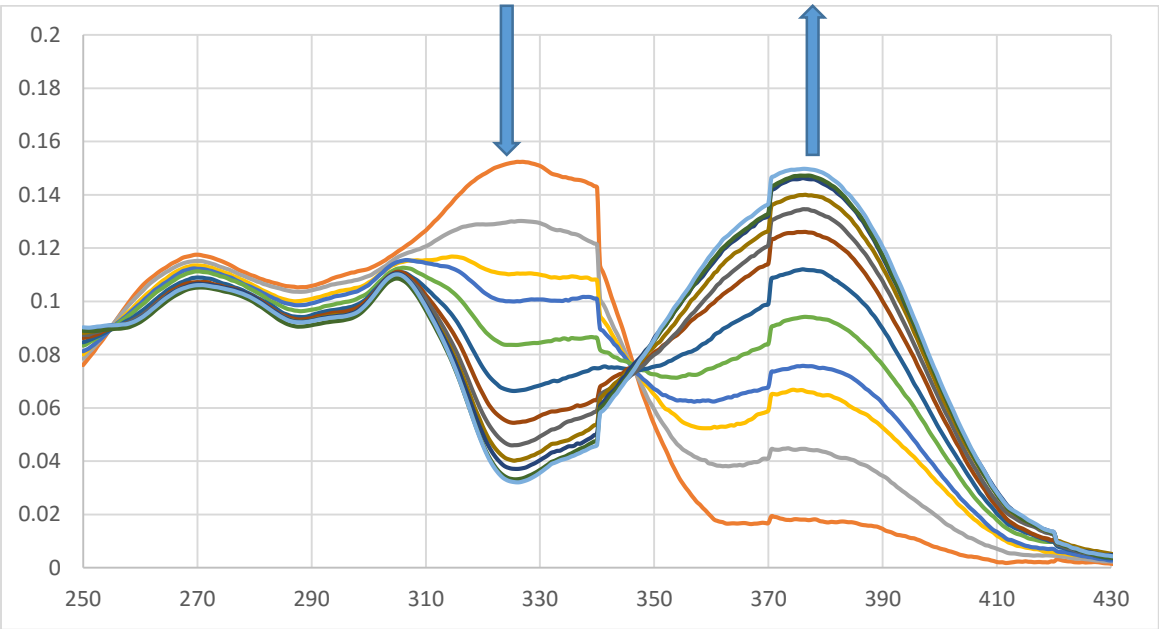

Figure 19. Representative UV-VIS spectra for the titration of *N*-methyl amide **29** with $Zn(OAc)_2$ in 50:50 methanol:H_2O. $[Zn]^{2+}$ range from 0-125μM.

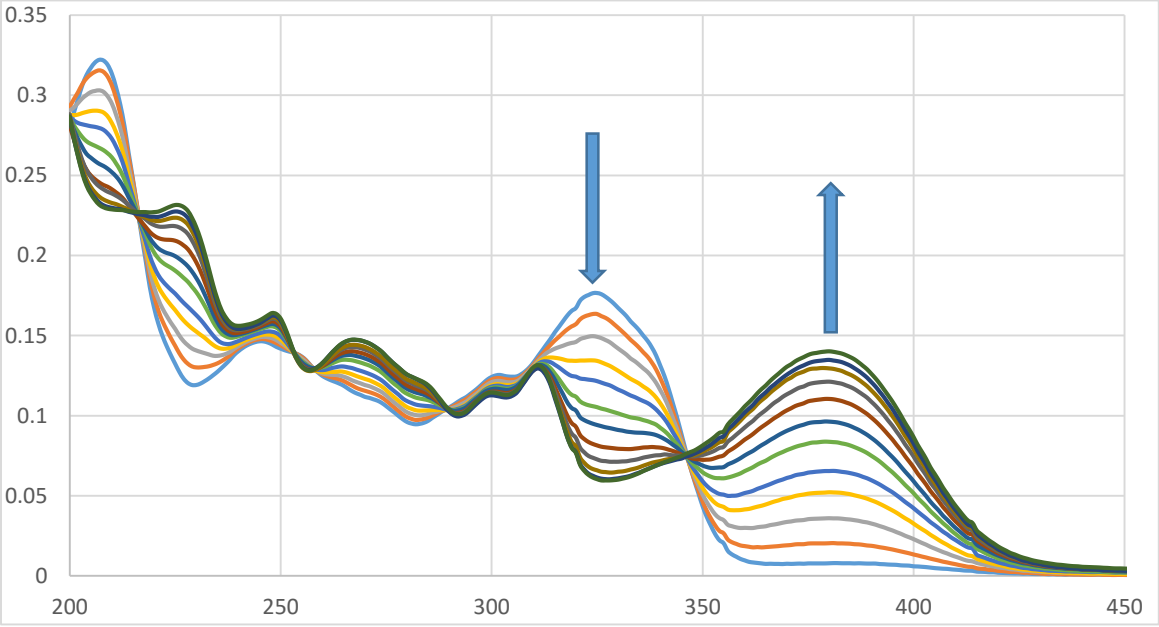

Figure 20. Representative UV-VIS spectra for the titration of benzimidazole **12** with $Zn(OAc)_2$ in 50:50 methanol:H_2O. $[Zn]^{2+}$ range from 0-245μM.

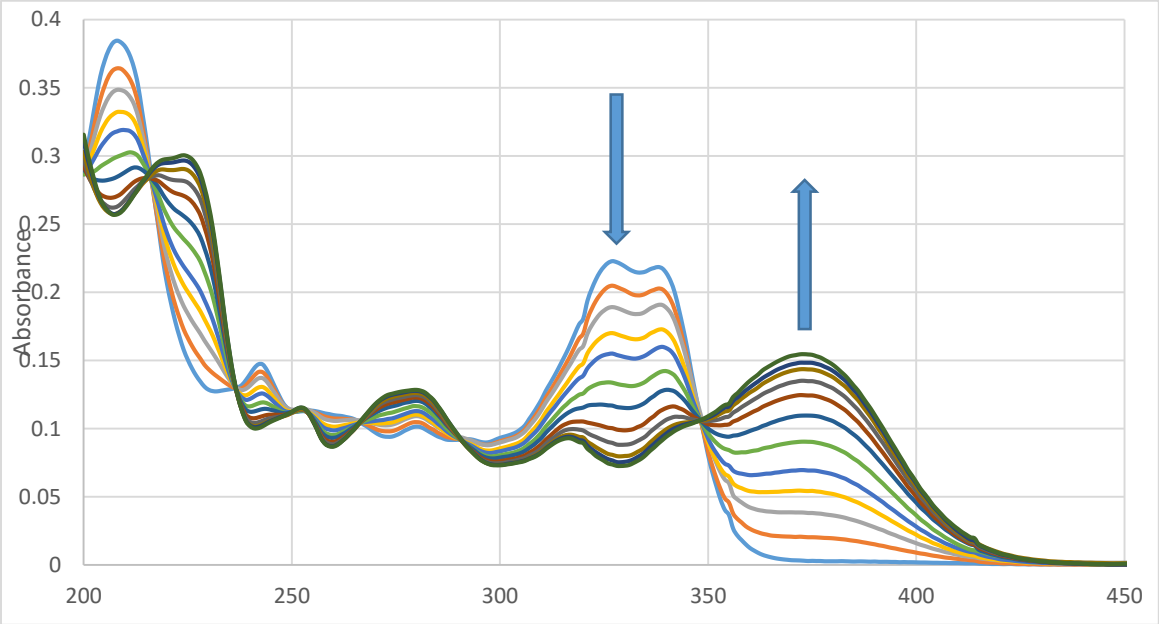

Figure 21. Representative UV-VIS spectra for the titration of thiol **19** with $Zn(OAc)_2$ in 50:50 methanol:H_2O. $[Zn]^{2+}$ range from 0-25μM.

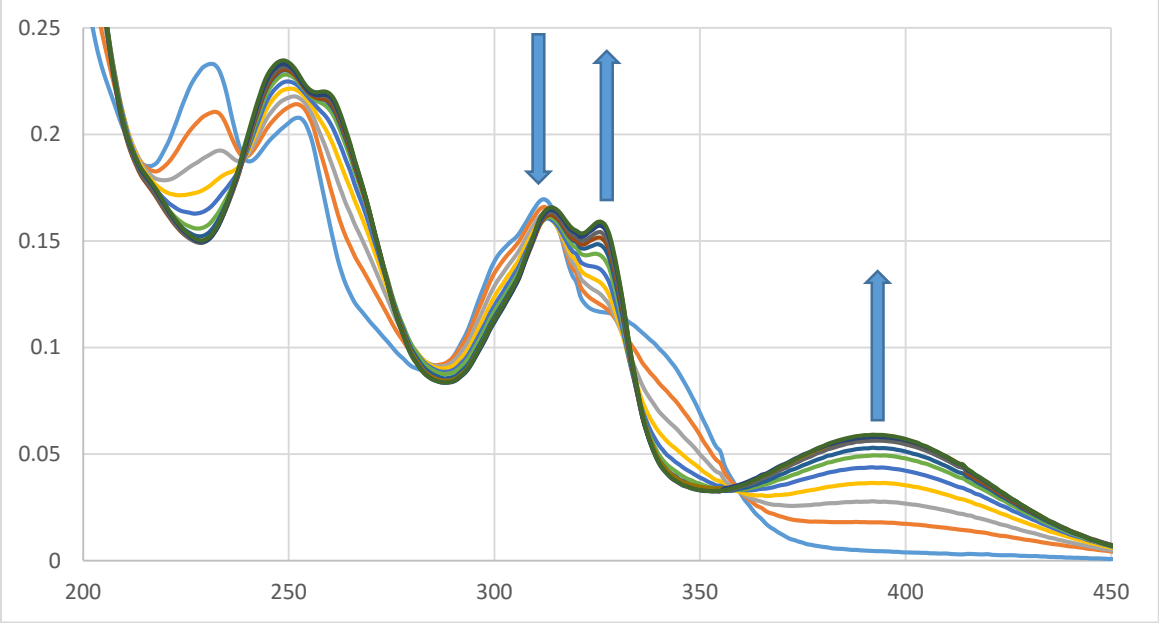

D. Biological Results and Discussion

All compounds were evaluated for selective antiviral activity on the replication of HCV in a HCV replicon assay using either a luciferase reporter or *via* quantitative analysis of viral RNA production (**Tables 1-5**).[60,77] Compounds for which Zn^{2+} binding constants were measured can be found in **Table 1**. Among lead methyl ester **3**, acid **8,** and methyl amide **29,** the acid has the highest affinity for zinc as well as the lowest EC_{50} value. Replacing the benzoxazole with a benzimidazole unexpectedly decreased the zinc affinity, but also decreased inhibitor efficacy. Thiol analog **19** has the highest affinity for zinc as well as the lowest EC_{50} value of all compounds for which zinc binding was measured. There was a correlation between K_d and EC_{50} values, with the exception of amide **29**, consistent with the hypothesis that inhibitor efficacy may be related to zinc coordination within the HCV proteome.

Table 1. Inhibition of HCV replication in a HCV replicon assay and Zn^{2+} dissociation constants for lead **3** and analogs **8, 29**, **12**, and **19**.

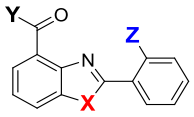

Compound ID	X=	Y=	Z=	K_d (μM)[a]	EC_{50} (μM)[b]	CC_{50} (μM)[c]	SI[d]
3	O	OCH_3	OH	65	40	71	1.8
8	O	OH	OH	0.50	4.9	25	5.1
29	O	NHMe	OH	53	117	>186	1.6
12	NH	OCH_3	OH	190	106	132	1.3
19	O	OCH_3	SH	0.23	2.5	4.1	1.6

a. Zinc dissociation constants measured *via* equilibrium titration experiments monitored by UV-VIS spectroscopy in 50/50 methanol/water. Results are an average of three independent trials. b. The concentration of compound that inhibits 50% of viral RNA replication, measured in the HCV subgenomic replicon assay using a luciferase reporter. This assay was conducted using Huh 5-2 cells containing the hepatitis C virus genotype 1b I389luc-ubi-neo/NS3-3'/5.1 replicon. c. The concentration of compound at which the metabolic activity of the cells is reduced by 50% as compared to untreated cells. d. The ratio of CC_{50} to EC_{50}.

A series of amides related to **29** were synthesized to examine the effects of sterics/hydrophobicity and hydrogen bonding about the 4-postion of the benzoxazole (**Table 2**). The larger benzyl and butyl groups were the most active of the amides. If these compounds are coordinating a structural zinc ion, this additional hydrophobic bulk may be further perturbing protein structure, increasing inhibitor efficacy. The primary amide was roughly twice as effective as the methyl and dimethyl analogs, which were the least effective within the amide series. The additional hydrogen bond donating ability of the primary amide seems to have improved the activity compared to the smaller *N*-alkyl amides.

Table 2. Inhibition of HCV replication in a HCV replicon assay for benzoxazole amides **29**-**33**.

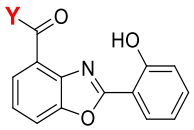

Compound ID	Y=	EC_{50} (μM)[a]	CC_{50} (μM)[b]	SI[c]
29	$NHCH_3$	117	186	1.59
30	NHBn	10	>50	>5
31	NHBu	7.2	39	5.4
32	NMe_2	109	>177	>1.6
33	NH_2	47	>197	>4.2

a. The concentration of compound that inhibits 50% of viral RNA replication, measured in the HCV subgenomic replicon assay using a luciferase reporter. This assay was conducted using Huh 5-2 cells containing the hepatitis C virus genotype 1b I389luc-ubi-neo/NS3-3'/5.1 replicon. b. The concentration of compound at which the metabolic activity of the cells is reduced by 50% as compared to untreated cells. c. The ratio of CC_{50} to EC_{50}.

All benzimidazole analogs evaluated are shown in **Table 3**. Interestingly, unlike benzoxazole leads **3**, **8**, and **29**, the benzimidazole methyl amide (**16**) was the most effective among the methyl ester and acid (**12** and **15**, respectively). The effect of

introducing hydrophobic/steric bulk about the imidazole core was investigated *via N*-benzylated analogs **35, 39,** and **38.** In all cases, benzylation of the benzimidazole nitrogen provided more active inhibitors than the analogous non-benzylated precursors. Acid **39** is the most effective compound tested with an EC_{50} value of 2.6 μM and a selectivity index greater than 55.

Table 3. Inhibition of HCV replication in a HCV replicon assay for benzimidazoles **12, 15, 16** and comparable *N*-benzylated analogs **35, 39,** and **38**.

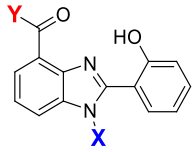

Compound ID	X=	Y=	EC_{50} (μM)[a]	CC_{50} (μM)[b]	SI[c]
12	H	OCH_3	106	132	1.25
35	Bn	OCH_3	7.5	>140	>19
15	H	OH	24	>197	>8.2
39	Bn	OH	2.6	>145	>55
16	H	NHMe	16	>187	>12
38	Bn	NHMe	8.4	101	12

a. The concentration of compound that inhibits 50% of viral RNA replication, measured in the HCV subgenomic replicon assay using a luciferase reporter. This assay was conducted using Huh 5-2 cells containing the hepatitis C virus genotype 1b I389luc-ubi-neo/NS3-3'/5.1 replicon. b. The concentration of compound at which the metabolic activity of the cells is reduced by 50% as compared to untreated cells. c. The ratio of CC_{50} to EC_{50}.

The effect of introducing additional steric/hydrophobic bulk about the phenolic ring was investigated using naphthol and quinoline analogs **41-43** and **45**. Only slightly improved efficacy, compared to lead phenol **3**, was found for naphthol analogs **42** and **43** (**Table 4**).

Table 4. Inhibition of HCV replication in a HCV replicon assay for naphthol and quinoline analogs **41-43** and **45**.

Compound ID	Structure	EC_{50} (μM)[a]	CC_{50} (μM)[b]	SI[c]
41	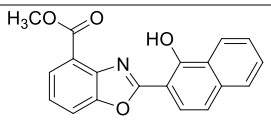	52	64	1.2
42	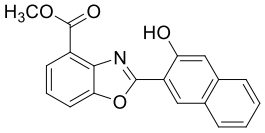	31	>50	>1.6
43	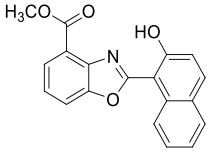	28	>50	>1.8
45	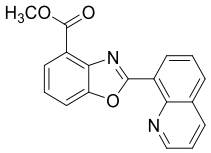	>50	>50	NA

a. The concentration of compound that inhibits 50% of viral RNA replication, measured in the HCV subgenomic replicon assay using a luciferase reporter. This assay was conducted using Huh 5-2 cells containing the hepatitis C virus genotype 1b I389luc-ubi-neo/NS3-3'/5.1 replicon. b. The concentration of compound at which the metabolic activity of the cells is reduced by 50% as compared to untreated cells. c. The ratio of CC_{50} to EC_{50}.

As a validation step, the most active compounds were also evaluated in replicons using Huh 9-13 cells as opposed to Huh 5-2; viral RNA production was quantified *via* real-time quantitative one-step PCR (RT-qPCR) to confirm inhibitor potency and explore efficacy in another cell line (**Table 5**). With the exception of **38**, all compounds retested proved more active as HCV replication inhibitors and were far less toxic in Huh 9-13 cells. *N*-Benzyl acid **39** was identified once again as the most active compound within the series, with an EC_{50} value of 0.6 μM and a selectivity index greater than 167; this data is consistent with the data that were obtained in Huh 5-2 cells, identifying **39** as a significantly active inhibitor of HCV replication.

Table 5. Validation of the inhibition of HCV replication in a HCV replicon assay in Huh 9-13 cells.

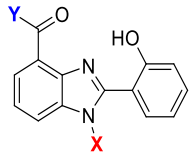

Compound ID	X=	Y=	EC_{50} (μM)[a]	CC_{50} (μM)[b]	SI[c]
15	H	OH	23	>100	>4.3
16	H	NHMe	3.1	47	15
35	Bn	OCH_3	0.9	95	106
39	Bn	OH	0.6	>100	>167
38	Bn	NHMe	21	38	1.8

a. The concentration of compound that inhibits 50% of viral RNA replication, measured in the HCV subgenomic replicon system in Huh 9-13 cells. Replicon RNA content was quantified using a real-time quantitative one-step RT-PCR method (RT-qPCR). b. The concentration of compound at which the metabolic activity of the cells is reduced by 50% as compared to untreated cells. c. The ratio of CC_{50} to EC_{50}.

E. Conclusions and Future Work

Several novel inhibitors of HCV replication have been identified. The possible role zinc binding may play in inhibitor efficacy was explored through a comparison of Zn^{2+} affinity and inhibitor efficacy, for a representative group of compounds. With one exception (**29**), there was a direct correlation between K_d and EC_{50} values, suggesting zinc binding may indeed play a key role in the efficacy of these inhibitors. It should be noted that many of the compounds for which zinc binding was measured were quite toxic, with selectivity indices ranging from 1.3-5.1. The HCV replicon assay used to determine inhibitor efficacy is sensitive to inhibitor cell-toxicity. Adverse effects on the cell can cause a non-virus specific decrease in viral proliferation. Further work is required to determine whether or not these compounds are specifically targeting HCV replication, which will involve modifications to inhibitors aimed to decrease cell-toxicity.

Exploration of the structure-activity relationship has led to the development of an inhibitor (**39**) with a low to sub-micromolar EC_{50} value (depending on the cell-line) and selectivity indices that are sufficiently high for this compound to be considered a selective inhibitor of HCV replication. Work is currently in progress to identify the mechanism of inhibition and to further improve upon inhibitor efficacy.

Chapter 3: Novel Inhibitors of the HCV NS3 Helicase

A. The HCV NS3 Helicase

The HCV NS3 helicase (NS3h) is located in the carboxy-terminus two-thirds of non-structural protein three and unwinds double-stranded RNA in an NTP-dependent fashion.[8] HCV is a positive-sense RNA virus that replicates outside the nucleus, however the NS3 helicase is also capable of unwinding double-stranded DNA.[78] The relevance of the NS3h substrate specificity remains unknown, as does the exact role this enzyme plays in the HCV life-cycle. It is generally accepted that NS3h separates double-stranded RNA produced during viral proliferation, to aid in the transcription process; however, other roles in the HCV viral life-cycle have been speculated (as discussed in Chapter 1).

Helicase enzymes are classified into families, and then superfamilies, based on structural sequence-motif homology. The HCV helicase is a member of the viral DEx/CH box family (so-named for highly conserved residues in a particular motif) and the helicase superfamily 2 (SF2), along with the helicase of dengue virus.[8] Within SF1 and SF2, there are a total of seven highly conserved sequence motifs.[79] All known helicases contain an NTP-binding domain, formed by the two highly conserved structural motifs: 'Walker A and Walker B' sites.[8,80] The 'Walker A' site binds phosphate and the 'Walker B' binds Mg^{2+} *via* an aspartic acid residue. Helicases also have at least one three-dimensional fold comprising a motor-domain, first discovered in the bacterial recombination protein 'RecA'.[81] The HCV helicase has two, so called RecA-like, motor domains. Most models assume the HCV helicase separates double-stranded nucleic acid by moving along the nucleotides, similar to an inchworm, by rotating the two RecA-

motor domains and hydrolyzing NTP for fuel; however other models have been suggested.[8]

NS3h was the first RNA helicase to be crystallized.[81] Since then, at least ten atomic structures of NS3h have been solved and deposited in the Protein Data Bank; each has provided unique structural data integral to the understanding of its function. The NTP and nucleic acid binding sites have been identified and resolved.[81-83] Two orientations of the RecA-like motor domains, 'open' or 'closed,' have been identified and their structures have been resolved.[84,85] A structure with a portion of NS4A, a co-factor for helicase activity, tethered to NS3h has been published.[86] In addition, crystal structures have been used to visualize how the protein conformation changes upon both binding and hydrolyzing ATP.[83] The wealth of structural information available for the HCV NS3 helicase has contributed to the design of a number of inhibitors of this enzyme. However, the extensively conserved sequence homology among all helicases has complicated the design of virus-specific helicase inhibitors.

B. HCV NS3 Helicase Assays

The first biochemical assays developed to monitor HCV NS3 helicase activity use radiolabeled double-stranded oligonucleotides.[87] Following helicase mediated separation of double-stranded nucleic acid, the products are separated using non-denaturing gels and detected with autoradiography or another analogous method. These prototypical helicase assays are highly accurate and are still used widely today; however, they require working with hazardous radioactive material.

The most commonly used NS3h assays incorporate fluorescently labeled oligonucleotides and Forster resonance energy transfer (FRET) to detect double-stranded nucleic acid separation. Early FRET-based assays use two complementary oligonucleotides; one labeled with a FRET-donor and the other with an acceptor.[88] Upon separation of the double-stranded substrate, the donor/acceptor fluorophores are no longer in close proximity and the donor fluoresces. As a result, helicase activity can be directly measured as an increase in fluorescence. It was later discovered however, that the nucleic acid 'traps' required in these assays to prevent reannealing of single-stranded oligonucleotides significantly interfere with measured reaction rates.[89] A second-generation FRET-based assay was developed that doesn't require 'traps'. This assay utilizes a hairpin-forming oligonucleotide substrate (a 'molecular beacon'), labeled with both donor and acceptor chromophores.[90] A complementary DNA or RNA oligonucleotide is added that anneals to the molecular beacon. Upon separation by the helicase, the molecular beacon forms a hairpin that places the FRET-donor and acceptor in close proximity, thus quenching fluorescence. Helicase activity is measured as a decrease in fluorescence. This assay has since been optimized for use in high throughout screens and has led to the identification of a number of NS3h inhibiting compounds.

C. Inhibitors of the HCV NS3 Helicase

Although the exact role NS3h plays in the hepatitis c viral lifecycle remains unknown, an active helicase is required for viral proliferation, validating this protein as a drug target.[8,16,17] Numerous strategies for helicase inhibition have been investigated, however there are currently no HCV helicase inhibitors approved by the FDA. NS3

helicase activity is dependent upon ATP hydrolysis. As such, various compounds have been developed which inhibit NTPase activity (**Figure 22**).[91-96]

Figure 22. HCV NS3 helicase inhibitors (**A**-**E**) targeting the NTPase activity.

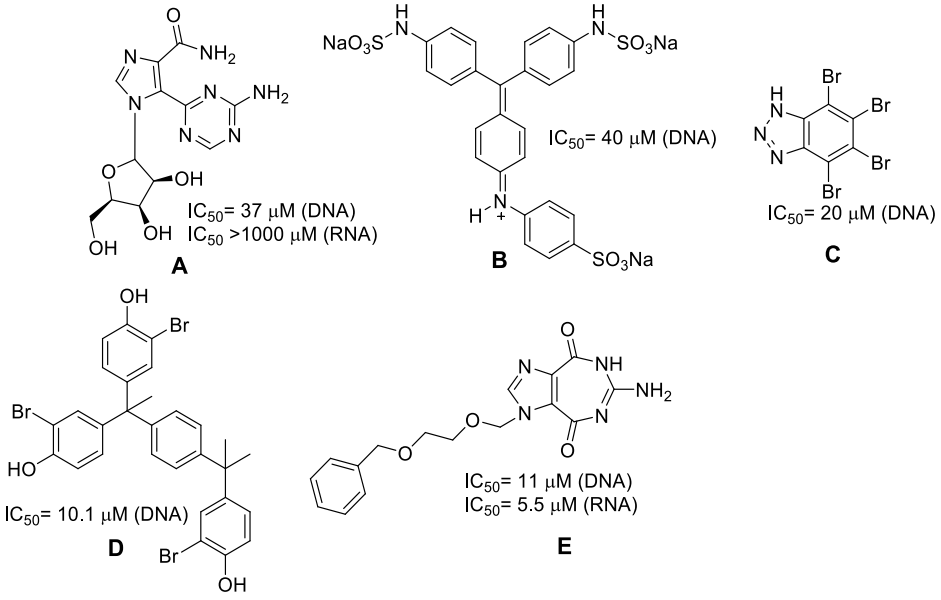

A nucleoside analog (**Figure 22**, **A**) inhibits NS3h, but only with a DNA substrate. This compound was more active against the related helicase of West Nile virus (IC_{50}= 23μM).[95] The dye Blue HT (**Figure 22**, **B**) is similarly effective as a NS3h inhibitor with a DNA substrate.[96] A halogenated benzotriazole (**Figure 22**, **C**) inhibits the NS3h with a DNA substrate, but was more effective against the helicase of West Nile virus (IC_{50}= 1.7 μM).[92] A triphenylmethane derivative has been shown to inhibit the HCV helicase, but also only with a DNA substrate (**Figure 22**, **D**).[96] Ring-expanded, so-called 'fat nucleosides', (**Figure 22**, **E**) are active against NS3h with both a DNA and RNA substrate, but were also active against the helicases of Japanese encephalitis and West Nile virus.

Other helicase inhibitors include compounds that coordinate directly to the nucleic acid binding site of the helicase, preventing binding of the natural RNA/DNA substrate (**Figure 23**).

Figure 23. HCV NS3 helicase inhibitors binding to the nucleic acid site (**A**) and to allosteric or unknown sites (**B**-**D**).

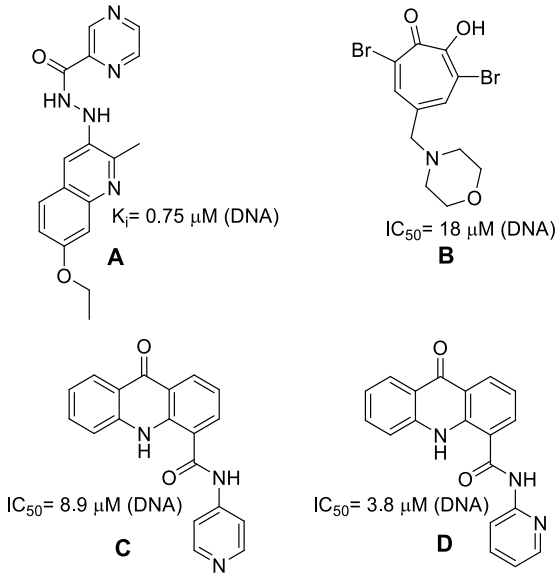

A quinoline analog (**Figure 23**, **A**) inhibits NS3h unwinding of DNA with a K_i=0.75 μM, but has never been tested as an HCV replication inhibitor.[97] In addition, various compounds have been identified as NS3h inhibitors that bind at unknown allosteric sites (**Figure 23, B**-**D**).[85,86,97-100] A tropolone analog (**Figure 23**, **B**) inhibits the NS3h with a DNA a substrate, but does not appear to compete with binding of NTP or nucleic acid.[98] Acridone analogs (**Figure 23**, **C** and **D**) have also been shown to inhibit DNA unwinding, but their binding site(s) are yet to be identified.[100]

Two UK-1 analogs (**1** and **2**), briefly mentioned in Chapter 2, have been designed and identified as inhibitors of hepatitis C virus replication in a replicon assay (**Figure 24**). Importantly, these compounds also inhibit the HCV NS3 helicase with both a DNA and

RNA substrate. In addition, no activity against the helicases of the closely related *Flaviviridae* viruses, Japanese encephalitis or dengue, is observed.[59]

Figure 24. UK-1 analogs **1** and **2** inhibit HCV replication and target the NS3 helicase.

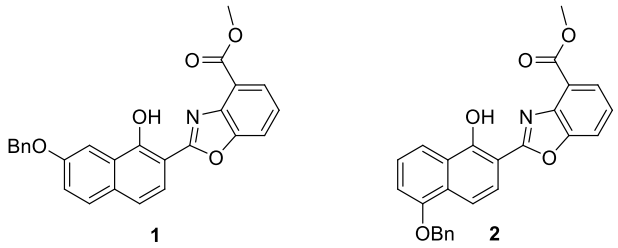

D. Synthesis of Novel NS3h Inhibitors

For the synthesis of HCV NS3 helicase inhibitors **1** and **2**, the same methodology was used; the synthesis of **2** is shown in **Scheme 9**. This began with carboxylation of 1,5-dihydroxynapthalene, using magnesium methyl carbonate as previously described.[101] The resulting acid was dibenzylated using benzyl chloride, which upon ester hydrolysis gave **46**. The acid was subsequently activated with 1,1'-carbonyldiimidazole (CDI) and coupled to methyl 3-hydroxyanthranilate, giving compound **47**. Refluxing **47** in *m*-xylene with PPTS resulted in cyclodehydration as well as monodebenzylation, to give target compound **2**. Compound **1** was synthesized similarly, starting with 1,7-dihydroxynaphthalene.

Scheme 9. Synthesis of lead compound **2**. An analogous route was used for the synthesis of **2**, starting from the 1,7-diol.[a]

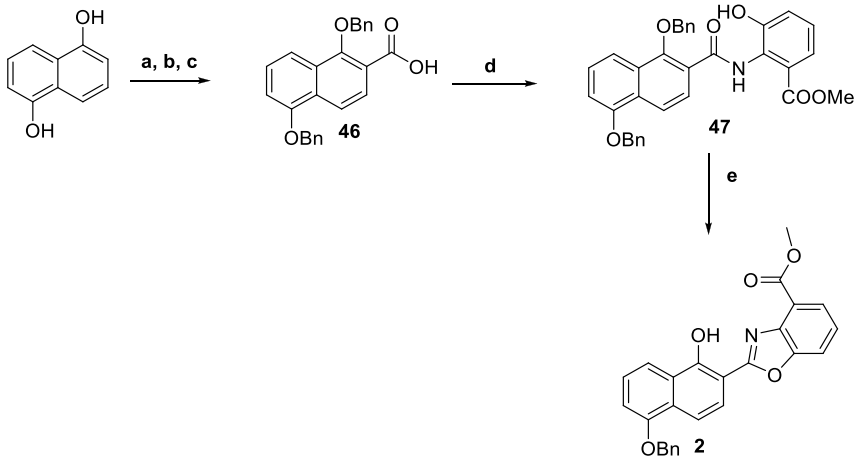

[a]Reagents, conditions, and yields: **(a)** Magnesium methyl carbonate, DMF, 140 °C, 55%. **(b)** BnCl, DMF, K_2CO_3, reflux, 78%. **(c)** NaOH, MeOH, reflux, 97%. **(d)** i) CDI, THF, R.T. ii) Methyl-3-hydroxyanthranilate, reflux 72%. **(e)** PPTS, m-xylene, 140 °C, 89%.

It was not initially clear which benzyl group had been removed during the last step in the synthesis of compounds **1** and **2**. Both compounds have a hydroxyl group correctly situated for excited state intramolecular proton transfer (ESIPT), giving rise to large Stoke shifts in their emission spectra (**Scheme 10**).[69]

Scheme 10. 2-(2'-hydroxyphenyl) benzoxazoles undergoes ESIPT.

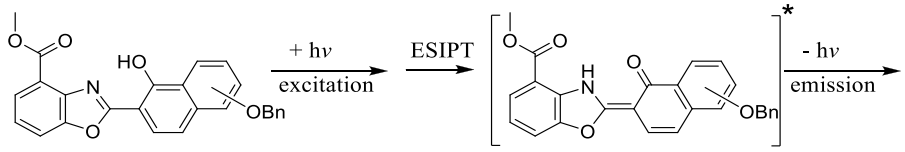

The emission spectra of compounds **1** and **2** were measured and compared to that of a negative control **48** (**Figure 25**), incapable of ESIPT (the synthesis of **48** follows the same methodology used for the synthesis of **1** and **2**, but starting from 1-hydroxy-2-

naphthoic acid). The results of the experiment show that compounds **1** and **2** ($\Delta\lambda_{max}$ =145 nm, and 145nm; respectively) exhibit large Stoke shifts of magnitudes consistent with ESIPT. Negative control **48** showed a much smaller Stokes shift ($\Delta\lambda_{max}$ = 43 nm), confirming the structure of target compounds **1** and **2**.

Figure 25. Negative control **48**, incapable of ESIPT, used in fluorescence experiments to confirm the structure of target compounds **1** and **2**.

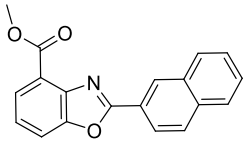

48

E. Biological Results and Discussion

Potential inhibition of the helicases of *Flavivirdae* viruses hepatitis c, Japanese encephalitis (JEV), and dengue (DENV) was investigated for compounds **1** and **2** using previously described methods.[107,108] Neither of the compounds inhibit JEV or DENV helicases (IC_{50}>700μM) (data not shown). Importantly, both of the compounds did inhibit the activity of the HCV helicase with a DNA substrate, with low micromolar IC_{50} values (**Table 6**, **Figure 26**).

Table 6: Helicase inhibition and viral replication inhibition data for **1** and **2**.

Compound	Helicase[a]		Replicon[c, d]		
	DNA	RNA			
	$IC_{50}(\mu M)^b$	$IC_{50}(\mu M)^b$	$EC_{50}(\mu M)^e$	$CC_{50}(\mu M)^f$	SI_{50}^g
1	2.6	20	0.54	>20	>37
2	3.8	20	2.1	>20	>10

a. Strand separation of radiolabeled oligonucleotides was monitored using gel electrophoresis. b. The concentration of compound required to inhibit 50% of helicase activity. c. Experiments were carried out at Southern Research Institute, Frederick, MD. d. Results are the averages of 2-4 independent dose-response experiments using a combination of luciferase reporter-based and RNA (qRT-PCR) assays. e. The concentration of compound that inhibits 50% of viral RNA replication. f. The concentration of compound that kills 50% of the cells. g. The ratio of CC_{50} to EC_{50}.

Figure 26: Inhibition of the unwinding activity of HCV helicase using DNA substrate. Strand separation of radiolabeled oligonucleotides was monitored using gel electrophoresis. UK-1 (■), **1** (▲), and **2** (●). Results presented are representatives of three independent experiments.

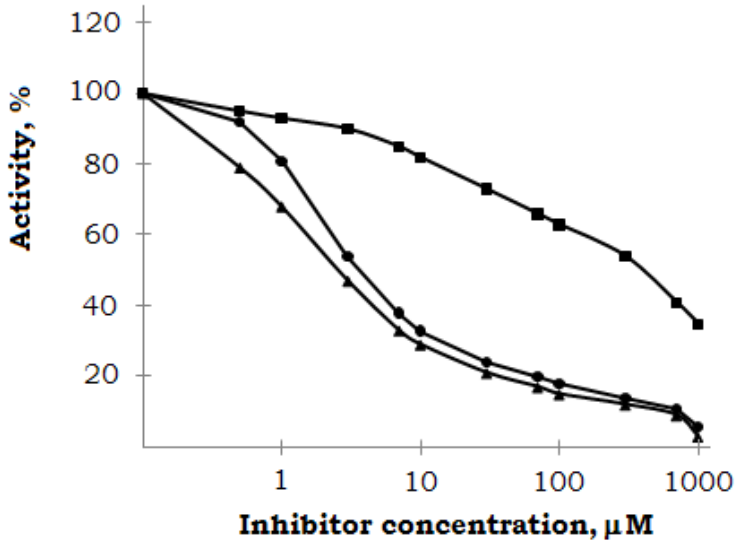

Both **1** and **2** are also active using an RNA substrate, albeit slightly less effective (IC_{50}= 20µM). Neither of the compounds inhibit the ATPase activity of the HCV helicase

(IC_{50}>1200 μM), eliminating this as a possible mechanism of action. In addition, compounds **1** and **2** do not affect the gel mobility of RNA, suggesting inhibition results from direct helicase interaction, rather than simple nucleic acid binding (**Figure 27**). The compounds were also screened against the HCV RNA-dependent RNA polymerase, NS5B. Very little inhibition was observed (inhibition ≤ 30% at 100μM; data not shown), eliminating this as a possible mechanism of action.

Figure 27. Gel shift assay using the EcoRI-digested pT7-7 plasmid in the presence of inhibitors UK-1 (lanes 1-3), **2** (lanes 4-6), **1** (lanes 7-9), without inhibitor (lane 13), and in the presence of the RNA intercalator epirubicin (lane 14).[a]

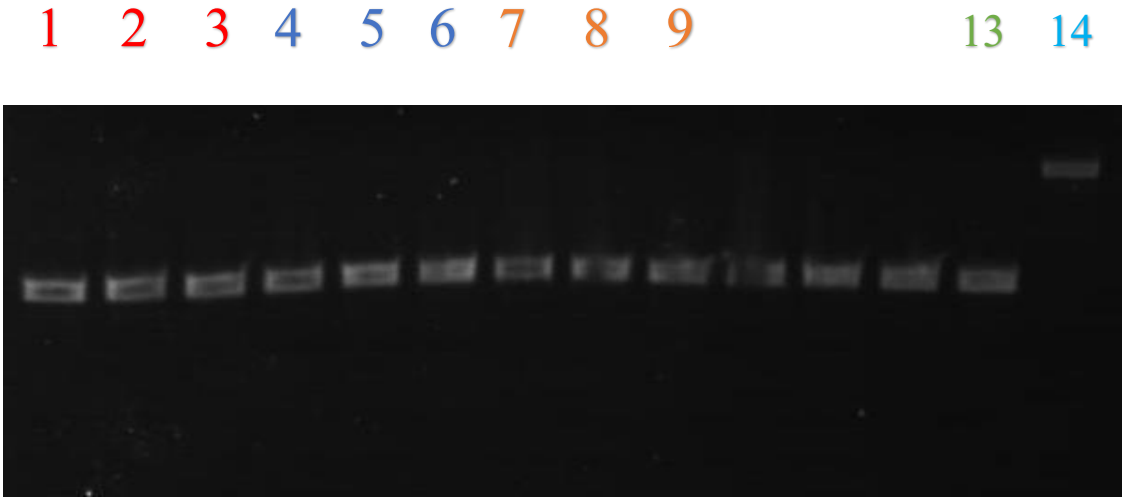

[a] Lane numbers containing compounds not included in this document were omitted for clarity.

To determine if the compounds were active against HCV replication in cells, they were screened in a replicon assay (**Table 6**). Quite interestingly, both **1** and **2** were active, with EC_{50} of 0.54 μM and 2.1 μM, respectively. Compounds **1** and **2** exhibit cell toxicity values greater than 20 μM, giving selectivity indices greater than 37 and 10, respectively.

F. Conclusions and Future Work

The HCV NS3 helicase is an essential protein for viral replication and is not currently targeted by the FDA approved therapeutic options. Two HCV helicase inhibitors (**1** and **2**) have been identified which are highly selective over the closely related helicases of DENV and JEV. These compounds show activity in whole cells and exhibit minimal cytotoxicity. It has been speculated that inhibition is a result of direct interaction with the helicase, as neither ATPase inhibition nor direct RNA binding is observed. The compounds are also ineffective against the NS5B RNA polymerase. Future work is currently underway to identify the binding site within the NS3 helicase and, using structure-based drug design, further improve upon inhibitor efficacy.

Chapter 4: Identifying an Inhibitor Binding Pocket Within the HCV NS3 Helicase

A. Photoaffinity Labeling: Overview

Identifying and analyzing the interactions between a ligand and a macromolecule is essential to the understanding of how drugs function. Knowledge of the location and structure of an inhibitor binding pocket within its substrate, allows for structure-based drug design which can lead to the development of more effective inhibitors. Historically, the most common technique for gathering this information has been X-ray crystallography. However, this technique is dependent upon the ability to grow crystals of the ligand-substrate complex which can be extremely difficult in many cases. Photoaffinity labeling is an increasingly useful technique for identifying a ligand's binding site, with no prior knowledge of its location, that has revolutionized this field.[102] In this process, a photoreactive functional group is synthetically introduced into a ligand/inhibitor and the ligand is incubated with its substrate. Upon irradiation of the inhibitor-substrate complex, the photoreactive group generates a highly unstable species which covalently inserts into the target macromolecule, irreversibly linking the bioactive inhibitor to its receptor. After the location of the receptor within the target has been identified using chromatography and mass spectrometry, molecular modeling can be used to elucidate the structure of the binding pocket. This technique has been used to identify numerous inhibitor binding sites, inhibitor-receptor interactions, unknown enzyme

targets, as well as amino acid residues at protein-protein and protein-lipid interfaces.[103-105]

An ideal photoreactive group should have a number of features.[103-105] The functional group should be relatively small in size, such that the photoactivatable analog has a close resemblance to the original inhibitor, with a similar affinity for the respective substrate. The reactive group should be relatively stable prior to activation, for ease of handling and synthesis. Irradiation, at a wavelength suitable for working with biological systems (>300nm), should generate a short-lived and highly reactive species that forms stable covalent bonds with molecules in close proximity. Ideally, the activated intermediate should be capable of covalently linking to a broad range of functional groups. Although some photoreactive groups are more successful than others, no single group meets all of these criteria.[103-105] There are three major classes of commonly used photoactivatable groups in photoaffinity labeling experiments: aromatic azides, benzophenones, and diazirines (**Figure 28**).[103] Each group has both positive and negative attributes as photoaffinity labeling agents.[103-105]

Figure 28. Commonly used photoactivatable groups for photoaffinity labeling: (left) aryl azides, (middle) benzophenones, and (right) diazirines.

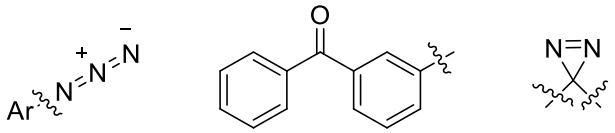

Aryl azides dispel nitrogen gas and generate nitrenes upon irradiation. Although relatively easy to synthesize, nitrenes have been shown to require activation at wavelengths damaging to biological systems (250 nm). Additionally, nitrenes are prone

to rearrangement upon irradiation to nonreactive and/or electrophilic species.[106,107] These rearrangement products both decrease labeling efficiency and lead to nonspecific labeling by nucleophilic amino acid residues. Benzophenones are activated at much longer wavelengths (~350 nm) and form triplet-state carbonyls.[103-107] This photoreactive group is very stable prior to irradiation and is also quite easy to synthesize. However, benzophenones are very large and such an inhibitor modification can significantly alter the affinity for a respective substrate. Additionally, this photoreactive group has been shown to require very long irradiation times which can lead to nonspecific labeling.[103, 108]

Diazirines are the smallest of the commonly used photoactivatable groups and their success in photoaffinity labeling has drastically increased in the past decade.[103-105] Upon irradiation, diazirines generate highly reactive and short-lived carbenes with lifetimes in the range of nanoseconds (**Figure 29**, path a).[109,110]

Figure 29. Radiative processes reported for trifluoromethyl aryldiazirines. The starting diazirine can generate the desired carbene *via* path **A** or can form the rearrange diazo-intermediate *via* path **B**. The diazo compound can react with nucleophiles (path **C**) or decompose to the orginal desired carbene (path **D**).

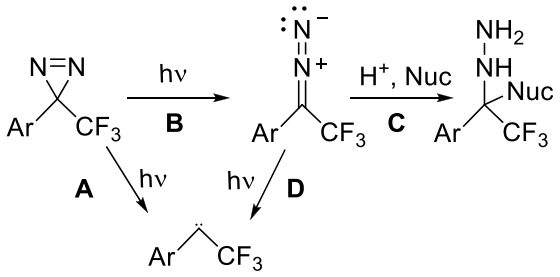

Carbenes are bivalent carbon species and can exist in two different states based on the arrangement of the two non-bonding electrons; the electrons can be spin-paired in the same orbital resulting in singlet carbenes, or they can be in different orbitals with parallel

spins, giving triplet-state species.[105] It has been shown that the singlet-state carbenes are the more reactive species, capable of inserting into almost any C-H bond, including traditional unreactive alkyl bonds. The majority of solution-phase reactivity has been shown to come from the singlet-state carbene.[105] Electron-donating substituents attached to the diazirine carbon have been shown to stabilize the singlet-state, which causes undesired rearrangements to linear diazo-species (**Figure 29**, path b).[103,105] The diazo-product has an increased lifetime, which results in decreased photoaffinity labeling efficiency. These long-lived diazo-products have also been shown to react with acidic amino acid residues, generating an electrophilic species (**Figure 29**, path c). This can result in nonspecific modification at nucleophilic residues of the substrate, following diffusion from the binding pocket.[105,111,112]

Trifluoromethyl aryldiazirines (**Figure 29**) have been shown to both decrease the formation of the linear diazo-product and decrease the extent to which the diazo-product reacts in a manner that results in nonspecific labeling.[105,111,112] It has been shown that the rearranged diazo-product resulting from irradiation of trifluoromethyl aryldiazirines will readily decompose to the original desired carbene (**Figure 29**, path d).[103,112] Trifluoromethyl aryldiazirines are quite stable to both high and low pH, and also elevated temperature, and nucleophilic reagents.[111] This photoreactive group is also stable to visible light, so there is no need to work with them in the dark.[111] In a recent review of photoaffinity labeling publications, 72% of the photoreactive analogs use a trifluoromethyl aryldiazirine.[103]

Our first attempt to identify the binding location within the NS3 helicase for lead helicase inhibitors **1** and **2** (**Figure 30**) was *via* crystal growth with the purified protein,

through an in-house collaboration with Dr. Elsa Garcin. Unfortunately, these efforts have yet to yield crystals. We have since turned to the photoaffinity labeling approach; the trifluoromethyl aryl photoreactive group was chosen to identify the binding site within the HCV NS3 helicase, for novel inhibitors **1** and **2**.

Figure 30. Previously described (Chapter 3) HCV NS3 helicase inhibitors **1** and **2**.

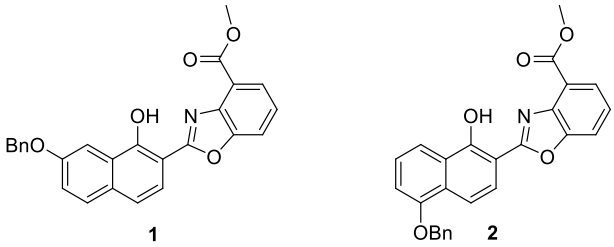

B. A Photoactivatable HCV NS3 Helicase Inhibitor: Design

As previously described in Chapter 2, naphthol analog (**41**) was synthesized and screened as an HCV replication inhibitor (**Figure 31**).

Figure 31. Naphthol analog **41**.

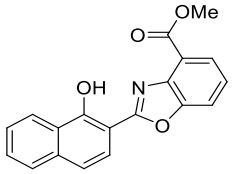

Naphthol **41** was additionally screened in an NS3 helicase assay, where the compound proved quite ineffective compared to leads **1** and **2** (**Table 7**). The benzyl ether at the 5- or 7- positions of the naphthol ring significantly increases the potency of these compounds against the NS3 helicase. It was therefore hypothesized that the benzyl ring is in close proximity to the helicase in its respective binding pocket. Thus, a

photoactivatable inhibitor analog was designed with the photoreactive trifluoromethyl diazirine conjugated to the benzene ring of the benzyl ether (**Figure 32**).

Table 7. HCV NS3 helicase inhibition data for leads **1** and **2**, as well as analog **41**.

Compound	**HCV Helicase**[a]	
	DNA	RNA
	$IC_{50}(\mu M)$[b]	$IC_{50}(\mu M)$[b]
1	2.6	20
2	3.8	20
41	**540**	**590**

a. Strand separation of radiolabeled oligonucleotides was monitored using gel electrophoresis. b. The concentration of compound required to inhibit 50% of helicase activity.

Figure 32. Lead compound **1** and the photoactivatable NS3 helicase inhibitor analog **64**.

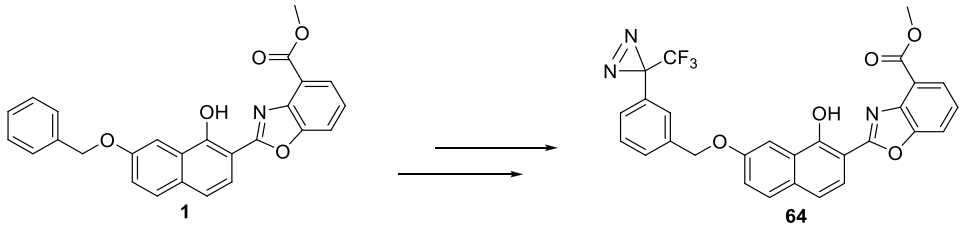

C. A Photoactivatable HCV NS3 Helicase Inhibitor: Synthesis

The synthesis of photoactivatable NS3 helicase inhibitor analog **64** utilizes lead compound **1** as a key starting material. However, a synthetic route different from that described in Chapter 3 was employed for the synthesis of **1,** which can be found in **Scheme 11**. This began with the demethylation of commercially available 7-

methoxytetralone using aluminum chloride, which gave 7-hydroxytetralone **48**. *O*-Benzylation using benzyl bromide and potassium carbonate gave benzyl ether **49**. Enolate formation using sodium hydride, followed by a crossed-Claisen reaction with diethylcarbonate gave beta-ketoester **50**, which was brominated using pyridinium tribromide yielding **51**. Aromatization of **51** using DBU in ACN gave ester **52**, which was then hydrolyzed to **53**. Acid activation of **53** with CDI and subsequent coupling to methyl-3-hydroxyanthranilate, gave intermediate amide **54**. PPTS mediated cyclization of **54** gave lead compound **1**.

Scheme 11. A new route to lead NS3 helicase inhibitor **1**.[a]

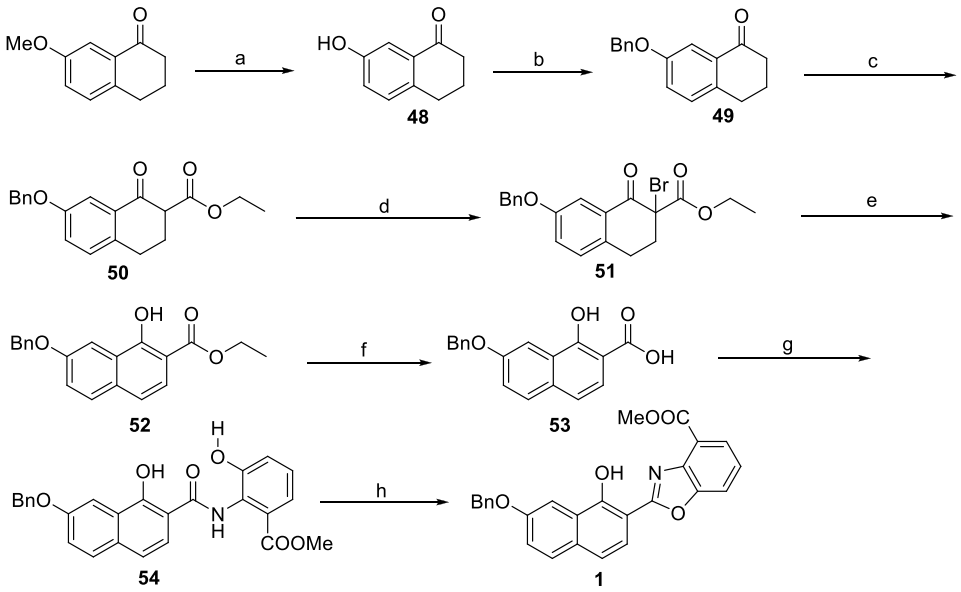

[a]Reagents, conditions, and yields: **(a)** $AlCl_3$, toluene, 99%. **(b)** BnBr, K_2CO_3, acetone, reflux, 98%. **(c)** NaH, diethylcarbonate, THF. **(d)** Pyridinium tribromide, AcOH. **(e)** DBU, ACN, reflux 75% (three steps). **(f)** KOH, THF, reflux, 99%. **(g)** (i) CDI, THF. (ii) Methyl-3-hydroxyanthranilate, reflux, 45%. **(h)** PPTS, *p*-xylene, reflux, 86%.

The photoreactive trifluoromethyl aryldiazirine was synthesized as the corresponding benzyl bromide **60**, as previously described (**Scheme 12**).[103,112] This began with Grignard formation from commercially available *m*-bromotoluene. Subsequent trifluoroacetic acid addition gave trifluoromethyl ketone **55**. Oxime formation using hydroxylamine hydrochloride in pyridine and ethanol gave **56**. The oxime was then *O*-tosylated using tosyl chloride, diisopropylethylamine, and catalytic dimethylaminopyridine to give **57**. Addition of liquid ammonia in diethyl ether at -70°C in a bomb, gave intermediate diaziridine **58**, which was then oxidized with iodine and trimethylamine to yield diazirine **59**. Bromination of **59** using *N*-bromosuccinimide and azobisisobutyronitrile provided target photoreactive benzyl bromide **60**.

Scheme 12. Synthesis of photoreactive trifluoromethyl aryldiazirine as the corresponding benzyl bromide **60**.[a]

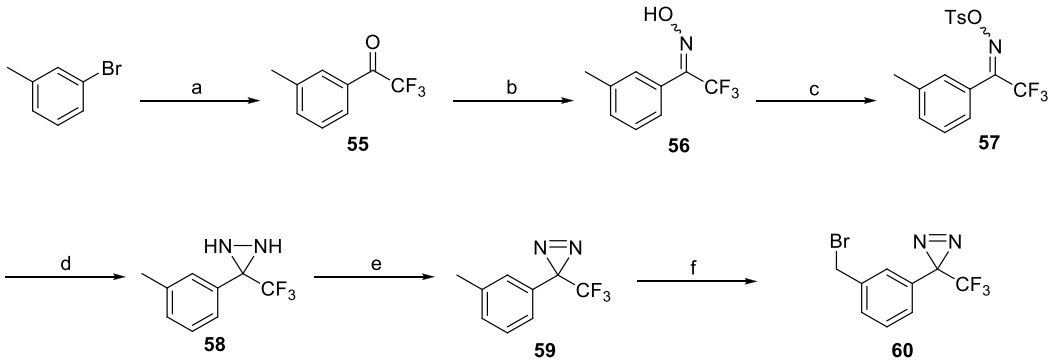

[a]Reagents, conditions, and yields: **(a)** (ii) Mg(s), ultra-sonication, ether. (ii)Trifluoroacetic acid. **(b)** hydroxylamine HCl, pyridine, EtOH, 81% (two steps). **(c)** TsCl, DIEA, DMAP, DCM, 85%. **(d)** NH_3(l), ether, -70°C-RT, (85%). **(e)** I_2(s), TEA, DCM. **(f)** NBS, AIBN, CCl_4.

For alkylation of lead compound **1** at the 7-hydroxyl with photoreactive bromide **60**, a synthetic route was devised where the 1-position hydroxyl of **1** was first orthogonally protected as the corresponding triflate (**Scheme 13**). Addition of triflic anhydride and trimethylamine to **1** gave triflate **61**. Selective deprotection of the 7-hydroxyl using thioethane and boron trifluoride etherate gave intermediate triflate **62**. Alkylation of **62** with photoreactive bromide **60** and potassium carbonate in acetone, provided **63**, although pure compound was unable to be obtained. Selective deprotection of the 1-position hydroxyl using tetrabutylammonium fluoride gave target photoactivatable inhibitor analog **64**. However, following deprotection of **64**, a small amount (3%, based on ^{1}HNMR) of unknown impurity was unable to be removed from the desired product. (It was later found this may have been a result of acidic NMR solvent, however another route to **64** had already been investigated).

Scheme 13. Triflate-route to photoactivatable target **64**.[a]

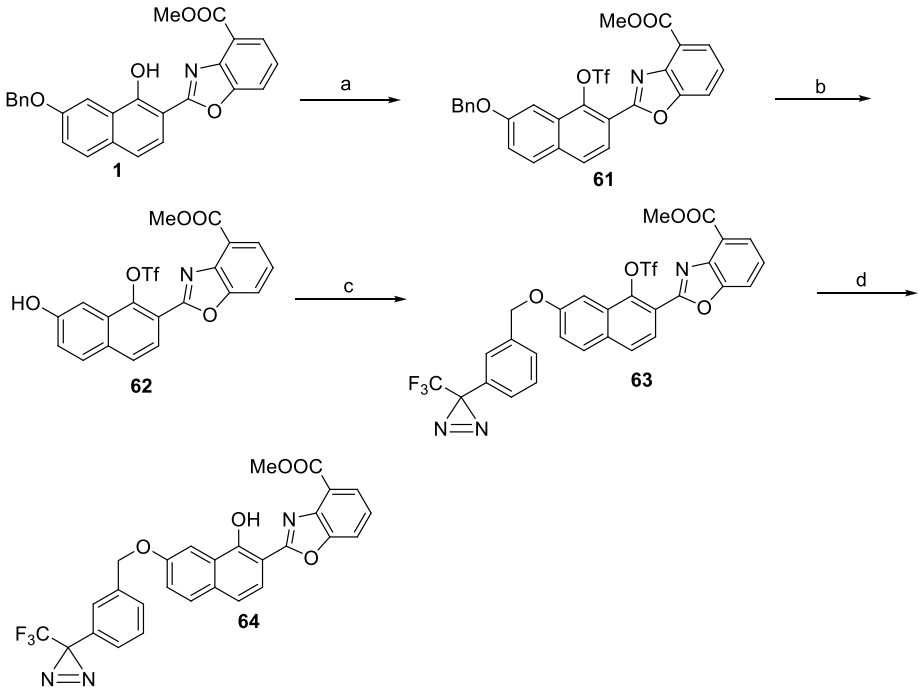

[a]Reagents, conditions, and yields: **(a)** $Tf(O)_2$, TEA, DCM, 0°C, 95%. **(b)** EtSH, BF_3 Et_2O, DCM, 70%. **(c)** K_2CO_3, **60**, acetone, reflux. **(d)** TBAF, THF, ~18% (two steps, slightly impure).

As such, a new route was designed for the synthesis of **64**, again starting from the lead inhibitor **1** (**Scheme 14**). Hydrogen gas (60 PSI) and a Pd/C (10%) catalyst in ethanol was used for deprotection of the 7-position hydroxyl. This benzyl ether was surprisingly stable, requiring an increased pressure of hydrogen, mass of Pd/C, and reaction time (>48 hours). The resulting diol **65** was alkylated using one equivalent of the photoreactive bromide **60** and potassium carbonate in DMF:acetone (1:3). It was hypothesized that some degree of selectivity for alkylation of the 7- versus the 1-hydroxyl may be achieved, due to the steric hindrance of the heterocycle about the 1-position. This route was successful in providing the pure photoactivatable compound **64**, albeit in low yield.

Scheme 14. Successful route to the synthesis of photoactivatable inhibitor analog **64**.[a]

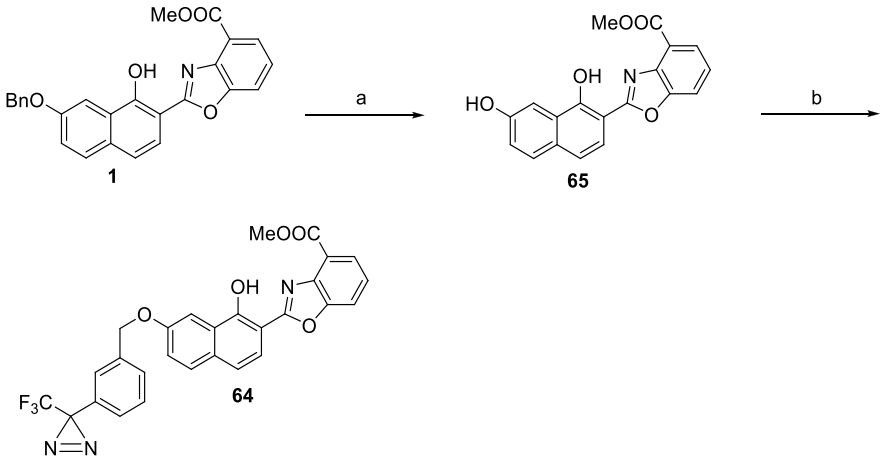

[a]Reagents, conditions, and yields: **(a)** H_2, 60 PSI, EtOH, 71%. **(b)** K_2CO_3, **60**, acetone:DMF (3:1), reflux, 10%.

D. A Photoactivatable HCV NS3 Helicase Inhibitor: Helicase Activity and Photolytic Properties

Following synthesis, it was necessary to determine if the photoactivatable analog retains activity against the HCV NS3 helicase. As such, **64** was sent to a collaborator, Dr. Andrea Baier at the John Paul II Catholic University of Lublin, for testing in an NS3 helicase assay (the same assay conditions were used for the testing of **1** and **2**). It was confirmed that **64** is similarly active as **1** against NS3h and is thus a suitable photoreactive inhibitor analog to probe the binding pocket within the enzyme (**Table 8**).

Table 8. NS3h inhibition data for the photoactivatable inhibitor analog **64** and lead **1**.

Compound	**HCV Helicase**[a]	
	DNA	RNA
	$IC_{50}(\mu M)$[b]	$IC_{50}(\mu M)$[b]
1	2.6	20
64	3.8	16

a. Strand separation of radiolabeled oligonucleotides was monitored using gel electrophoresis. b. The concentration of compound required to inhibit 50% of helicase activity. The results are an average of 2-3 independent trials.

Photolysis experiments were performed to confirm photoactivatable inhibitor analog **64** is indeed reactive upon exposure to irradiation of a suitable wavelength. A solution of **64** in methanol was irradiated using a mercury lamp with a 320nm cutoff filter, for varying lengths of time (1-60 minutes) and monitored *via* UV-VIS spectroscopy (**Figure 33**).

Figure 33. UV-VIS Spectra monitoring the photolysis of **64** over 60 minutes of irradiation.[a]

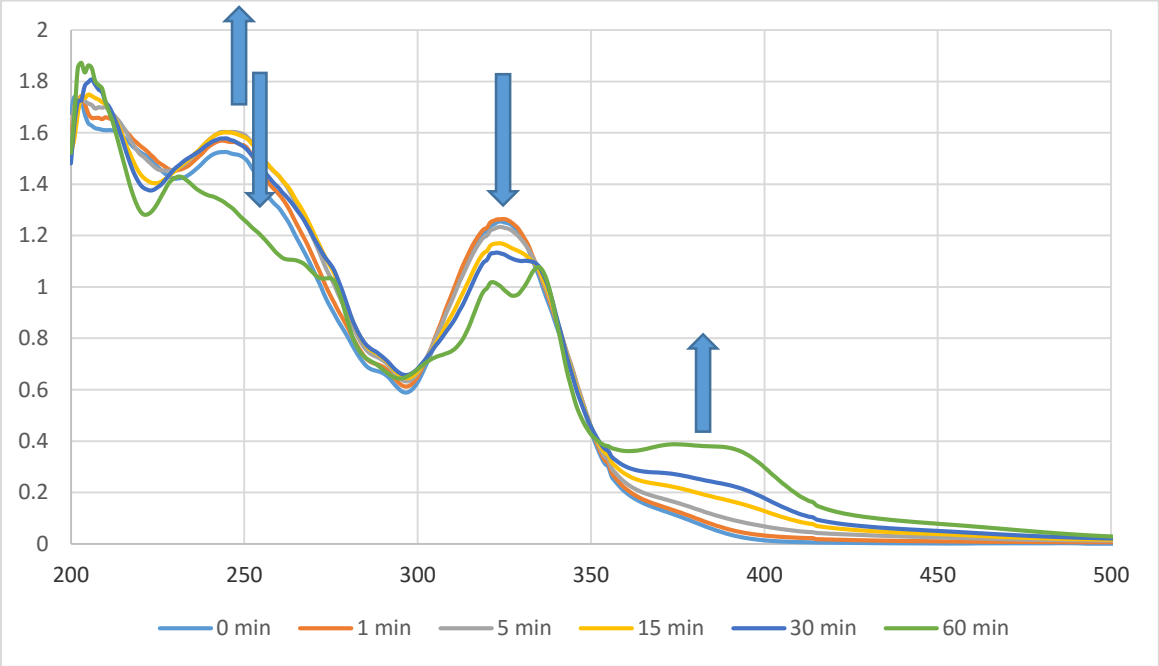

[a] Additional photolysis conditions: A mercury lamp equipped with a 320nm cutoff filter, held ~6cm from the sample, was used for irradiation. A solution of **64** in methanol (2.5mL, 50μM) was held at constant temperature (~23°C) during irradiation using a water bath.

The λ_{max} at ~325nm, corresponding to the starting material diazirine, decreases upon irradiation as the desired carbene is formed.[112,113] Consistent with the literature, the λ_{max} at ~240nm initially increases upon irradiation. This has been attributed to the previously discussed diazo-rearrangement product (see **Figure 29**).[113] However, as irradiation time increases, the diazo intermediate decomposes to give the desired carbene, as indicated by the eventual decrease in this maximum.[113]

To ensure a carbene, capable of covalent insertion into a substrate, was being formed upon irradiation, **64** was analyzed by mass spectrometry (MS) both before and after the previously described photolysis experiment (**Figure 34**). Prior to irradiation, the two

major peaks in the spectrum correspond to the molecular weight of **64** (MW=533.1 g/mol) complexed with a sodium ion (556.2 g/mol) or a potassium ion (572.2 g/mol).

Figure 34. Mass spectrum (zoomed in for clarity) of photoactivatable compound **64** in methanol, prior to irradiation. The two major peaks (shown) correspond to **64** (MW=533.12 g/mol) complexed with Na^+ (556.2 g/mol) or with K^+ (572.2 g/mol). [a]

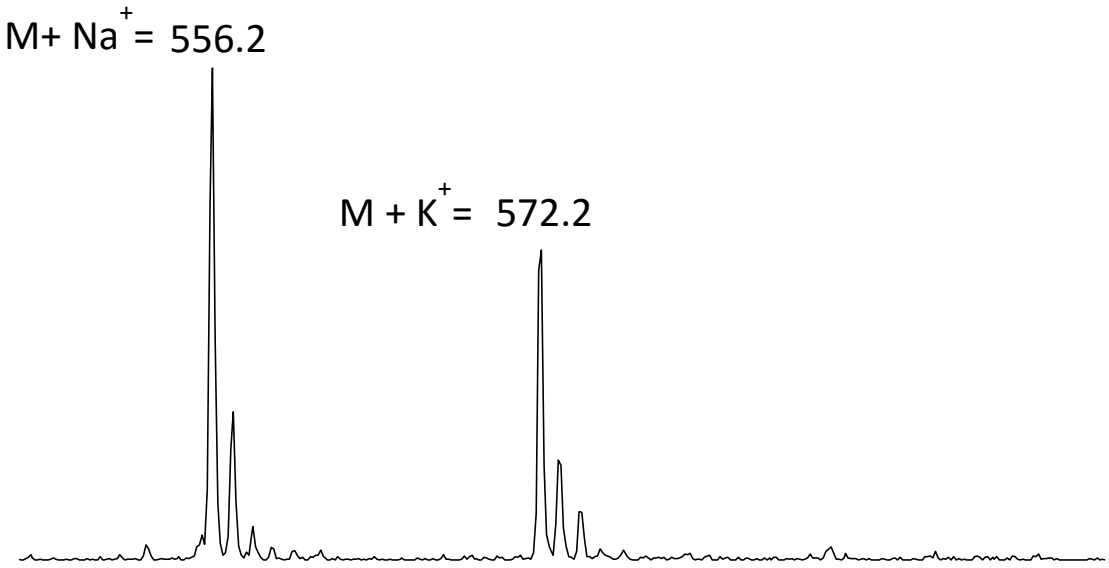

[a] Experiment details and conditions: A solution of **64** (50μM in methanol) was injected into a Bruker Amazon Speed Ion Trap equipped with an Apollo II Electrospray Ionizer.

Following irradiation of the same solution of **64** with a mercury lamp for 60 minutes followed by MS analysis, the two main peaks now correspond to the molecular weight of the carbene covalently (MW=505.1 g/mol) inserted into methanol (MW=537.1 g/mol), similarly complexed with a sodium ion (560.2 g/mol) or a potassium ion (576.2 g/mol) (**Figure 35**).

Figure 35. Mass spectrum (zoomed in for clarity) of photoactivatable compound **64** in methanol, after 60 minutes of irradiation. The two major peaks (shown) correspond to the carbene generated from **64** covalently inserted into methanol (MW=537.1 g/mol), complexed with Na^+ (560.2) or with K^+ (576.2).

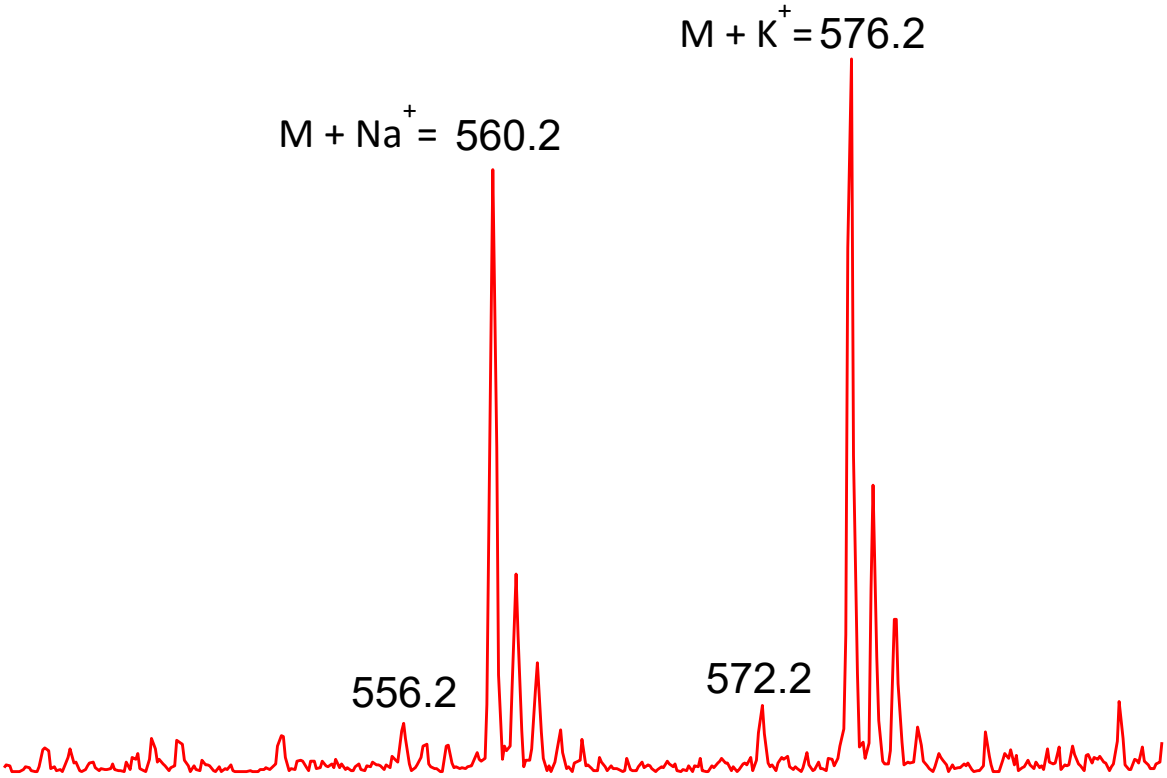

[a] Experiment details and conditions: A solution of **64** (50μM in methanol) was irradiated for 60 minutes with mercury lamp at constant temperature (~23°C). The solution was then injected into a Bruker Amazon Speed Ion Trap equipped with an Apollo II Electrospray Ionizer.

The carbene covalent-insertion product could be one of two isomers, resulting from carbene insertion into methanol at one of the carbon-hydrogen bonds (**Figure 36**, left) or the oxygen-hydrogen bond (**Figure 36**, right). This experiment confirms the photoactivatable analog is indeed reactive with desired carbene formation, following irradiation using a 320nm cutoff filter. Importantly, the carbene is capable of covalent insertion into a substrate.

Figure 36. Two possible carbene covalent insertion products following the photolysis of **64** in methanol. The carbene can insert into methanol at one of the carbon-hydrogen bonds (left) or the oxygen-hydrogen bond (right).

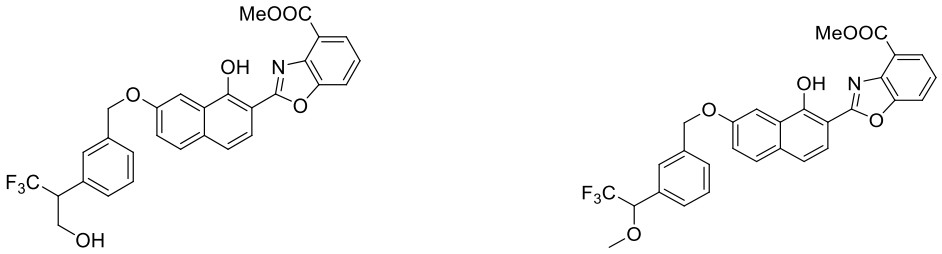

E. Photoaffinity Labeling of HCV NS3 Helicase: Approach

The first step in our photoaffinity labeling approach is incubation of the photoreactive inhibitor analog (**64**) with the protein of interest (NS3h), where the inhibitor should coordinate to its respective binding pocket. The inhibitor-protein complex is then irradiated with a mercury lamp for one hour at 0°C. Ideally, the photoreactive analog will covalently insert into the binding pocket. NS3h is then enzymatically digested; resulting peptides are separated using a nanoflow HPLC and subsequently analyzed by MS/MS on a Bruker 12T Apex IV Fourier Transform ICR equipped with a nano-electrospray ionizer. The resulting spectra are then analyzed using Peaks® software, which systematically identifies MS/MS peptide fragmentation patterns consistent with a preprogrammed protein sequence and enzymatic digest. Peaks® provides the user with a percent protein sequence coverage, which corresponds to the number of peptides identified with high confidence divided by the total number of peptides that should be found based on the enzymatic digest. The program is also capable of identifying peptide(s) covalently linked to an inhibitor based on a change in mass, thus identifying the binding pocket within the protein. Once modified amino acid residues have been identified, molecular modeling

(likely through a collaboration) can be used to identify interactions between the inhibitor and protein within the binding pocket.

Prior to photoaffinity labeling NS3h, it was first necessary to optimize the denaturation and enzymatic digestion conditions for the protein. A poor enzymatic digest (large number of missed cleavages), would likely result in a low percent protein sequence coverage; Peaks® identifies peptide fragmentation patterns consistent with an optimal enzyme digest. In addition, a poor digest will lead to larger peptide fragments due to missed cleavages. Peptides of large mass are increasingly difficult to identify using MS/MS fragmentation patterns.

For denaturation of NS3h, Rapigest® (a surfactant), was used along with standard heating protocols. Disulfide bonds were subsequently reduced with beta-mercaptoethanol (BME). These conditions resulted in 20% protein sequence coverage by Peaks® (following HPLC separation and MS/MS analysis). In an attempt to increase coverage, thiols were alkylated using iodoacetamide following reduction. However, this did not change the results. Next, urea was used for denaturation instead of the surfactant. Once again, Peaks® only identified 20% of the digested protein. Changing the denaturing reagent to guanidine hydrochloride similarly resulted in no increase of coverage. Interestingly, when guanidine hydrochloride was used along with dithiothreitol (DTT) and iodoacetamide, the sequence coverage increased to 36%. In an attempt to identify additional peptide fragments, chymotrypsin was used for digestion. Using the previously optimized denaturing conditions, the chymotrypsin digest similarly resulted in 36% sequence coverage. Unfortunately, a large number of peptide fragments identified in the

chymotrypsin digest significantly overlap with those found using trypsin. As a result, the combined protein sequence coverage was only increased to 49% (**Figure 37**).

Figure 37. Snapshot of combined NS3h sequence coverage (49%) using Peaks®. Both chymotrypsin and trypsin were used for enzymatic digestion. Peptide fragments underlined in blue were identified by Peaks® with low probability of error. Fragments underline in grey, are *de novo* identified sequences which are only a partial match of the desired peptide fragment; *de novo* fragments are not included in the total percent coverage. Post-translational modifications are represented by 'd' (deamidation), 'c' (acetamide alkylated cysteine), and 'o' (oxidation).

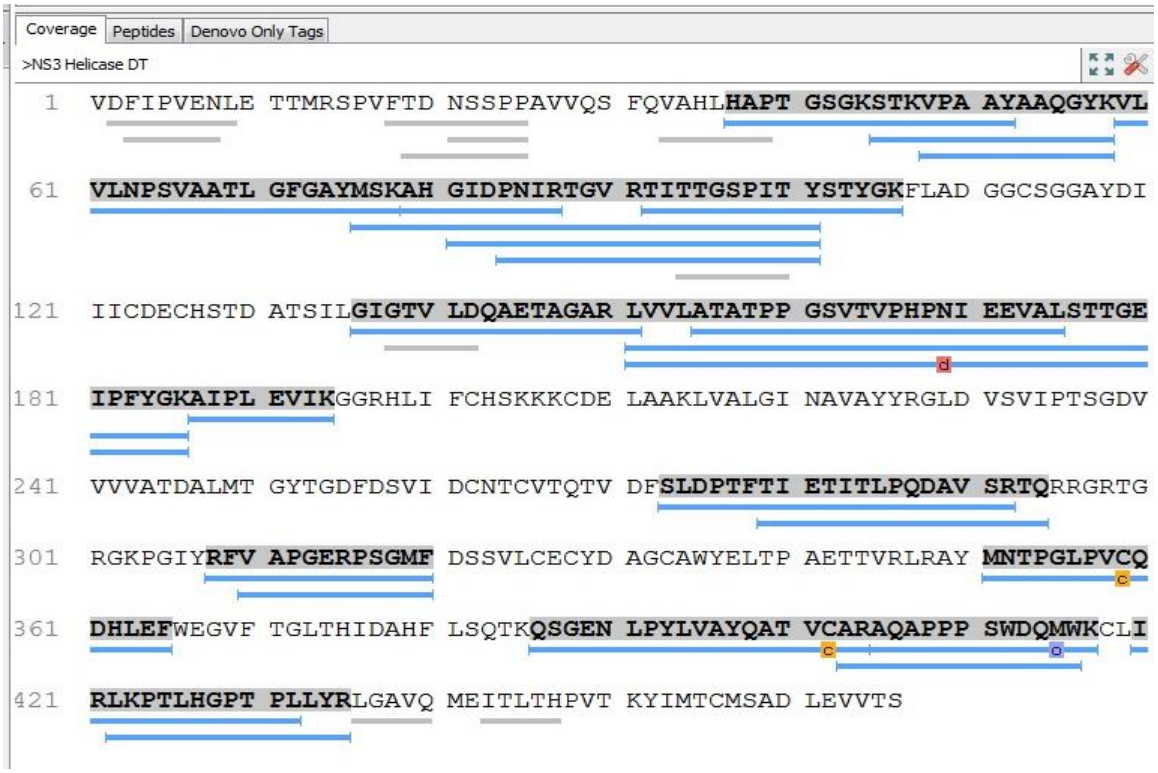

Although the sequence coverage was not ideal, the photoaffinity labeling experiment was conducted with NS3h (~40 μM) and various concentrations (0.5-500 μM) of photoaffinity probe **64**. Following irradiation of the inhibitor-protein complex, the enzyme was denatured and digested using the previously described conditions which provided the highest percent sequence coverage. At all inhibitor concentrations tested,

Peaks® was only able to identify a maximum of 36% protein coverage in both the trypsin and chymotrypsin digests, for a combined coverage of 49%. Unfortunately, no inhibitor-bound peptides were identified. It is likely that the covalent modification lies somewhere in the 51% of unidentified protein.

F. Future Work

In order to increase the probability of identifying inhibitor-bound peptide(s), the protein sequence coverage using Peaks® needs to be increased. This can likely be accomplished through further optimization of the denaturing/digesting conditions of NS3h. Using the described conditions, Peaks® has only identified two peptides that contain cysteine. It is it therefore hypothesized that the conditions used to denature the protein, and subsequently reduce/alkylate cysteine residues, are inefficient. Intact disulfide bonds could lead to large undigested protein segments and complicate the peptide identification process. To further increase protein sequence coverage, other enzymes can be used for digestion in hopes of identifying peptide fragments that do not overlap with those found using trypsin and chymotrypsin.

Chapter 5: Experimental

A. General: *Chemistry Methods*

Proton and carbon nuclear magnetic resonance spectra (^{1}H NMR and ^{13}C NMR) were obtained using a JEOL ECX400 spectrometer. Abbreviations used for peak multiplicity in ^{1}H NMR data are: s=singlet, bs=broad singlet, d=doublet, dd=doublet of doublets, t=triplet, td=triplet of doublets, q=quartet, m=multiplet. High resolution mass spectra were obtained on a Bruker Apex IV ITCR spectrometer. Low resolution mass spectra were obtained on a PerkinElmer AxION 1 DSA TOF or a Bruker Amazon Speed Ion Trap equipped with an Apollo II Electrospray Ionizer.

Thin layer chromatography on silica gel was performed using EMD 60F glass plates. Fisher Scientific silica gel 60 (230-400 mesh) was used for flash chromatography. ACS grade solvents were used for chromatography without further purification.

Reactions ran "under inert atmosphere" were conducted under argon gas. Reaction vessels were arranged so that the system could be flame dried *in vacuo* and subsequently filled with argon using a mercury bubbler, and left under positive argon pressure. Anhydrous solvents were used in all reactions ran under inert atmosphere. THF was purchased from Fisher Scientific, distilled from sodium metal, and stored over 4 Å molecular sieves under argon. Anhydrous dioxane was purchased from Acros Organics. Anhydrous chloroform was obtained *via* distillation following stirring over molecular sieves (4 Å, powder). All other solvents were purchased from Fisher Scientific and used without further purification. Deuterated chloroform was purchased from Acros Organics.

Deuterated DMSO was purchased from Cambridge Isotope Laboratories Inc. All other chemicals were obtained from commercial sources and used without further purification.

"Concentrated under reduced pressure" refers to the removal of solvent on a rotary evaporator at 40-55˚C and subsequent drying under lower pressure with a direct drive high-vacuum pump. All percent yields are based on ^{1}H NMR spectra.

B. Synthesis

i. Chapter 2

2-Benzyloxybenzoic acid (5). K_2CO_3 (5.01g, 36.4 mmol) was added to a solution of salicylic acid (2.00g, 14.5 mmol) in acetone (26.4mL) under inert atmosphere. The slurry was refluxed for 45 minutes and cooled to room temperature. A solution of benzyl bromide (4.34mL, 36.3 mmol) in acetone (16.5mL) was added slowly over a ten minute period. The reaction mixture was refluxed for 36 hours and then cooled to room temperature. Solids were removed via filtration and washed with CH_2Cl_2 (2x10mL). The filtrate was diluted with 80mL CH_2Cl_2 and transferred to a separatory funnel. The solution was washed with H_2O (2x100mL) and brine(100mL), dried with $MgSO_4$, filtered, and concentrated under reduced pressure to give a pale yellow oil (5.67g). Crude benzyl-2-benzyloxybenzoate was used without further purification. ^{1}H NMR (400 MHz, $CDCl_3$) δ 7.85 (1H, dd, J=7.8Hz, J=1.8Hz), δ 7.27-7.45 (11H, m), δ 7.00 (2H, m), δ 5.34 (2H, s), δ 5.16 (2H, s). NaOH (1.74g, 43.5mmol) was dissolved in 21mL 90% EtOH(aq). The alkali solution was added to a flask containing 5.67g crude benzyl-2-benzyloxybenzoate. The reaction was refluxed for 20 hours. The reaction mixture was

cooled to room temperature and acidified to pH=1-2 with 50mL 1M HCl. The solution was transferred to a separatory funnel and extracted with EtOAc (3x75mL). The combined organic phases were extracted with saturated $NaHCO_3$ (3x100mL). The aqueous phase was acidified to pH=1-2 with 6M HCl and extracted with EtOAc (3x100mL). The combined organic phases were washed with brine (100mL), dried with $MgSO_4$, filtered, and concentrated under reduced pressure to give a yellowish brown oily solid (3.02g). Product was recrystallized from EtOAc:hexane to give 2.30g white crystalline solid (70% yield;two steps). ^{1}H NMR (400MHz, $CDCl_3$) δ 8.21 (1H, dd, J= 7.8Hz, J= 1.8Hz), δ 7.56 (1H, m), δ 7.37-7.45 (5H, m), δ 7.15 (2H, m), δ 5.30 (2H, s).

Methyl 2-((2-benzyloxybenzoyl)amino)-3-hydroxybenzoate (6). Methyl 3-hydroxyanthranilate (0.250g, 1.50 mmol) and **5** (0.512g, 2.24 mmol) were dissolved in chloroform (29.7mL) under inert atmosphere. Dichlorotriphenylphosphorane (1.79g, 5.39 mmol) was then added and the reaction mixture was refluxed 2.5 hours. The solution was cooled to room temperature and transferred to a separatory funnel with 30mL $CHCl_3$. The solution was washed with 4M HCl (2x25mL), saturated $NaHCO_3$ (2x 25mL), and brine (25mL), dried with $MgSO_4$, filtered, and concentrated under reduced pressure to give a brown oil with clumps of white solid. Crude product was purified via flash chromatography (100% CH_2Cl_2) to give 0.423g of a brown solid (76% yield). ^{1}H NMR (400 MHz, $CDCl_3$) δ 12.31 (1H, s), δ 9.25 (1H, bs), δ 8.26 (1H, dd, J=7.9Hz, J= 1.9Hz), δ 7.58 (1H, dd, J= 7.7Hz, J= 1.6Hz), δ 7.40-7.49 (3H, m), δ 7.26-7.34 (4H, m), δ 7.20 (1H, t, J= 8.2Hz), δ 7.08 (1H, J= 7.6Hz), δ 7.02 (1H, d, J= 8.4Hz), δ 5.47 (2H, s), δ 3.77 (3H, s).

Methyl 2-(2-benzyloxyphenyl)benzoxazole-4-carboxylate (7). Toluene (22.4mL) was added to a flask containing **6** (0.386g, 1.02mmol) and pyridinium *p*-toluene sulfonate (0.514g, 2.05mmol) equipped with a Dean-Stark trap. The reaction mixture was refluxed for 23 hours and then cooled to room temperature. The resulting slurry was transferred to a separatory funnel containing 50mL saturated $NaHCO_3$. The solution was extracted with EtOAc (3x50mL). Combined organic phases were washed with brine (50mL), dried with $MgSO_4$, filtered, and concentrated under reduced pressure to give a brown solid. Crude product was purified via flash chromatography (5% EtOAc in CH_2Cl_2) to give 0.336g desired compound as a yellow solid (91% yield). ^{1}H NMR (400 MHz, $CDCl_3$) δ 8.27 (1H, dd, J= 7.8Hz, J= 1.8Hz), δ 8.04 (1H, dd, J= 7.8Hz, J= 0.9Hz), δ 7.75 (1H, dd, J= 8.2Hz, J= 1.4Hz), δ 7.65 (2H, d, J= 7.8Hz), δ 7.50 (1H, m), δ 7.41 (3H, m), δ 7.32 (1H, m), δ 7.13 (2H, m), δ 5.30 (2H, s), δ 4.01 (3H, s).

Methyl 2-(2-phenyl)benzoxazole-4-carboxylate (3). Compound **7** (0.200g, 0.556 mmol) was shaken with Pd/C (10%, 0.0200g) in methanol (10mL) under 45 PSI of H_2 for 4 hours. Pd/C was removed *via* vacuum filtration through celite. The filtrate was concentrated under reduced pressure to give 0.144 g pure product as a yellowish-white solid (99% yield). ^{1}H NMR (400MHz, $CDCl_3$) δ 11.84 (1H, s), δ 8.09 (1H, d, J= 8.0 Hz), δ 8.05 (1H, dd, J= 7.6 Hz, J= 1.6 Hz), δ 7.82 (1H, d, J= 9.2 Hz), δ 7.48–7.44 (2H, m), δ 7.16 (1H, d, J= 8.0 Hz), δ 4.06 (3H, s). Previously characterized via ^{13}C and HRMS.[73]

2-(2-Phenyl)benzoxazole-4-carboxylic acid (8). NaOH (0.553 mL, 5M (aq)) was added to a solution of **3** (0.044 g, 0.163 mmol) in THF (1.1 mL) and the mixture was refluxed overnight. The reaction mixture was cooled to RT and concentrated under

reduced pressure. The remaining solids were resuspended in HCl (5 mL, 1M) and isolated *via* vacuum filtration. Solids were washed with H_2O (3 x 5 mL) and dried under reduced pressure to give 0.029 g of desired compound as a white solid. ^{1}H NMR (400 MHz, d6-DMSO) δ 11.80 (1H, bs), δ 8.10 (1H, d, J= 7.6Hz), δ 8.03 (1H, dd, J= 7.6 Hz, J= 1.6 Hz), δ 7.97 (1H, dd, J= 7.6 Hz, J= 0.80 Hz), δ 7.57-7.51 (2H, m), δ 7.13 (1H, d, J= 8.4 Hz), δ 7.10-7.06 (1H, m). Previously characterized via ^{13}C and HRMS.[54]

Methyl 2,3-diaminobenzoate (9). Methyl 2-amino-3-nitrobenzoate (1.00g, 5.10 mmol) was shaken with Pd/C (10%, 0.0980g) in ethanol (30mL) under 45 PSI of H_2 for 4 hours. Pd/C was removed via vacuum filtration through celite. The filtrate was concentrated under reduced pressure to give 0.850g pure product as a dark brown solid (99% yield). ^{1}H NMR (400MHz, $CDCl_3$) δ 7.47 (1H, dd, J= 8.2Hz, J= 1.4Hz), δ 6.84 (1H, dd, J= 7.3Hz, J= 1.4Hz), δ 6.59 (1H, t, J= 7.8Hz).

Methyl 2-amino-3-((2-(benzyloxy)benzoyl)amino)benzoate (10). 1-1'-Carbonyldiimidazole (0.586g, 3.61 mmol) and **5** (0.687g, 3.01 mmol) and were dissolved in THF and stirred for 30 minutes under inert atmosphere. **9** (0.500g, 3.01 mmol) was added and the reaction mixture was refluxed for 18 hours The reaction mixture was cooled to room temperature and transferred to a separatory funnel along with EtOAc (50mL). The solution was washed with saturated $NaHCO_3$ (2x50mL), H_2O (2x50mL), and brine (50mL), dried with $MgSO_4$, filtered, and concentrated under reduced pressure to give 1.36g of a reddish-brown oil. Crude product was purified *via* flash chromatography (5% EtOAc in CH_2Cl_2) to give 0.679g pure product as an orange-yellow glassy solid (59% yield). ^{1}H NMR (400MHz, $CDCl_3$) δ 9.16 (1H, bs), δ 8.27 (1H, dd, J=

7.8Hz, J= 1.8Hz), δ 7.74 (1H, dd, J= 8.2Hz, J= 1.4Hz), δ 7.41−7.53 (7H, m), δ 7.16 (2H, m), δ 6.64 (1H, t, J= 8.3Hz), δ 5.56 (2H, bs), δ 5.26 (2H, s), δ 3.85 (3H, s).

Methyl 2-(2-(benzyloxy)phenyl)-1*H*-benzimidazole-4-carboxylate (11). Glacial acidic acid (11mL) was added to a flask containing **10** (0.424g, 1.11 mmol) and the solution was refluxed for 19 hours under inert atmosphere. The reaction mixture was cooled to room temperature and transferred to a flask containing approximately 25g of ice and 30mL H_2O. The acid was neutralized with 50mL saturated $NaHCO_3$ and the aqueous phase was extracted with CH_2Cl_2 (3x75mL). Combined organic phases were washed with saturated $NaHCO_3$ (1x50mL), H_2O (2x75mL), and brine (75mL), dried with $MgSO_4$, filtered, and concentrated under reduced pressure to give 0.432g pure desired product as a reddish brown solid (99% yield). ^{1}H NMR (400MHz, $CDCl_3$) δ 11.54 (1H, bs), δ 8.59 (1H, dd, J= 7.8Hz, J= 1.8Hz), δ 8.00 (1H, d, J= 8.3Hz), δ 7.88 (1H, dd, J= 7.8Hz, J= 0.9Hz), δ 7.53 (2H, m), δ 7.35−7.47 (4H, m), δ 7.30 (1H, t, J= 7.8Hz), δ 7.18 (2H, m), δ 5.36 (2H, s), δ 3.65 (3H, s).

Methyl 2-(2-(hydroxy)phenyl)-1*H*-benzimidazole-4-carboxylate (12). **11** (0.215g, 0.600 mmol) was shaken with Pd/C (10%, 0.0200g) in methanol (10mL) under 45 PSI of H_2 for 4 hours. Pd/C was removed *via* vacuum filtration through celite. The filtrate was concentrated under reduced pressure to give 0.159g pure product as a yellowish-white solid (99% yield). ^{1}H NMR (400MHz, $CDCl_3$) δ 10.72 (1H, bs), δ 7.94 (2H, m), δ 7.68 (1H, dd, J= 8.2Hz, J= 1.4Hz), δ 7.40 (2H, m), δ 7.14 (1H, dd, J= 7.4Hz, J= 0.9Hz), δ 7.00 (1H, m), δ 4.04 (3H, s). Previously characterized via ^{13}C and HRMS.[73]

2-(2-(Benzyloxy)phenyl)-1*H*-benzimidazole-4-carboxylic acid (13). To a flask containing **11** (0.432g, 1.21 mmol) in THF (8.80mL), was added 5M NaOH (5.42mL). The reaction mixture was refluxed for 22 hours and then cooled to room temperature. The solution was acidified to pH=1-2 with 6M HCl (10mL) and solids were removed *via* vacuum filtration. Solid precipitate was washed with H_2O (2x10mL) and dried under reduced pressure to provide 0.269g of pure product as a brownish-white solid (65% yield). ^{1}H NMR (400MHz, d_6-DMSO) δ 8.20 (1H, d, J= 7.4Hz), δ 8.00 (1H, d, J= 8.2Hz), δ 7.91 (1H, d, J= 7.4Hz), δ 7.50–7.60 (3H, m), δ 7.38–7.50 (2H, m), δ 7.24–7.38 (2H, m), δ 7.18 (1H, t, J= 7.4Hz), δ 5.39 (2H, s).

2-(2-(Benzyloxy)phenyl)-*N*-methyl-1*H*-benzimidazole-4-carbamide (14). Methylamine (2M in THF, 0.149mL, 0.297 mmol) and **13** (0.0950g, 0.270 mmol) were dissolved in chloroform (5.4mL) under inert atmosphere. Dichlorotriphenylphosphorane (0.414g, 1.24 mmol) was then added and the reaction mixture was refluxed for 21 hours. The solution was cooled to room temperature and transferred to a separatory funnel with 50 mL H_2O. The aqueous phase was extracted with EtOAc (3x50mL). Combined organic phases were washed with 1M HCl (50mL), saturated $NaHCO_3$ (50mL), and brine (50mL), dried with $MgSO_4$, filtered, and concentrated under reduced pressure to give an off-white solid. Crude product was purified via flash chromatography (50% EtOAc in CH_2Cl_2) to give 0.0225g desired compound as an off-white solid (23% yield). ^{1}H NMR (400MHz, $CDCl_3$) δ 10.72 (1H, bs), δ 9.91 (1H, bs), δ 8.60 (1H, dd, J= 7.3Hz, J= 1.8Hz), δ 8.14 (1H, dd, J= 7.3Hz, J= 1.4Hz), δ 7.45-7.54 (5H, m), δ 7.29-7.37(2H,m), δ7.18 (3H, m), δ 5.33 (2H, s), δ 3.18 (3H, d, J= 4.1Hz). ^{13}C NMR (100 MHz, $CDCl_3$) δ166.4, 156.4, 150.9, 143.7, 135.7, 134.2, 131.7, 130.6, 129.0, 128.6,

128.0, 124.6, 124.3, 122.0, 121.8, 118.0, 113.5, 113.0, 71.4, 51.8. HRMS calculated for $C_{22}H_{19}N_3O_2$ $[M+D]^+$ 359.1477, found; 359.1396‡.

2-(2-(Hydroxy)phenyl)-1*H*-benzimidazole-4-carboxylic acid (15). **13** (0.0500g, 0.145 mmol) was shaken with Pd/C (10%, 0.020g) in methanol (10mL) under 45 PSI of H_2 for 4 hours. Pd/C was removed *via* vacuum filtration through celite. The filtrate was concentrated under reduced pressure to give 0.0210g pure product as an off-white solid (57% yield). ^{1}H NMR (400MHz, d_6-DMSO) δ 8.28 (1H, d, J= 7.8Hz), δ 7.95 (1H, d, J= 8.2Hz), δ 7.86 (1H, d, J= 7.4Hz), δ 7.41 (2H, t, J= 7.3Hz), δ 7.07 (1H, d, J= 7.8Hz), δ 7.02 (1H, t, J= 7.3Hz). Previously characterized via ^{13}C and HRMS.[73]

2-(2-(Hydroxy)phenyl)-*N*-methyl-1*H*-benzimidazole-4-carbamide (16). **14** (0.0225g, 0.063 mmol) was shaken with Pd/C (10%, 0.0200g) in methanol (10mL) under 45 PSI of H_2 for 4 hours. Pd/C was removed *via* vacuum filtration through celite. The filtrate was concentrated under reduced pressure to give 0.0141g pure product as an off-white solid (84% yield). ^{1}H NMR (400MHz, d_6-DMSO) δ 9.40 (1H, bs), δ 8.27 (1H, m), δ 7.70–7.80 (2H, m), δ 7.36 (1H, t, J= 8.2Hz), δ 7.28 (1H, t, J= 7.8Hz), δ 7.04 (1H, m), δ 6.99 (1H, m), δ 2.94 (3H, bs). δ166.3, 156.5, 150.9, 143.6, 135.3, 134.6, 131.4, 130.4, 129.0, 128.4, 128.2, 124.5, 113.5, 113.1, 71.3, 51.8. LRMS calculated for $C_{15}H_{13}NO_2$, $[M+H]^+$ 268.10; found 268.13.

‡ Sample submitted for mass spectrometric analysis sat for approximately 24 hours in $CDCl_3$ prior to analysis.

Dimethyl 2,2'-((2,2'-disulfanediylbis(benzoyl))bis(azanediyl))bis(3-hydroxybenzoate) (17). 2,2'-Dithiodibenzoic acid (0.100g, 0.326 mmol) and 1-1'-carbonyldiimidazole (0.127g, 0.782 mmol) were dissolved in THF (3mL) and stirred for 30 minutes under inert atmosphere. Methyl 3-hydroxyanthranilate (0.109g, 0.652 mmol) was added and the reaction mixture was refluxed for 21 hours. The reaction mixture was cooled to room temperature and transferred to a separatory funnel along with 30mL H_2O and extracted with EtOAc (3x30mL). Combined organic phases were washed with H_2O (2x50mL) and brine (50mL), dried with $MgSO_4$, filtered, and concentrated under reduced pressure to give a light brown solid. Crude product was purified via flash chromatography (5% EtOAc in CH_2Cl_2) to give 0.0640g desired compound as a yellowish orange solid (33% yield). ^{1}H NMR (400MHz, $CDCl_3$) δ 11.92 (1H, s), δ 9.51 (1H, s), δ 7.90 (2H, d, J= 11.0Hz), δ 7.68 (1H, d, J= 7.4Hz), δ 7.46 (1H, t, J= 7.8Hz), δ 7.35 (2H, m), δ 7.21 (1H, m), δ 3.94 (3H, s).

Dimethyl 2,2'-(disulfanediylbis(2,1-phenylene))bis(benzoxazole-4-carboxylate) (18). Pyridinium *p*-toluene sulfonate (0.0465g, 0.185 mmol) and **17** (0.0560g, 0.0926 mmol) were dissolved in toluene (3mL) in a flask equipped with a Dean-Stark trap under inert atmosphere. The reaction mixture was refluxed for 17 hours. The solution was then cooled to room temperature and transferred to a separatory funnel along with 30mL EtOAc. The solution was washed with saturated $NaHCO_3$ (2x30mL), H_2O (30mL), and brine (30mL), dried with $MgSO_4$, filtered, and concentrated under reduced pressure to give a yellowish orange solid. Crude product was purified via flash chromatography (5% EtOAc in CH_2Cl_2) to give 0.0195 grams desired product as a dark yellow solid (37% yield). ^{1}H NMR (400MHz, $CDCl_3$) δ 8.30 (1H, dd, J= 7.3Hz, J= 1.4Hz), δ 8.09 (1H, d, J=

7.8Hz), δ 7.93 (1H, d, J= 7.8Hz), δ 7.83 (1H, d, J= 8.2Hz), δ 7.48 (1H, t, J= 7.8Hz), δ 7.43 (1H, m), δ 7.36 (1H, t, J= 6.8Hz), δ 4.07 (3H, s). LRMS calculated for $C_{30}H_{20}N_2O_6S_2$ $[M+H]^+$ 569.08, found; 569.08. HRMS calculated for $C_{30}H_{20}N_2O_6S_2$ $[M+Na]^+$ 591.0660, found; 591.0683.

Methyl 2-(2-sulfanylphenyl)benzoxazole-4-carboxylate (19). Triphenylphosphine (0.0646g, 0.246 mmol) and **18** (0.0700g, 0.123 mmol) were dissolved in a mixture of acetone (1mL) and methanol (3mL). HCl (0.300mL, 6M) was then added to the solution and the reaction mixture was stirred for 1 hour. The solution was then transferred to a separatory funnel along with H_2O (30mL) and extracted with EtOAc (3x30mL). Combined organic phases were washed with brine (30mL), dried with $MgSO_4$, filtered, and concentrated under reduced pressure to give a pinkish orange solid. Crude product was purified *via* flash chromatography (5% EtOAc in CH_2Cl_2) to give 0.0399g desired product as orange crystals (57% yield). ^{1}H NMR (400MHz, d_6-DMSO) δ 8.28 (1H, bs), δ 8.27 (1H, dd, J= 7.8Hz, J= 1.8Hz), δ 8.06 (1H, dd, J= 7.8Hz, J= 1.4Hz), δ 7.79 (1H, dd, J= 7.8Hz, J= 1.4Hz), δ 7.47 (2H, m), δ 7.35 (1H, td, J= 8.2Hz, J= 1.4Hz), δ 7.22–7.30 (1H, m), δ 4.05 (3H, s). ^{13}C (100MHz, $CDCl_3$) δ 166.0, 162.9, 150.8, 141.3, 138.8, 132.1, 130.1, 127.4, 126.9, 126.1, 125.1, 124.0, 122.5, 115.1, 52.9. HRMS calculated for $C_{15}H_{11}NO_3S$ $[M]^+$ 286.0532, found; 286.0532. LRMS calculated for $C_{15}H_{11}NO_3S$, $[M-H]^-$ 284.05; found, 284.03.

2-Chloro-4,6-dimethoxy-1,3,5-triazine. Cyanuric chloride (1.00g, 5.42 mmol) was added to a slurry of methanol (3.1mL), H_2O (0.271mL), and $NaHCO_3$ (0.911g, 10.84 mmol) and the reaction mixture was stirred until CO_2(g) production ceased. The reaction mixture was then refluxed for 30 minutes. The mixture was then cooled to room

temperature and solids were removed *via* vacuum filtration. The precipitate was washed with H_2O (3x10mL) and dried under reduced pressure to give 0.380g desired product as a white solid (40% yield). ^{1}H NMR (400MHz, d_6 -DMSO) δ 3.95 (6H, s). LRMS calculated for $C_5H_6ClN_3O_2$ $[M+H]^+$ 176.010, found; 176.007.

Dimethyl 3,3'-((2,2'-disulfanediylbis(benzoyl))bis(azanediyl))bis(2-aminobenzoate) (20). 2-Chloro-4,6-dimethoxy-1,3,5-triazine (0.115g, 0.652 mmol) was dissolved in THF (2.0mL) and cooled to -5°C under inert atmosphere. *N*-Methylmorpholine (0.717mL, 0.652 mmol) was added to the reaction mixture and the solution was stirred at -5°C for 10 minutes. 2,2'-Dithiodibenzoic acid (0.100g, 0.326 mmol) was then added to the solution and the mixture was stirred for 2 hours at -5°. **9** (0.109g, 0.652 mmol) and *N*-methylmorpholine (0.358mL, 0.326 mmol) were then added and the reaction mixture was stirred for 2 hours at -5°C. The solution was then stirred at room temperature for 18 hours. The reaction mixture was transferred to a separatory funnel along with CH_2Cl_2 (30mL) and washed with saturated NH_4Cl (30mL), saturated $NaHCO_3$ (30mL), H_2O (2x30mL), brine (30mL), dried with $MgSO_4$, filtered, and concentrated under reduced pressure to give a brown solid. Crude product was purified *via* flash chromatography (10% EtOAc in $CHCl_3$) to give 0.0482g pure product as a reddish brown solid (25% yield). ^{1}H NMR (400MHz, $CDCl_3$) δ 8.12 (1H, d, J= 7.8Hz), δ 7.99 (1H, dd, J= 8.2Hz, J= 1.4Hz), δ 7.69 (1H, m), δ 7.59 (1H, d, J= 8.2Hz), δ 7.47 (1H, m), δ 7.41 (1H, dd, J= 7.8Hz, J= 1.4Hz), δ 6.73 (1H, t, J= 8.0Hz), δ 6.08 (2H, bs), δ 3.89 (3H, s).

Dimethyl 2,2'-(disulfanediylbis(2,1-phenylene))bis(1*H*-benzimidazole-carboxylate) (21). **20** (0.196g, 0.326 mmol) was dissolved in glacial acetic acid (3.0mL)

and refluxed for 36 hours. The reaction mixture was cooled to room temperature and neutralized with saturated $NaHCO_3$ (75mL). The solution was extracted with CH_2Cl_2 (3x75mL). Combined organic phases were washed with saturated $NaHCO_3$ (75mL), H_2O (75mL), and brine (75mL), dried with $MgSO_4$, filtered, and concentrated under reduced pressure to give 0.120g desired product as a dark yellow crystalline solid (68% yield). ^1H NMR (400MHz, $CDCl_3$) δ 11.28 (1H, bs), δ 8.01 (1H, d, J= 8.3Hz), δ 7.94 (2H, m), δ 7.67 (1H, dd, J= 7.8Hz, J= 1.4Hz), δ 7.33 (1H, t, J= 7.8Hz), δ 7.22 (2H, m), δ 3.99 (3H, s).

Methyl 2-(2-sulfanylphenyl)-1*H*-benzimidazole-4-carboxylate (22). Sodium borohydride (9.21mg, 0.244 mmol) and **21** (0.0345g, 0.0609 mmol) were dissolved in a mixture of THF (0.400mL) and ethanol (0.400mL) under inert atmosphere and the solution was stirred for 2 hours. The reaction mixture was acidified with HCl (10mL, 1M), EtOAc (30mL) was added, and the phases were separated. The organic phase was washed with brine (10mL), dried with $MgSO_4$, filtered, and concentrated under reduced pressure to give 0.0156g desired product as a yellowish orange solid (90% yield). NMR (400MHz, *d*$_6$-DMSO) δ 7.97 (3H, m), δ 7.53 (2H, m), δ 7.12 (1H, m), δ 7.00 (1H, m), δ 3.97 (3H, s). ^{13}C (100MHz, $CDCl_3$) δ 166.9, 151.3, 144.1, 135.0, 134.6, 132.7, 130.6, 130.5, 128.5, 125.2, 122.1, 113.4, 52.4.

2-(2-Benzyloxyphenyl)benzoxazole-4-carboxylic acid (23). To a flask containing **7** (0.334g, 0.929 mmol) in THF (6.2mL), was added 5M NaOH (3.12mL). The reaction mixture was refluxed for 2.5 hours and then cooled to room temperature. The solution was acidified to pH=1-2 with 1M HCl (30mL) and transferred to a separatory funnel. The aqueous phase was extracted with EtOAc (3x50mL). Combined organic phases were

washed with H_2O (2x50mL) and brine (50mL), dried with $MgSO_4$, filtered, and concentrated under reduced pressure to give 0.299g of pure product as a viscous yellow oil (92% yield). ^{1}H NMR (400MHz, $CDCl_3$) δ 8.23 (1H, dd, J= 7.8Hz, J= 1.8Hz), δ 8.13 (1H, d, J= 7.8Hz), δ 7.78 (1H, dd, J= 8.3Hz, J= 0.9Hz), δ 7.53–7.59 (3H, m), δ 7.50 (1H, t, J= 8.2Hz), δ 7.43 (2H, m), δ 7.36 (1H, m), δ 7.12-7.20 (2H, m), δ 5.30 (2H, s).

2-(2-Benzyloxyphenyl)-*N*-methyl-benzoxazole-4-carbamide (24). Methylamine (2M in THF, 0.138mL, 0.278 mmol) and **23** (0.145g, 0.415 mmol) were dissolved in chloroform (5.5mL) under inert atmosphere. Dichlorotriphenylphosphorane (0.331g, 0.994 mmol) was then added and the reaction mixture was refluxed for 21 hours. The solution was cooled to room temperature and transferred to a separatory funnel along with 50mL CH_2Cl_2. The solution was washed with 1M HCl (2x25mL), saturated $NaHCO_3$ (2x 50mL), and brine (50mL), dried with $MgSO_4$, filtered, and concentrated under reduced pressure to give a brown solid. Crude product was purified via flash chromatography (20% EtOAc in CH_2Cl_2) to give 0.0715g pure desired compound as an off-white solid (72% yield). ^{1}H NMR (400MHz, $CDCl_3$) δ 9.00 (1H, bs), δ 8.20 (2H, t, J= 6.4Hz), δ 7.68 (1H, d, J= 8.2Hz), δ 7.55 (3H, m), δ 7.27-7.45 (4H, m), δ 7.16-7.20 (2H, m), δ 5.27 (2H, s), δ 2.83 (3H, d, J= 4.6Hz). ^{13}C NMR (100 MHz, $CDCl_3$) δ 165.1, 162.0, 158.0, 150.2, 139.6, 136.4, 133.5, 131.5, 128.7, 128.2, 127.2, 125.5, 124.9, 124.1, 121.2, 115.8, 113.8, 113.3, 70.8, 26.3. HRMS calc. for $C_{22}H_{18}N_2O_3$ $[M+Na]^+$ 381.1198; found 381.1216.

***N*-Benzyl-2-(2-benzyloxyphenyl)benzoxazole-4-carbamide (25).** Benzylamine (0.048mL, 0.440 mmol) and **23** (0.154g, 0.440 mmol) were dissolved in chloroform

(9mL) under inert atmosphere. Dichlorotriphenylphosphorane (0.528g, 1.58 mmol) was then added and the reaction mixture was refluxed for 19 hours. The solution was cooled to room temperature and transferred to a separatory funnel with $CHCl_3$ (50mL). The solution was washed with 4M HCl (2x50mL), saturated $NaHCO_3$ (2x 50mL), and brine (50mL), dried with $MgSO_4$, filtered, and concentrated under reduced pressure to give 0.815g of a brown solid. Crude product was purified via flash chromatography (10% EtOAc in CH_2Cl_2) to give 0.152g pure desired compound as a yellowish white solid (80% yield). ^{1}H NMR (400MHz, $CDCl_3$) δ 9.62 (1H, bs), δ 8.23 (1H, dd, J= 7.8Hz, J= 1.3Hz), δ 8.13 (1H, dd, J= 7.8Hz, J= 1.8Hz), δ 7.70 (1H, dd, J= 6.9Hz, J= 0.9Hz), δ 7.45-7.50 (4H, m), δ 7.18-7.37 (8H, m), δ 7.10 (2H, m), δ 5.17 (2H, s), δ 4.64 (2H, d, J= 5.5Hz). ^{13}C NMR (100 MHz, $CDCl_3$) δ 164.5, 162.3, 157.8, 150.4, 139.7, 138.8, 136.6, 133.5, 131.5, 128.6, 128.5, 128.0, 127.6, 127.1, 126.8, 125.7, 124.8, 123.9, 121.1, 115.8, 114.0, 113.5, 70.6, 43.6. HRMS calc. for $C_{28}H_{22}N_2O_3$ $[M+H]^+$ 435.1630; found 435.1711.

2-(2-Benzyloxyphenyl)-*N,N*-dimethyl-benzoxazole-4-carbamide (27) .

Dimethylamine, (2M in THF, 0.190mL, 1.50 mmol) and **23** (0.132g, 0.379 mmol) were dissolved in chloroform (7.5mL) under inert atmosphere. Dichlorotriphenylphosphorane (0.328g, 0.985 mmol) was then added and the reaction mixture was refluxed for 17 hours. The solution was cooled to room temperature and transferred to a separatory funnel with $CHCl_3$ (30mL). The solution was washed with 1M HCl (30mL), H_2O (2x 30mL), and brine (30mL), dried with $MgSO_4$, filtered, and concentrated under reduced pressure to give 0.592g of brown solid. Crude product was purified via flash chromatography (CH_2Cl_2:EtOAc, 1:2) to give 0.103g pure desired compound as an off-white solid (73%

yield). ^{1}H NMR (400MHz, $CDCl_3$) δ 8.17 (1H, dd, J= 7.8Hz, J= 1.4Hz), δ 7.59 (3H, m), δ 7.50 (1H, m), δ 7.38-7.46 (4H, m), δ 7.34 (1H, m), δ 7.12 (2H, m), δ 5.23 (2H, s), δ 3.16 (3H, s), δ 2.88 (3H, s). ^{13}C NMR (100 MHz, $CDCl_3$) δ 168.3, 162.5, 157.7, 150.4, 139.0, 136.6, 133.0, 131.8, 128.6, 127.9, 127.3, 125.0, 123.7, 122.8, 121.2, 116.7, 113.8, 111.5, 70.9, 39.0, 35.4. HRMS calc. for $C_{23}H_{20}N_2O_3$ $[M+H]^+$ 373.1474; found 373.1546.

2-(2-Benzyloxyphenyl)benzoxazole-4-carbamide (28). 1-1'-Carbonyldiimidazole (0.0717g, 0.442 mmol) and **23** (0.129g, 0.373 mmol) were dissolved in THF and stirred for 30 minutes under inert atmosphere. Ammonia (0.5M in THF, 7.37mL, 3.69 mmol) was added and the reaction mixture was refluxed for 18 hours. The reaction mixture was cooled to room temperature and transferred to a separatory funnel along with EtOAc (30mL). The solution was washed with 1M HCl (2x15mL), H_2O (30mL), and brine (30mL), dried with $MgSO_4$, filtered, and concentrated under reduced pressure to give a brown oil. Crude product was purified *via* flash chromatography (20% EtOAc in $CHCl_3$) to give 0.0840g pure product as a white crystalline solid (66% yield). ^{1}H NMR (400MHz, $CDCl_3$) δ 8.77 (1H, bs), δ 8.24 (1H, dd, J= 8.2, J= 1.8Hz), δ 8.13 (1H, dd, J= 7.8Hz, J= 1.4Hz), δ 7.70 (1H, dd, J= 7.8Hz, J= 0.9Hz), δ 7.54-7.59 (3H, m), δ 7.39-7.46 (4H, m), δ 7.21 (1H, d, J= 8.3Hz), δ 7.16 (1H, td, J= 7.8Hz, J= 0.9Hz), δ 5.45 (1H, bs), δ 5.23 (2H,s). ^{13}C NMR (100 MHz, $CDCl_3$) δ 161.8, 158.2, 150.0, 136.3, 133.6, 131.2, 128.7, 128.5, 128.0, 125.7, 124.8, 121.1, 113.8, 113.4, 71.0. HRMS calc. for $C_{21}H_{16}N_2O_3$ $[M+H]^+$ 345.1161; found 345.1240.

2-(2-Hydroxyphenyl)-*N*-methyl-benzoxazole-4-carbamide (29). **24** (0.0682g, 0.190 mmol) was shaken with Pd/C (10%, 0.050g) in methanol (4mL) under 45 PSI of H_2 for 4 hours. Pd/C was removed *via* vacuum filtration through celite. The filtrate was

concentrated under reduced pressure to give 0.0516g pure product as an off-white solid (99%). ^{1}H NMR (400MHz, $CDCl_3$) δ 10.48 (1H, bs), δ 8.22 (1H, d, J= 8.2Hz), δ 8.09 (1H, d, J= 7.8Hz), δ 7.80 (1H, bs), δ 7.75 (1H, d, J= 8.2Hz), δ 7.51 (2H, m), δ 7.15 (1H, d, J= 8.2Hz), δ 7.10 (1H, t, J= 7.3Hz), δ 3.15 (3H, d, J= 4.6Hz). ^{13}C (100MHz, $CDCl_3$) δ 164.7, 163.6, 158.4, 149.1, 137.3, 134.7, 127.9, 126.7, 125.6, 124.1, 120.4, 117.6, 113.7, 110.1, 26.8. HRMS calculated for $C_{15}H_{12}N_2O_3$ $[M]^+$ 269.0920, found; 269.0919.

***N*-Benzyl-2-(2-hydroxyphenyl)benzoxazole-4-carbamide (30). 25** (0.081g, 0.186 mmol) was shaken with Pd/C (10%, 0.050g) in 5mL methanol under 45 PSI of H_2 for 6 hours. Pd/C was removed *via* vacuum filtration through celite. The filtrate was concentrated reduced pressure to give 0.0580g pure product as solid white needles (90%). ^{1}H NMR (400MHz, $CDCl_3$) δ 10.14 (1H, bs), δ 8.25 (1H, dd, J= 7.8Hz, J= 0.9Hz), δ 8.18 (1H, bs), δ 8.06 (1H, dd, J= 8.2Hz, J= 1.8Hz), δ 7.76 (1H, dd, J= 8.2Hz, J= 0.9Hz), δ 7.38-7.54 (6H, m), δ 7.33 (1H, m), δ 7.10 (1H, dd, J= 8.2Hz, J= 0.9Hz), δ 7.04 (1H, td, J= 7.6Hz, J= 0.9Hz), δ 4.80 (2H, d, J= 6.0Hz). ^{13}C (100MHz,$CDCl_3$) δ 163.9, 163.6, 158.5, 149.2, 138.1, 137.6, 134.37, 129.1, 127.9, 127.8, 127.7, 126.8, 125.6, 124.0, 120.3, 117.7, 113.8, 110.0, 44.2. HRMS calculated for $C_{21}H_{16}N_2O_3$ $[M]^+$ 345.1233, found; 345.1232.

Synthesis of *N*-Butyl-2-(2-hydroxyphenyl)benzoxazole-4-carbamide (31):[§]

[§] A different route than that reported in the document was used for the synthesis of **31**. This route proved less efficient and was thus not used for the synthesis of any other benzoxazole amides. **31** was included in **Scheme 5** for ease of interpretation. Intermediate **27** was in fact, never synthesized due to the change in synthetic route.

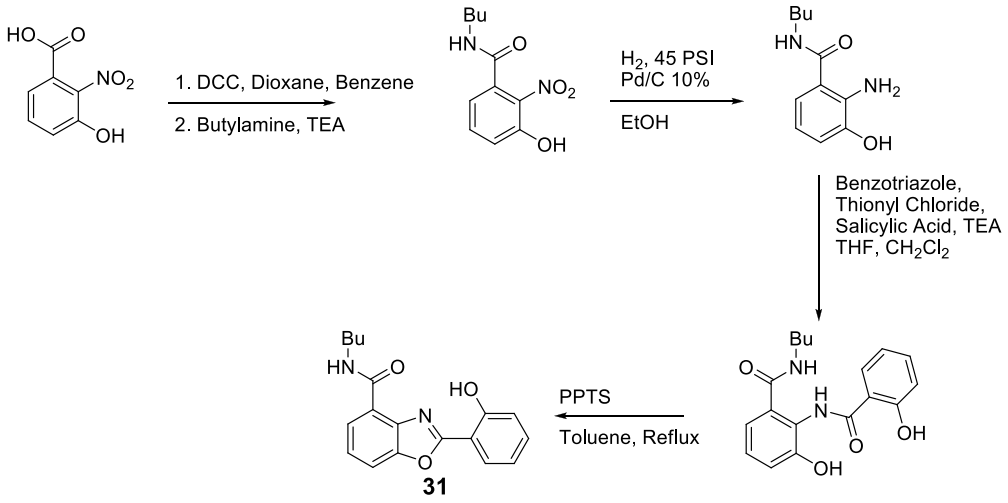

***N*-Butyl-3-hydroxy-2-nitrobenzamide**. 3-Hydroxy-2-nitrobenzoic acid (0.250g, 1.37 mmol) was dissolved in dioxane (2.74mL) under inert atmosphere. A solution of dicyclohexylcarbodiimide (0.311g, 1.51 mmol) and benzene (0.010mL) in dioxane (1.35mL) was added to the reaction mixture and the mixture was stirred for 15 minutes. A solution of butylamine (0.135mL, 1.37 mmol) and triethylamine (0.210mL, 1.51 mmol) in dioxane (1.37mL) was then added and the reaction mixture was stirred for 20 hours. The slurry was then transferred to a separatory funnel and acidified to pH=1-2 with 50mL 1M HCl. The aqueous phase was extracted with EtOAc (3x50mL). Combined organic phases were washed with H_2O (50mL) and brine (50mL), dried with $MgSO_4$, filtered, and concentrated under reduced pressure to yield a yellowish-brown oil. Desired product was achieved *via* flash chromatography (50% EtOAc in CH_2Cl_2) as a light brown oil (0.303g, 93% yield). ^{1}H NMR (400MHz, $CDCl_3$) δ 7.52 (1H,m), δ 7.19 (1H, dd, J= 8.2Hz, J= 1.4Hz), δ 6.95 (1H, dd, J= 7.4Hz, J= 1.4Hz), δ 5.74 (1H, bs), δ 3.46 (2H, m), δ 1.63 (2H, m), δ 1.42 (2H, m), δ 0.97 (3H, t, J= 7.3Hz).

2-Amino-*N*-butyl-3-hydroxybenzamide. *N*-Butyl 3-hydroxy-2-nitrobenzamide (0.300g, 1.64 mmol) was shaken with Pd/C (10%, 0.0550g) in ethanol (11mL) under 45 PSI of H_2 for 2 hours. Pd/C was removed *via* vacuum filtration through celite. The filtrate was concentrated under reduced pressure to give 0.260g pure product as a brown solid (76% yield). ^{1}H NMR (400MHz, d_6-DMSO) δ 9.39 (1H, bs), δ 8.08 (1H, bs), δ 6.96 (1H, dd, J= 7.8Hz, J= 1.4Hz), δ 6.70 (1H, dd, J= 7.8Hz, J= 1.4Hz), δ 6.36 (1H, t, J= 7.8Hz), δ 3.16 (2H, q, J= 6.9Hz), δ 1.44 (2H, m), δ 1.29 (2H, m), δ 0.86 (3H, t, J= 7.3Hz).

***N*-Butyl-3-hydroxy-2-((2-hydroxybenzoyl)amino)benzamide.** Benzotriazole (0.468g, 3.93 mmol) was dissolved in 7.5mL 50% THF in CH_2Cl_2 under inert atmosphere. Thionyl chloride (0.0911mL, 1.25 mmol) was added and the solution was stirred for 45 minutes. Salicylic acid (0.173g, 1.25 mmol) and THF (5mL) was then added and the solution was stirred for 2 hours. A solution of 2-amino-*N*-butyl-3-hydroxybenzamide (0.260g, 1.25 mmol) and triethylamine (0.261mL, 1.87 mmol) in THF (7mL) was then added and the reaction mixture was stirred for 18 hours. The reaction mixture was transferred to a separatory funnel along with 50mL saturated $NaHCO_3$ and extracted with EtOAc (3x50mL). The combined organic phases were washed with H_2O (4x50mL) and brine (50mL), dried with $MgSO_4$, filtered, and concentrated under reduced pressure to give a brownish yellow solid. Crude product was purified via flash chromatography (20% EtOAc in $CHCl_3$) to give 0.199g of a yellowish white powder (49% yield). ^{1}H NMR (400MHz, $CDCl_3$) δ 12.37 (1H, bs), δ 11.51(1H, s), δ 9.23 (1H, s), δ 7.83 (1H, dd, J= 8.2Hz, J= 1.4Hz), δ 7.47(1H, m), δ 7.21 (2H, m), δ 7.09 (1H, dd, J= 7.4Hz, J= 2.3Hz), δ 7.01 (2H, m), δ 6.24 (1H, bs), δ 3.45 (2H, m), δ 1.59 (2H, m), δ 0.95 (3H, t, J= 7.3Hz).

***N*-Butyl-2-(2-hydroxyphenyl)benzoxazole-4-carbamide (31)**. *N*-Butyl-3-hydroxy-2-((2-hydroxybenzoyl)amino)benzamide (0.199g, 0.606 mmol) was added to a solution of pyridinium *p*-toluene sulfonate (0.305g, 1.21 mmol) in toluene (13.3mL) under inert atmosphere. The reaction vessel was equipped with a Dean-Stark trap and refluxed for 23 hours. The solution was cooled to room temperature and transferred to a separatory funnel along with 50mL saturated $NaHCO_3$. The solution was extracted with EtOAc (3x50mL). Combined organic phases were washed with H_2O (3x50mL) and brine (50mL), dried with $MgSO_4$, filtered, and concentrated under reduced pressure to give a solid yellow powder. Pure product was achieved *via* flash chromatography (10% EtOAc in $CHCl_3$) as a white powder (0.0324g, 17% yield). ^{1}H NMR (400MHz, $CDCl_3$) δ 10.47 (1H, s), δ 8.22 (1H, dd, J= 7.8Hz, J= 1.4Hz), δ 8.09 (1H, dd, J= 8.3Hz, J= 1.8Hz), δ 7.86 (1H, bs), δ 7.75 (1H, dd, J= 7.8Hz, J= 0.9Hz), δ 7.51 (2H, m), δ 7.16 (1H, dd, J= 8.3Hz, J= 0.9Hz), δ 3.61 (2H, m), δ 1.72 (2H, m), δ 1.50 (2H, m), δ 1.01 (3H, t, J= 7.3Hz). ^{13}C (100MHz, $CDCl_3$) δ 164.0, 163.6, 158.5, 149.1, 137.4, 134.7, 127.9, 126.6, 125.6, 124.2, 120.3, 117.6, 113.6, 110.0, 39.8, 31.7, 20.4, 13.9. HRMS calculated for $C_{18}H_{18}N_2O_3$ $[M]^+$ 311.1390, found; 311.1387.

2-(2-Hydroxyphenyl)-*N*,*N*-dimethyl-benzoxazole-4-carbamide (32). **27** (0.934g, 0.251 mmol) was shaken with Pd/C (10%, 0.01g) in methanol (5mL) under 45 PSI of H_2 for 3 hours. Pd/C was removed *via* vacuum filtration through celite. The filtrate was concentrated under reduced pressure to give 0.0667g pure product as a glassy yellow solid (94%). ^{1}H NMR (400MHz, $CDCl_3$) δ 8.04 (1H, dd, J= 7.8Hz, J= 1.4Hz), δ 7.66 (1H, d, J= 7.8Hz), δ 7.42-7.51 (3H, m), δ 7.11 (1H, d, J= 8.2Hz), δ 7.03 (1H, td, J= 7.8Hz, J= 0.9Hz), δ 3.23 (3H, s), δ 2.99 (3H, s). ^{13}C (100MHz, $CDCl_3$) δ 167.9, 163.7,

158.9, 148.9, 136.8, 134.2, 127.9, 127.4, 125.8, 124.5, 119.9, 117.6, 111.8, 110.2, 39.0, 35.4. HRMS calculated for $C_{16}H_{14}N_2O_3$, $[M]^+$ 283.1077, found; 283.1075.

2-(2-Hydroxyphenyl)benzoxazole-4-carbamide (33). 28 (0.0844g, 0.245 mmol) was shaken with Pd/C (10%, 0.020g) in 10mL ethanol under 45 PSI of H_2 for 6 hours. Pd/C was removed *via* vacuum filtration through celite. The filtrate was concentrated under reduced pressure to give 0.0600g pure product as a glassy yellow solid (96%). ^{1}H NMR (400MHz, $CDCl_3$) δ 10.40 (1H, bs), δ 8.23 (1H, dd, J= 7.8Hz, J= 0.9Hz), δ 8.09 (1H, dd, J= 7.8Hz, J= 1.8Hz), δ 7.80 (1H, dd, J= 8.2Hz, J= 0.9Hz), δ 7.74 (1H, bs), δ 7.50-7.55 (2H, m), δ 7.15 (1H, dd, J= 8.2Hz, J= 0.9Hz), δ 7.08 (1H, td, J= 7.8Hz, J= 0.9Hz), δ 5.97 (1H, bs). ^{13}C (100MHz, d_6-DMSO) δ 165.6, 163.2, 158.1, 150.0, 138.8, 134.7, 130.0, 125.7, 125.6, 125.1, 120.4, 118.0, 114.4, 111.8. HRMS calculated for $C_{14}H_{10}N_2O_3$ $[M]^+$ 255.0764, found; 255.0764.

Methyl 1-benzyl-2-(2-(benzyloxy)phenyl)benzimidazole-4-carboxylate (34). DMF (2mL) was added to a flask containing **11** (0.100g, 0.279 mmol) and Cs_2CO_3 (0.137g, 0.419 mmol) under inert atmosphere. Benzyl bromide (0.0365mL, 0.307 mmol) was added to the slurry and the reaction mixture was stirred for 18 hours at room temperature. The reaction mixture was transferred to a separatory funnel along with H_2O (30mL). The aqueous phase was extracted with CH_2Cl_2 (3x30mL). Combined organic phases were washed with brine (50mL), dried with $MgSO_4$, filtered, and concentrated under reduced pressure to give a yellowish oil. Crude product was purified *via* flash chromatography (10% EtOAc in CH_2Cl_2) to give 0.0770g pure product as a fluffy off-white solid (61.4% yield). ^{1}H NMR (400MHz, $CDCl_3$) δ 7.95 (1H, dd, J= 7.3Hz, J= 1.4Hz), δ 7.65 (1H, dd,

J= 7.3Hz, J= 1.8Hz), δ 7.43 (1H, m), δ 7.31 (2H, m), δ 7.12–7.24 (6H, m), δ 7.08 (1H, m), δ 7.01 (1H, m), δ 6.93 (2H, m), δ 5.26 (2H, s), δ 5.01 (2H, s), δ 4.04 (3H, s). HRMS calc. for $C_{29}H_{24}N_2O_3$ $[M+H]^+$ 449.1787; found 449.1860.

Methyl 1-benzyl-2-(2-(hydroxy)phenyl)benzimidazole-4-carboxylate (35). **34** (0.0730g, 0.163 mmol) was shaken with Pd/C (5%, 6.00mg) in methanol (8mL) under 30 PSI of H_2 for 4 hours. Pd/C was removed *via* vacuum filtration through celite. The filtrate was concentrated under reduced pressure to give a bright yellow solid. Crude product was purified via flash chromatography (5% EtOAc in CH_2Cl_2) to give 0.0450g of a bright yellow solid (77% yield). ^{1}H NMR (400MHz, $CDCl_3$) δ 8.07 (1H, dd, J= 7.3Hz, J= 1.4Hz), δ 7.33–7.47 (7H, m), δ 7.16–7.20 (3H, m), δ 6.80 (1H, m), δ 5.69 (2H, s), δ 4.09 (3H, s). ^{13}C (100MHz, $CDCl_3$) δ 166.8, 159.9, 153.5, 139.3, 136.6, 135.3, 132.4, 129.5, 128.3, 126.8, 126.5, 125.8, 123.1, 120.5, 118.9, 118.6, 114.7, 112.3, 52.4. HRMS calculated for $C_{22}H_{18}N_2O_3$ $[M]^+$ 359.1390, found; 359.1389.

1-Benzyl-2-(2-(benzyloxy)phenyl)benzimidazole-4-carboxylic acid (36). Benzyl bromide (0.415mL, 0.349 mmol) and **11** (0.100g, 0.279 mmol) were dissolved in THF (2mL) under inert atmosphere. NaH (0.0335g, 1.40 mmol) was added and the reaction mixture was stirred for 4 hours. The reaction was then quenched with HCl (30mL, 1M), transferred to a separatory funnel, and extracted with EtOAc (3x30mL). Combined organic phases were washed with H_2O (2x30mL) and brine (30mL), dried with $MgSO_4$, filtered, and concentrated under reduced pressure to give a yellow solid. Crude product was recrystallized from EtOAc:Hexane which gave 0.0671g desired product as a white crystalline solid (55% yield). ^{1}H NMR (400MHz, $CDCl_3$) δ 8.08 (1H, dd, J= 6.4Hz, J=

2.3Hz), δ 7.48–7.54 (3H, m), δ 7.27–7.32 (5H, m), δ 7.17–7.21 (5H, m), δ 7.12 (2H, m), δ 6.96 (2H, m), δ 5.29 (2H, s), δ 5.06 (2H, s). ^{13}C NMR (100 MHz, $CDCl_3$) δ 166.4, 157.7, 156.8, 152.5, 136.0, 135.0, 134.6, 133.0, 132.6, 129.0, 128.8, 128.32, 128.25, 127.2, 126.8, 125.8, 123.7, 121.7, 119.4, 116.1, 113.5, 71.0, 49.3. HRMS calc. for $C_{28}H_{22}N_2O_3$ $[M+H]^+$ 435.1630; found 435.1710.

1-Benzyl-2-(2-(benzyloxy)phenyl)-*N*-methyl-benzimidazole-4-carbamide (37). **36** (0.141g, 0.323 mmol) was dissolved in CH_2Cl_2 (1.5mL) and cooled to -5°C under inert atmosphere. *N*-Methylmorpholine (0.0355mL, 0.323 mmol) and 2-chloro-4,6-dimethoxy-1,3,5-triazine (0.0567g, 0.323 mmol) were then added to the solution and the mixture was stirred for 2 hours at -5°. Methylamine (2M in THF, 0.808mL, 1.61 mmol) and *N*-methylmorpholine (0.0355mL, 0.323 mmol) were then added and the reaction mixture was stirred for 2 hours at -5°C. The solution was then stirred at room temperature for 23 hours. The reaction mixture was transferred to a separatory funnel along with CH_2Cl_2 (30mL) and washed with 1M HCl (3x30mL), saturated $NaHCO_3$ (30mL), H_2O (30mL), brine (30mL), dried with $MgSO_4$, filtered, and concentrated under reduced pressure to give a yellowish-white solid. Crude product was purified via flash chromatography (20% EtOAc in CH_2Cl_2) to give 0.0863g pure product as a white solid (60% yield). ^{1}H NMR (400MHz, $CDCl_3$) δ 7.95 (1H, dd, J= 7.8Hz, J= 1.2Hz), δ 7.65 (1H, dd, J= 7.3Hz, J= 1.4Hz), δ 7.43 (1H, m), δ 7.31 (2H, dd, J= 8.2Hz, J= 0.9Hz), δ 7.12–7.24 (8H, m), δ 7.08 (1H, td, J= 7.3Hz, J= 0.9Hz), δ 7.02 (1H, d, J= 8.7Hz), δ 6.92 (2H, m), δ 5.26 (2H, s), δ5.01 (2H, s), δ 4.04 (3H, s).

1-Benzyl-2-(2-hydroxyphenyl)-*N*-methyl-benzimidazole-4-carbamide (38). **37** (0.0863g, 0.193 mmol) was shaken with Pd/C (5%, 8.0mg) in methanol (8mL) under 30 PSI of H_2 for 4 hours. Pd/C was removed *via* vacuum filtration through celite. The filtrate was concentrated under reduced pressure to give 0.0795g desired product as a white solid (98% yield). ^{1}H NMR (400MHz, $CDCl_3$) δ 10.61 (1H, s), δ 8.76 (1H, bs), δ 8.23 (1H, dd, J= 5.5Hz, J= 3.2 Hz), δ 7.35–7.43 (7H, m), δ 7.15–7.19 (3H, m), δ 6.87–6.90 (1H, m), δ 5.61 (2H, s), δ 3.16 (3H, d, J= 4.6Hz). ^{13}C (100MHz, $CDCl_3$) δ 165.9, 157.4, 152.2, 138.8, 135.8, 135.4, 132.7, 129.5, 128.3, 127.9, 125.8, 125.4, 123.8, 123.3, 119.9, 118.0, 113.9, 112.9, 49.4, 26.6. HRMS calculated for $[M]^+$ 358.1550, found; 358.1547.

1-Benzyl-2-(2-(hydroxy)phenyl)benzimidazole-4-carboxylic acid (39). 36 (0.0671 g, 0.154 mmol) was shaken with Pd/C (5%, 0.020g) in methanol (8mL) under 30 PSI of H_2 for 4 hours. Pd/C was removed *via* vacuum filtration through celite. The filtrate was concentrated under reduced pressure to give the desired product as a grey solid. (57% yield). ^{1}H NMR (400MHz, d_6-DMSO) δ 8.29 (1H, bs), δ 7.82 (1H, d, J= 7.3Hz), δ 7.75 (1H, d, J= 7.8Hz), δ 7.50 (1H, d, J= 6.4Hz), δ 7.33–7.40 (2H, m), δ 7.19–7.27 (3H, m), δ 7.02 (2H, t, J= 6.9Hz), δ 6.90–6.96 (1H, m), δ 5.58 (2H, s). ^{13}C (100MHz, d_6-DMSO) δ 166.9, 153.7, 141.1, 136.8, 136.2, 132.6, 131.0, 129.3, 128.2, 127.1, 125.2, 123.2, 119.7, 117.2, 116.3, 115.7, 49.2, 31.2. HRMS calculated for $C_{21}H_{16}N_2O_3$ $[M]^+$ 345.1234, found; 345.1232.

Methyl 2-(1-hydroxynaphthalen-2-yl)benzoxazole-4-carboxylate (41). 1-Hydroxy-2-napthoic acid (0.200g, 1.06 mmol) and 1-1'-carbonyldiimidazole (0.207g, 1.28 mmol) were dissolved in THF (6mL) and stirred for 30 minutes under inert atmosphere. Methyl 3-hydroxyanthranilate (0.210g, 1.06 mmol) was added and the reaction mixture was

refluxed for 19 hours. The reaction mixture was cooled to room temperature and transferred to a separatory funnel along with H_2O (50mL) and extracted with EtOAc (3x50mL). Combined organic phases were washed with H_2O (50mL) and brine (50mL), dried with $MgSO_4$, filtered, and concentrated under reduced pressure to give 0.558g of a light brown solid. Crude product amide **40** was dissolved in *m*-xylene (34.4mL) and pyridinium *p*-toluene sulfonate (0.816g, 3.25 mmol) was added to the solution. The reaction mixture was refluxed overnight. The solution was then cooled to room temperature and 75mL saturated $NaHCO_3$ was added. The solution was extracted with EtOAc (3x100mL). Combined organic phases were washed with H_2O (2x100mL) and brine (100mL), dried with $MgSO_4$, filtered, and concentrated under reduced pressure to give a dark brown solid. Crude product was purified via flash chromatography (10% EtOAc in $CHCl_3$) to give 0.105g desired compound as a reddish brown solid (30% yield; two steps). ^{1}H NMR (400MHz, $CDCl_3$) δ 8.52 (1H, d, J= 8.2Hz), δ 8.08 (1H, dd, J= 7.8Hz, J=1.0 Hz), δ 8.00 (1H, d, J= 8.7Hz), δ 7.82 (2H, d, J= 8.3Hz), δ 7.62–7.57 (2H, m), δ 7.46–7.42 (2H, m), δ 4.09 (3H, s). ^{13}C (100MHz, $CDCl_3$) δ 166.4, 165.7, 162.3, 149.6, 138.0, 135.7, 130.9, 129.4, 128.7, 128.5, 127.7, 124.6, 124.4, 124.0, 120.7, 119.7, 115.0, 101.9, 52.6. HRMS calculated for $C_{19}H_{13}NO_4$ $[M]^+$ 320.0917, found; 320.0917.

Methyl 2-(3-hydroxynaphthalen-2-yl)benzoxazole-4-carboxylate (42). 3-Hydroxy-2-napthoic acid (0.200g, 1.06 mmol) and 1-1'-carbonyldiimidazole (0.207g, 1.28 mmol) were dissolved in THF (6mL) and stirred for 30 minutes under inert atmosphere. Methyl 3-hydroxyanthranilate (0.210g, 1.06 mmol) was added and the reaction mixture was refluxed overnight. The reaction mixture was cooled to room temperature and transferred to a separatory funnel along with 50mL H_2O and extracted with CH_2Cl_2 (3x50mL).

Combined organic phases were washed with H_2O (50mL) and brine (50mL), dried with $MgSO_4$, filtered, and concentrated under reduced pressure to give 0.359g of a dark brown solid. Crude amide was dissolved in *m*-xylene (22mL) and pyridinium *p*-toluene sulfonate (0.523g, 2.08 mmol) was added to the solution. The reaction mixture was refluxed for 22 hours. The solution was then cooled to room temperature and 75mL saturated $NaHCO_3$ was added. The solution was extracted with CH_2Cl_2 (3x75mL). Combined organic phases were washed with H_2O (2x100mL) and brine (100mL), dried with $MgSO_4$, filtered, and concentrated under reduced pressure to give a greenish brown solid. Crude product was purified *via* flash chromatography (10% EtOAc in $CHCl_3$) to give 0.0950g desired compound as a reddish brown solid (28% yield; two steps). ^{1}H NMR (400MHz, $CDCl_3$) δ 8.65 (1H, s) δ 8.10 (1H, dd, J= 7.8Hz, J= 1.4Hz), δ 7.87 (2H, m) δ 7.74 (1H, d, J= 8.3Hz), δ 7.47–7.54 (3H, bm), δ 7.37 (1H, m), δ 4.08 (3H, s). ^{13}C (100MHz, $CDCl_3$) δ 165.6, 164.0, 154.7, 150.0, 139.5, 137.2, 129.1, 128.9, 127.7, 127.5, 126.7, 125.3, 124.2, 121.7, 115.1, 112.2, 112.0, 52.6. HRMS calculated for $C_{19}H_{13}NO_4$ $[M]^+$ 320.0917, found; 320.0917.

Methyl 2-(2-hydroxynaphthalen-1-yl)benzoxazole-4-carboxylate (43). 2-Hydroxy-1-napthoic acid (0.200g, 1.06 mmol) and 1-1'-carbonyldiimidazole (0.207g, 1.28 mmol) were dissolved in THF (6mL) and stirred for 30 minutes under inert atmosphere. Methyl 3-hydroxyanthranilate (0.210g, 1.06 mmol) was added and the reaction mixture was refluxed for 17 hours. The reaction mixture was cooled to room temperature and transferred to a separatory funnel along with H_2O (50mL) and extracted with EtOAc (3x50mL). Combined organic phases were washed with H_2O (50mL) and brine (50mL), dried with $MgSO_4$, filtered, and concentrated under reduced pressure to give 0.548g of a

light brown solid. Crude product amide was dissolved in *m*-xylene (34.4mL) and pyridinium *p*-toluene sulfonate (0.816g, 3.25 mmol) was added to the solution. The reaction mixture was refluxed overnight. The solution was then cooled to room temperature and 75mL saturated $NaHCO_3$ was added. The solution was extracted with EtOAc (3x100mL). Combined organic phases were washed with H_2O (2x100mL) and brine (100mL), dried with $MgSO_4$, filtered, and concentrated under reduced pressure to give a dark brown solid. Crude product was purified *via* flash chromatography (10% EtOAc in $CHCl_3$) to give 0.0980g desired compound as a reddish brown solid (28% yield; two steps). ^{1}H NMR (400MHz, $CDCl_3$) δ 9.09 (1H, d, J= 8.7Hz), δ 8.13 (1H, d, J= 7.8Hz), δ 7.93 (2H, dd, J= 8.3Hz, J= 3.6Hz), δ 7.84 (1H, d, J= 7.8Hz), δ 7.69 (1H, m), δ 7.47 (2H, m), δ 7.35 (1H, d, J= 9.2Hz), δ 4.09 (3H, s). ^{13}C (100MHz, $CDCl_3$) δ 166.4, 165.7, 162.3, 149.6, 138.0, 135.7, 130.9, 129.4, 128.7, 128.5, 127.7, 124.6, 124.4, 124.0, 120.7, 119.7, 115.0, 101.9, 52.6. HRMS calculated for $C_{19}H_{13}NO_4$ $[M]^+$ 320.0917, found; 320.0917.

Methyl 3-hydroxy-2-((quinolin-8-ylcarbonyl)amino)benzoate (44). Oxalyl chloride (0.527mL, 5.77 mmol) was added to a solution of quinoline-8-carboxylic acid (0.125g, 0.722 mmol) in CH_2Cl_2 (36.1mL) under inert atmosphere. DMF (5-7 drops) was then added and the solution was stirred for 2 hours. Solvent was removed *via* distillation and remaining residue was dried *in vacuo* for 30 minutes. The residue was then dissolved in CH_2Cl_2 (54mL). A solution of pyridine (1.80mL, 22.4 mmol) and methyl 3-hydroxyanthranilate (0.142g, 0.722 mmol) in CH_2Cl_2 (22mL) was then added and the reaction mixture was stirred for 19 hours. The reaction was quenched with H_2O (50mL) and transferred to a separatory funnel along with CH_2Cl_2 (50mL). The organic phase was

washed with H_2O (4x100mL) and brine (100mL), dried with $MgSO_4$, filtered, and concentrated under reduced pressure to give a brown solid. Crude product was purified *via* flash chromatography (5% EtOAc in CH_2Cl_2) to give 0.136g desired compound as a yellow solid (59% yield). ^{1}H NMR (400MHz, $CDCl_3$) δ 9.10 (1H, dd, J= 4.6Hz, J=1.8Hz), δ 8.94 (1H, dd, J= 7.3Hz, J= 1.4Hz), δ 8.35 (1H, dd, J= 8.2Hz, J= 1.8Hz), δ 8.07 (1H, dd, J= 8.2Hz, J= 1.4Hz), δ 7.74 (1H, t, J= 7.8Hz), δ 7.58–7.62 (2H, m), δ 7.34 (1H, dd, J= 8.2Hz, J= 1.8Hz), δ 7.22–7.28 (1H, m), δ 3.84 (3H, s). ^{13}C (100MHz, $CDCl_3$) δ 167.3, 165.4, 151.5, 149.5, 145.3, 137.6, 134.7, 133.1, 128.5, 127.6, 127.4, 126.6, 126.5, 125.3, 124.2, 123.1, 121.5, 52.2. HRMS calculated for $C_{18}H_{14}N_2O_4$ $[M+Na]^+$ 345.0852, found; 345.0852.

Methyl 2-(quinolin-8-yl)benzoxazole-4-carboxylate (45). *m*-Xylene (7mL) was added to a flask containing **44** (0.104g, 0.323 mmol) and pyridinium *p*-toluene sulfonate (0.162g, 0.646 mmol) under inert atmosphere. The reaction mixture was refluxed for 18 hours. The reaction mixture was then cooled to room temperature and 50mL saturated $NaHCO_3$ was added. The solution was transferred to a separatory funnel and extracted with EtOAc (3x50mL). Combined organic phases were washed with H_2O (3x50mL) and brine (50mL), dried with $MgSO_4$, filtered, and concentrated under reduced pressure to give a reddish purple solid. Crude product was purified *via* flash chromatography (5% EtOH in $CHCl_3$) to give 0.0810g desired compound as a reddish brown solid (84% yield). ^{1}H NMR (400MHz, $CDCl_3$) δ 9.12 (1H, dd, J= 4.2Hz, J= 1.8Hz), δ 8.60 (1H, dd, J= 7.3Hz, J= 1.4Hz), δ 8.26 (1H, dd, J= 8.2Hz, J= 1.8Hz), δ 8.08 (1H, dd, J=7.8Hz, J=0.9Hz), δ 8.04 (1H, dd, J= 7.8Hz, J= 1.4Hz), δ 7.90 (1H, dd, J= 8.2Hz, J=0.9Hz), δ 7.70 (1H, t, J= 7.8Hz), δ 7.52 (1H, dd, J= 8.2Hz, J= 4.1Hz), δ 7.46 (1H, t,

J=7.8Hz), δ 4.06 (3H, s). ^{13}C (100MHz, $CDCl_3$) δ 166.1, 164.7, 152.1, 151.8, 146.1, 141.4, 136.8, 133.7, 132.2, 128.7, 127.2, 126.1, 124.6, 122.4, 121.9, 115.5, 52.7. HRMS calculated for $C_{18}H_{12}N_2O_3$ $[M]^+$ 305.0921, found; 305.0919.

ii. Chapter 3

Benzyl 1,5-bis-benzyloxy-naphthalene-2-carboxylate. Benzyl chloride (1.5mL, 13mmol) was added to a mixture of 1,5-dihydroxynaphthalene-2-carboxylic acid (0.539g, 2.64mmol), K_2CO_3 (2.45g, 17.7mmol), and DMF (5.4mL) under inert atmosphere and the mixture was refluxed for four hours. The reaction mixture was then cooled to room temperature, diluted with H_2O (100mL), and extracted with EtOAc (3x200mL). Combined organic phases were washed with H_2O (5x200mL) and brine (200mL), dried over Na_2SO_4, filtered, and concentrated under reduced pressure. Crude product was purified *via* flash chromatography (SiO_2, 15% Hexanes in CH_2Cl_2, R_f 0.38) to give 0.68g desired product as a brown oil (55% yield). ^1H NMR (400 MHz, $CDCl_3$) δ 8.14 (d, J = 8.7 Hz, 1H), δ 7.89 (d, J = 8.7 Hz, 1H), δ 7.83 (d, J = 8.7 Hz, 1H), δ 7.53-7.30 (m, 16H), δ 6.98 (d, J = 7.3 Hz, 1H), δ 5.40 (s, 2H), δ 5.25 (s, 2H), δ 5.12 (s, 2H). The isomeric ester *en route* to compound **2**, **benzyl 1,7-bis-benzyloxy-naphthalene-2-carboxylate**, was synthesized analogously and purified *via* flash chromatography (SiO_2, 40% hexanes in CH_2Cl_2, R_f 0.39) to give desired product as a brown oil (64% yield). ^1H NMR (400 MHz, $CDCl_3$) δ 7.78 (d, J = 8.6 Hz, 1H), δ 7.75 (d, J = 8.7 Hz, 1H), δ 7.56 (d, J = 8.7 Hz, 2H), δ 7.52-7.28 (m, 16H), δ 5.40 (s, 2H), δ 5.06 (s, 2H), δ 4.99 (s, 2H).

1,5-Bis-benzyloxynaphthalene-2-carboxylic acid (46). Benzyl 1,5-bis-benzyloxynaphthalene-2-carboxylate (0.556g, 1.17mmol) was dissolved in MeOH (6.4mL). NaOH (1.25mL, 40% aqueous) was added and the reaction mixture was refluxed for 18 hours. The reaction mixture was then cooled to room temperature, diluted with H_2O (65mL), and acidified to a pH~4 with citric acid. The mixture was extracted with EtOAc (3x100mL) and the combined organic phases were washed with H_2O (2x100mL) and brine (100mL), dried over $MgSO_4$, filtered, and concentrated under reduced pressure. Crude product was purified *via* flash chromatography (SiO_2, 40% hexanes in CH_2Cl_2, R_f 0.13) to give 0.507g desired product as an off-white solid (92% yield). ^{1}H NMR (400 MHz $CDCl_3$) δ 8.26 (d, J = 8.7 Hz, 1H), δ 8.08 (d, J = 8.7 Hz, 1H), δ 7.83 (d, J = 8.7 Hz, 1H), δ 7.55-7.38 (m, 11H), δ 7.06 (d, J = 7.3 Hz, 1H), δ 5.28 (s, 2H), δ 5.23 (s, 2H). The isomeric acid *en route* to compound **2**, **1,7-bis-benzyloxynaphthalene-2-carboxylic acid**, was synthesized analogously and purified *via* flash chromatography (SiO_2, 40% hexanes in CH_2Cl_2, R_f 0.13) to give desired product as a white solid (90% yield). ^{1}H NMR (400 MHz, $CDCl_3$) δ 7.96 (d, J = 8.2 Hz, 1H), δ 7.84 (d, J = 8.7 Hz, 1H), δ 7.68 (d, J = 8.7 Hz, 1H), δ 7.51-7.30 (m, 12H), δ 5.14 (s, 2H), δ 5.12 (s, 2H).

Methyl 2[((1,5-bis-benzyloxy-naphthalene-2-carboxyl)-amino)]-3-hydroxybenzoate (47). CDI (0.245g, 1.51mmol) was dissolved in THF (7.4mL). Acid **46** (0.484g, 1.26mmol) was added and the mixture was stirred under inert atmosphere at room temperature until CO_2(g) production ceased. Methyl 3-hydroxyanthranilate (0.211g, 1.26mmol) was then added and the mixture was refluxed for 19 hours. The reaction mixture was cooled to room temperature, diluted with H_2O (50mL), and

extracted with CH_2Cl_2 (3x50mL). Combined organic phases were washed with H_2O (50mL) and brine (50mL), dried over Na_2SO_4, filtered, and concentrated under reduced pressure. Crude product was purified *via* flash chromatography (SiO_2, 20% hexanes in CH_2Cl_2, R_f 0.40) to give 0.225g desired compound as a reddish-brown oil (33% yield). ^{1}H NMR (400 MHz, $CDCl_3$) δ 8.24 (d, J = 8.7 Hz, 1H), δ 8.03 (d, J = 8.7 Hz, 1H), δ 7.91 (d, J = 8.7 Hz, 1H), δ 7.60 (dd, J = 7.8 Hz, J = 1.4 Hz, 1H), δ 7.54 (d, J = 7.3 Hz, 2H), δ 7.49-7.42 (m, 3H), δ 7.39-7.36 (m, 6H), δ 7.32 (dd, J = 9.6 Hz, J = 1.4 Hz, 1H), δ 7.21 (t, J = 7.8 Hz, 1H), δ 7.03 (d, J = 7.8 Hz, 1H), δ 5.29 (s, 2H), δ 5.18 (s, 2H), δ 3.77 (s, 3H). The amide *en route* to compound **2**, **methyl 2[((1,7-bis-benzyloxy-napthalene-2-carboxyl)-amino)]-3-hydroxybenzoate**, was synthesized analogously and purified *via* flash chromatography (SiO_2, 20% hexanes in CH_2Cl_2, R_f 0.31) to give desired product as a reddish-brown oil (43% yield). ^{1}H NMR (400 MHz, $CDCl_3$) δ 7.92 (d, J = 8.7 Hz, 1H), δ 7.81 (d, J = 8.7 Hz, 1H), δ 7.67 (d, J = 8.7 Hz, 1H), δ 7.61 (dd, J = 7.8 Hz, J = 1.8 Hz, 1H), δ7.56 (d, J = 2.2 Hz, 1H), δ 7.43-7.27 (m, 12H), δ 7.22 (t, J = 7.8 Hz , 1H), δ 5.10 (s, 2H), δ 5.06 (s, 2H), δ 3.80 (s, 3H).

Methyl 2'-(5-benzyloxy-1-hydroxynaphthlen-2-yl)benzoxazole-4'-carboxylate (**2**). Compound **47** (0.223g, 0.418mmol) was added to a solution of PPTS (0.212g, 0.836mmol) in *m*-xylene (3.4mL) and the mixture was refluxed for 9 hours under inert atmosphere. The reaction mixture was then cooled to room temperature, $NaHCO_3$ (75 mL) was added, and the mixture was extracted with CH_2Cl_2 (3x50mL). Combined organic phases were washed with H_2O (2x50mL) and brine (50mL), dried over Na_2SO_4, filtered, and concentrated under reduced pressure. Crude product was purified *via* flash chromatography (SiO_2, 100% CH_2Cl_2, R_f 0.34) to give 0.110g desired product as a

yellow solid (52% yield). ^{1}H NMR (400 MHz, $CDCl_3$) δ 8.11 (d, J = 8.2 Hz, 1H), δ 8.09 (dd, J = 7.3 Hz, J = 1.0 Hz, 1H), δ 7.96 (q, J = 8.7 Hz, 2H), δ 7.83 (dd, J = 8.7 Hz, J = 1.0 Hz, 1H), δ 7.55-7.35 (m, 7H), δ 7.06 (d, J = 7.3 Hz, 1H), δ 5.27 (s, 2H), δ 4.10 (s, 3H). ^{13}C NMR (100 MHz, $CDCl_3$) δ 165.7, 165.4, 157.9, 154.4, 149.9, 139.7, 136.7, 128.7, 128.6, 128.2, 127.53, 127.49, 126.2, 124.5, 121.5, 121.1, 116.3, 115.0, 113.8, 108.7, 103.8, 70.4, 52.5. Anal. calcd for $C_{26}H_{19}NO_5$: C,73.40; H, 4.50; N, 3.29. Found: C, 73.43; H, 4.51; N, 3.17. m.p.; 183.5-185˚C. **Methyl 2'-(7-benzyloxy-1-hydroxynapthalen-2-yl)benzoxazole-4'-carboxylate (1)**, was synthesized analogously and purified *via* flash chromatography (SiO_2, CH_2Cl_2, R_f 0.31) to give 0.074g desired product as a yellow solid (34% yield). ^{1}H NMR (400 MHz, $CDCl_3$) δ 8.09 (dd, J = 7.8 Hz, J = 1.0 Hz, 1H), δ 7.91 (d, J = 2.2 Hz, 1H), δ 7.88 (d, J = 8.3 Hz, 1H), δ 7.82 (dd, J = 8.3 Hz, J = 1.0 Hz, 1H), δ 7.75 (d, J = 9.2 Hz, 1H), δ 7.53 (d, J = 7.3 Hz, 2H), δ 7.47-7.34 (m, 6H), δ 5.27 (s, 2H), δ 4.10 (s, 3H). ^{13}C NMR (100 MHz, $CDCl_3$) δ 165.8, 165.5, 157.23, 157.20, 149.9, 139.7, 136.8, 131.9, 129.4, 128.7, 128.2, 127.9, 127.5, 126.0, 124.5, 122.0, 121.0, 120.0, 119.3, 114.9, 103.6, 103.3, 70.3, 52.5. Anal. calcd for $C_{26}H_{19}NO_5$: C,73.40; H, 4.50; N, 3.29. Found: C, 72.81; H, 4.43; N, 3.22. m.p; 181.5-183 °C.

iii. Chapter 4

7-Hydroxy-3,4-dihydronaphthalen-1(2*H*)-one (48). 7-Methoxy-1-tetralone (3.00 g, 17.02 mmol) was added to a slurry of aluminum chloride (5.80 g, 42.56 mmol) and anhydrous toluene (75 mL) in a flame dried round bottom flask under inert atmosphere. The reaction mixture was refluxed for 30 minutes and then quenched with ice water (75

mL). The mixture was then extracted with EtOAc (3x75mL). Combined organic extracts were washed with H_2O (2x75mL) and brine (75mL). The organic phase was then dried over $MgSO_4$, filtered, and concentrated under reduced pressure to give a light-orange solid (3.06g). Crude product was recrystallized from EtOAc:Hexane to give a 2.80g of brown crystalline solid (~99% yield). ^{1}H NMR (400 MHz, d6-Acetone) δ 8.44 (1H, bs), δ 7.36 (1H, d, J = 3.2 Hz), δ 7.16 (1H, d, J = 8.4 Hz), δ 7.00 (1H, dd, J = 8.0 Hz, J = 2.8 Hz), δ 2.89-2.83 (2H, m), δ 2.5 (2H, t, J = 6.8 Hz), δ 2.07-1.99 (2H, m).

7-Benzyloxy-3,4-dihydronaphthalen-1(2*H*)-one (49). Anhydrous acetone (52 mL) was added to **48** (2.627 g, 16.20 mmol) and K_2CO_3 (4.48 g, 32.40 mmol) in a flame-dried round bottom flask under inert atmosphere. Benzyl bromide (2.91 g, 17.00 mmol) was added to the slurry and the reaction mixture was refluxed overnight. The slurry was then diluted with H_2O (50 mL) and the aqueous phase was extracted with EtOAc (3x50 mL). Combined organic phases were washed with brine (50 mL), dried over $MgSO_4$, filtered, and concentrated under reduced pressure to give a pale brown solid (4.509 g). Crude product was recrystallized from MeOH:H_2O to give 3.987 g white needle-like crystals (97% yield). ^{1}H NMR (400 MHz, $CDCl_3$) δ 7.62 (1H, d, J= 2.8 Hz), δ 7.45-7.30 (5H, m), δ 7.18-7.16 (1H, m), δ 7.13-7.10 (1H, m), δ 5.09 (2H, s), δ 2.9 (2H, t, J = 6.0 Hz), δ 2.64 (2H, t, J= 6 Hz), δ 2.15-2.08 (2H, m).

Ethyl 7-(benzyloxy)-1-oxo-1,2,3,4-tetrahydronaphthalene-2-carboxylate (50). NaH (853 mg, 34.70 mmol) was added to a solution of diethylcarbonate (5.59g, 5.7 mL, 47.4 mmol) in anhydrous THF (44 mL) in a flake dried round bottom flask equipped with an addition funnel under inert atmosphere. A solution of **49** (3.98 g, 15.8 mmol) in THF (25 mL) was added dropwise to the reaction mixture through the addition funnel, over a

period of 20 minutes. The solution was the refluxed overnight. The reaction was quenched with HCl (50 mL, 1M) and transferred to a separatory funnel. The aqueous phase was extracted with EtOAc (3 x 50 mL). Combined organic phases were washed with brine (1 x 75 mL), dried over $MgSO_4$, filtered, and concentrated under reduced pressured to give a dark brown oil (5.294). The crude product, a mixture of keto:enol (1:0.4) tautomers slightly contaminated with diethylcarbonate, was used without purification.

Ethyl 7-(benzyloxy)-2-bromo-1-oxo-1,2,3,4-tetrahydronaphthalene-2-carboxylate (51). Potassium acetate (1.55g, 15.8 mmol) and acetic acid (37 mL) were added to **50** (~5.117 g, ~15.8 mmol) in a round bottom flask under inert atmosphere and the solution was cooled on an ice bath for 5 minutes. Pyridinium tribromide (5.05 g, 15.8 mmol) was added to the slurry and the solution was stirred in an ice bath for 30 minutes and then overnight at RT. The reaction mixture was then diluted with CH_2Cl_2 (75 mL) and transferred to a separatory funnel. The organic phase was washed with H_2O (2 x 75 mL), $NaHCO_3$ (2 x 75 mL), and brine (75 mL), dried over $MgSO_4$, filtered, and concentrated under reduced pressure to give a brown oily solid (6.169 g). The crude product, slightly contaminated with diethylcarbonate, was used without purification.

Ethyl 7-(benzyloxy)-1-hydroxy-2-naphthoate (52). **51** (~1.00 g, ~2.48 mmol) was dissolved in anhydrous ACN (8 mL) in a flame dried round bottom flask equipped with an addition funnel under inert atmosphere. DBU (0.780 mL, 793mg, 5.21 mmol) was dissolved in ACN (2 mL) in attached addition funnel and the mixture was added dropwise to the reaction flask over 15 minutes. The reaction was then stirred overnight. The reaction was quenched with HCl (50 mL, 1 M) and transferred to a separatory

funnel. The mixture was extracted with EtOAc (3 x 50 mL). Combined organic phases were washed with H_2O (50 mL) and brine (50 mL), dried over $MgSO_4$, filtered, and concentrated under reduced pressure to give a light brown solid (0.826 g). Crude product was purified via flash chromatography (5% hexanes in $CHCl_3$, R_f 0.61) to give 597 mg desired compound as an off-white solid (75% yield). ^{1}H NMR (400 MHz, $CDCl_3$) δ 12.02 (1H, s), δ 7.93 (1H, d, J= 2.8 Hz), δ 7.67 (2H, t, J= 8.8 Hz), δ 7.51-7.50 (2H, m), δ 7.43-7.39 (2H, m), δ 7.37-7.32 (2H, m), δ 7.24 (1H, d, J= 8.4 Hz), δ 5.21 (2H, s), δ 4.46 (2H, q, J= 6.8 Hz), δ 1.45 (3H, t, J= 7.2 Hz). ^{13}C NMR (100 MHz, $CDCl_3$) δ 171.2, 159.8, 156.9, 136.7, 132.6, 129.1, 128.6, 128.1, 127.8, 125.7, 122.2, 122.1, 118.3, 106.2, 103.2, 70.2, 61.4, 14.3. HRMS calc. for $C_{20}H_{18}O_4$ $[M+Na]^+$ 345.1103; found 345.1103.

7-(Benzyloxy)-1-hydroxy-2-naphthoic acid (53) KOH (6.5 mL, 5 M) was added to a solution of **52** (0.597 g, 2.03 mmol) in THF (12.5 mL) and the solution was refluxed for 48 hours. The mixture was then acidified with HCl (50mL, 1M) and extracted with EtOAc (3 x 50 mL). Combined organic phases were washed with brine (50 mL), dried over $MgSO_4$, filtered, and concentrated under reduced pressure to give 0.481 g of the desired product as a light brown solid (88 % yield). ^{1}H NMR (400 MHz, d6-DMSO) δ 7.84 (1H, d, J= 8.4 Hz), δ 7.65 (1H, d, J= 2.8 Hz), δ 7.6 (1H, d, J= 8.8 Hz), δ 7.50-7.47 (2H, m), δ 7.40-7.36 (3H, m), δ 7.33-7.30 (2H, m), δ 5.23 (2H, s). ^{13}C NMR (100 MHz, *d6*-DMSO) δ 173.5, 159.6, 156.9, 137.3, 132.6, 129.9, 128.9, 128.4, 128.2, 125.5, 123.0, 122.3, 118.7, 106.8, 103.4, 69.9.

Methyl 2-(7-(benzyloxy)-1-hydroxy-2-naphthamido)-3-hydroxybenzoate (54). CDI (0.550 g, 3.39 mmol) was added to a solution of **53** (0.832 g, 2.83 mmol) in anhydrous THF (26 mL) in a flame dried round bottom flask under inert atmosphere. The

solution was stirred for 30 minutes. Methyl 3-hydroxyanthranilate (0.473 g, 2.83 mmol) was then added and the reaction was refluxed overnight. The mixture was then cooled to RT and concentrated under reduced pressure. EtOAc (20 mL) was then added and the mixture was filtered. Solids were further dried under reduced pressure (0.640 g). The crude product was suspended in EtOAc (10 mL), stirred for 10 minutes, and filtered. Solids were washed with cold EtOAc (10 mL), giving 0.490 g of the desired product as a yellow solid (40% yield). ^{1}H NMR (400 MHz, $CDCl_3$) δ 7.84 (1H, d, J= 2.4 Hz), δ 7.73-7.68 (3H,m), δ 7.53-7.50 (2H, m), δ 7.43-7.40 (3H, m), δ 7.38-7.33 (3H, m), δ 7.24-7.21 (1H, m), δ 5.23 (2H, s), δ 3.98 (3H, s).

Methyl 2-(7-(benzyloxy)-1-hydroxynaphthalen-2-yl)benzo[*d*]oxazole-4-carboxylate (1).[**] PPTS (0.555 g, 2.21 mmol) was added to a flame dried round bottom flask containing **53** (0.490 g, 1.11 mmol) in *p*-xylene (9 mL) and the mixture was stirred at 130°C for 48 hours. The solution was transferred to a separatory funnel with H_2O (50 mL) and extracted with $CHCl_3$(3 x 50 mL). Combined organic phases were washed with H_2O (50 mL) and brine (50 mL), dried over $MgSO_4$, filtered, and concentrated under reduced pressure to give 0.406 g of desired compound as a yellow solid (86% yield). ^{1}H NMR (400 MHz, $CDCl_3$) δ 8.08 (1H, dd, J= 7.6 Hz, J= 0.8 Hz), δ 7.90 (1H,d, J= 2.8 Hz), δ 7.88 (1H,d, J= 8.8 Hz), δ 7.82-7.80 (1H, m), δ 7.75 (1H, d. J= 8.8 Hz), δ 7.53-7.51 (2H, m), δ 7.45-7.32 (6H, m), δ 5.25 (2H, s), δ 4.09 (3H, s).

[**] Compound **1** was synthesized previously *via* a different route, as described in the experimental for Chapter 3. The compound was fully characterized in the experimental found for Chapter 3. The ^{1}H NMR of **1** *via* this route, matches that obtained in Chapter 3.

2,2,2-Trifluoro-1-*m*-tolylethanone (55). Magnesium turnings (0.332 g, 13.7 mmol) were added to a solution of *m*-bromotoluene (2.00 g, 11.7 mmol) in anhydrous ether (6.7 mL) in a flame dried round bottom flask equipped with an addition funnel under inert atmosphere. The slurry was vigorously stirred and agitated with an ultrasonicator for approximately 20 minutes or until reflux began. When the self-sustaining reflux ceased, the mixture was refluxed for 10 minutes and then chilled to 0°C in an ice bath. A solution of trifluoroacetic acid (0.298 mL, 3.90 mmol) in ether (6.7 mL) was slowly added through attached addition funnel and the reaction was stirred at 0°C for an hour. The mixture was then refluxed for 20 minutes and then cooled to RT. The reaction was pipetted into an acidic ice bath (30 g ice, 10 mL 12M HCl) and then extracted with ether (3 x 30 mL). Combined organic phases were washed with $NaHCO_3$ (2 x 50 mL) and brine (50 mL), dried over $MgSO_4$, and solvent was carefully removed *via* simple distillation as the product was found to be quite volatile (max heat source temperature~52°C). The crude product (~0.700 g), along with toluene dimers, was used without further purification.

2,2,2-Trifluoro-1-*m*-tolylethanone oxime (56). Hydroxlamine HCl (0.407 g, 5.85 mmol) was added to a round bottom flask containing **55** (~0.667 g, ~3.90 mmol) in a mixture of absolute ethanol (3.35 mL) and pyridine (7.36 mL) under inert atmosphere. The reaction was heated to 80°C for two hours and then cooled to RT. The solution was diluted with ether (50 mL) and washed with H_2O (3 x 30 mL) and brine (30 mL), dried over $MgSO_4$, filtered, and carefully concentrated on a rotary evaporator without heating to give a pale yellow oil. Crude product was purified *via* flash chromatography (CH_2Cl_2, R_f 0.43) to give 0.607 g of desired product as a yellow oil (81%, two step yield). ^{1}H NMR

(400 MHz, $CDCl_3$). All signals reported for both isomers obtained (E/Z), although it is not immediately clear which signals correspond to which isomer. δ 8.38 (1H, bs), δ 8.15 (0.63H, s), δ 7.38-7.33 (1H,m), δ 7.31-7.27 (6H, m), δ 2.40 (1.9H, s), δ 2.39 (3H, s).

2,2,2-Trifluoro-1-*m*-tolylethanone-*O*-tosyloxime (57). Diisopropylethylamine (0.247 g, 1.91 mmol) and dimethylaminopyridine (0.016 g, 0.130 mmol) were added to a round bottom flask containing **56** (0.328 g, 1.73 mmol) in anhydrous CH_2Cl_2 (3 mL) equipped with an addition tower under inert atmosphere. The solution was cooled in an ice bath and *p*-toluenesulfonyl chloride (0.331 g, 1.73 mmol) was added through the addition tower. The solution was stirred for 40 mins in ice bath followed by 3 hours at RT. The mixture was then diluted with CH_2Cl_2 (30 mL), transferred to a separatory funnel, and washed with H_2O (2 x 30 mL) and brine (30 mL), dried over $MgSO_4$, filtered, and concentrated under reduced pressure to give the desired compound (E/Z isomers) as an off-white solid (0.530 g, 89% yield). ^{1}H NMR (400 MHz, $CDCl_3$), All signals reported for both isomers obtained (E/Z). Some integral values are not integers, as some isomeric signals overlap, δ 7.91-7.87 (4.25H, m), δ 7.42-7.28 (7.9H, m), δ 7.24-7.13 (3.9H, m), δ 2.48 (1.73H, s), δ 2.46 (3H, s), δ 2.38 (1.73H, s), δ 2.37 (3H, s).

3-*m*-Tolyl-3-(trifluoromethyl)diaziridine (58). Anhydrous ether (8 mL) was added to a bomb containing **57** (0.530 g, 1.54 mmol) and the solution was chilled to -78°C under a stream of Ar(g). Ammonia was bubbled through the reaction mixture for 7 minutes at -78°C while stirring. The bomb was then sealed and the reaction was stirred at -78°C for 1.5 hours and then overnight at RT. The chamber was then opened and excess ammonia was allowed to escape. Once the majority of ammonia had dissipated, the solution was transferred to a separatory funnel using both CH_2Cl_2 and H_2O as needed.

The solution was diluted with CH_2Cl_2 (50mL) and washed with H_2O (3 x 30 mL) and brine (30 mL), dried over $MgSO_4$, filtered, and carefully concentrated using a rotorary evaporator without heating to give the desired product (0.249 g, 80% yield).). ^{1}H NMR (400 MHz, $CDCl_3$) δ 7.41-7.40 (2H, m), δ 7.30-7.28 (1H,m), δ 7.25-7.22 (1H,m), δ 2.77 (1H, bd, J= 8.4 Hz), δ 2.38 (3H, s), δ 2.22 (1H, bd, J= 9.2 Hz).

3-*m*-Tolyl-3-(trifluoromethyl)-3*H*-diazirine (59). Triethylamine (0.316 g, 3.12 mmol) was added to a solution of **58** (0.211 g, 1.04 mmol) in CH_2Cl_2 (5.6 mL) in a round bottom flask under inert atmosphere. The solution was cooled to 0°C and I_2 (0.291 g, 1.15 mmol) was added. The reaction was stirred at RT for 2 hours and then diluted with CH_2Cl_2 (30 mL) and transferred to a separatory funnel. The solution was washed with NaOH (2 x 30 mL, 1 M), H_2O (3 x 30 mL), Na_2SO_3 (2 x 30 mL), and brine (30 mL), dried over $MgSO_4$, filtered, and carefully concentrated using a rotary evaporator without heating to give 0.220 g of an oily dark brown liquid. Crude product was used without further purification.

3-(3-(Bromomethyl)phenyl)-3-(trifluoromethyl)-3*H*-diazirine (60). Compound **59** (~0.522 g, ~2.61 mmol) was dissolved in CCl_4 (10.4 mL) in a round bottom flask under inert atmosphere. The solution was heated to 85°C and NBS (0.511 g, 2.87 mmol, recrystallized from H_2O) was added and the mixture was stirred for 10 minutes. AIBN (0.128 g, 0.782 mmol) was then added and the reaction was refluxed for 2.5 hours. The mixture was cooled to RT and pentane (10 mL) was added and the slurry was stirred for 5 minutes. The mixture was then filter through glass wool and the filtrate was carefully concentrated on a rotaryevaporator to give a brown oil. Crude product was purified *via*

flash chromatography (pentane, R_f 0.58) to give the desired product plus dibrominated impurity (0.438 g), and was used without further purification.

Methyl 2-(7-(benzyloxy)-1-(((trifluoromethyl)sulfonyl)oxy)naphthalen-2-yl)benzo[*d*]oxazole-4-carboxylate (61). Triethylamine (0.0928g, 0.917 mmol) was added to a slurry of **1** (0.150 g, 0.353 mmol) in anhydrous CH_2Cl_2 (2 mL) in a flame dried round bottom flask equipped with an addition tower under inert atmosphere. The slurry was cooled to 0°C and triflic anhydride (0.129 g, 0.458 mmol) was slowly added. The reaction was stirred at 0°C for 20 minutes and then overnight at RT. The mixture was then pipetted into an acidic ice bath (10g ice, 20 mL 0.5M HCl) and stirred for 5 minutes. The solution was then transferred to a separatory funnel and extracted with CH_2Cl_2 (3 x 25 mL). Combined organic phases were washed with H_2O (30 mL) and brine (30 mL), dried over $MgSO_4$, filtered, and concentrated under reduced pressure to give the desired product as a brown solid (0.175 g, 89% yield) ^{1}H NMR (400 MHz, $CDCl_3$) δ 8.29 (1H, d, J= 8.8 Hz), δ 8.12 (1H,dd, J= 7.6 Hz, J= 1.2 Hz), δ 7.94 (1H,d, J= 8.4 Hz), δ 7.88-7.83 (2H, m), δ 7.61 (1H, d, J= 2 Hz), δ 7.53-7.49 (3H, m), δ 7.45-7.35 (4H, m), δ 5.24 (2H, s), δ 4.08 (3H, s). ^{13}C NMR (100 MHz, $CDCl_3$) δ 165.8, 158.8, 151.4, 142.9, 140.9, 135.9, 132.0, 129.8, 128.5, 128.4, 128.3, 127.7, 125.4, 124.2, 122.8, 120.5, 118.3, 115.1, 101.6, 70.3, 52.5. HRMS calc. for $C_{27}H_{18}F_3NO_7S$ $[M+H]^+$ 558.0756; found 558.0836.

Methyl 2-(7-(hydroxy)-1-(((trifluoromethyl)sulfonyl)oxy)naphthalen-2-yl)benzo[*d*]oxazole-4-carboxylate (62). Thioethane (1 mL) was added to a slurry of **61** (0.395 g, 0.709 mmol) in anhydrous CH_2Cl_2 (2 mL) in a round bottom flask equipped with an addition tower under inert atmosphere. Borontrifluoride etherate (1.11 g, 7.79 mmol) was slowly added and the reaction was heated to 40°C for 19 hours. The reaction

was cooled to RT and concentrated under reduced pressure using a secondary ice trap. Remaining solids were dissolved in CH_2Cl_2 (30 mL), transferred to a separatory funnel, and washed with H_2O (2 x 30 mL) and brine (30 mL), dried over $MgSO_4$, filtered, and concentrated under reduced pressure to give a yellow oil (0.373 g). Crude product was purified *via* flash chromatography (10% EtOAc in CH_2Cl_2, R_f 0.48) to give 0.233 g of desired product as a yellow solid (70% yield). ^{1}H NMR (400 MHz, $CDCl_3$) δ 8.17 (1H, d, J= 8.0 Hz), δ 8.13 (1H, dd, J= 8.0 Hz, J= 0.8 Hz), δ 7.86-7.82 (2H, m), δ 7.78 (1H, d, J= 8.8 Hz), δ 7.54-7.50 (2H, m), δ 7.27-7.26 (1H, m), δ 6.30 (OH), δ 4.09 (3H, s).

Methyl 2-(1-hydroxy-7-((3-(3-trifluoromethyl)-3*H*-diazirin-3-yl)benzyl)oxy)naphthalen-2-yl)benzo[*d*]oxazole-4-carboxylate (64). Bromide **60** (0.078 g, 0.279 mmol, 0.522 mL in CH_2Cl_2) was added to a flame dried round bottom flask containing **62** (0.087 g, 0.186 mmol) under inert atmosphere. Anhydrous acetone (1.5 mL) and K_2CO_3 (0.051 g, 0.372 mmol) were added and the reaction was refluxed overnight. The reaction mixture was diluted with CH_2Cl_2 (30 mL), transferred to a separatory funnel, washed with H_2O (2 x 30 mL) and brine (30 mL), dried over $MgSO_4$, filtered, and concentrated under reduced pressure to give a light brown solid (0.106 g). Crude product was purified *via* flash chromatography (CH_2Cl_2, R_f 0.39) to give 0.046g of an impure mixture containing the desired compound. The product (impure) was dissolved in anhydrous THF (1 mL) in a round bottom flask under inert atmosphere. TBAF (0.140 mL, 1 M in THF) was added and the solution was stirred at RT overnight. The reaction mixture was concentrated under reduced pressure to give a brown oil. Crude product was purified *via* flash chromatography (10% EtOAc in CH_2Cl_2, R_f 0.26) to give the desired compound **64** (~0.018g) with minor (~3%) impurities (~18 % yield). ^{1}H NMR (400 MHz,

$CDCl_3$) δ 8.18 (1H, d, J= 8.8 Hz), δ 8.07 (1H,dd, J= 8.0 Hz, J= 1.2 Hz), δ 7.83 (1H, d, J= 8.8 Hz), δ 7.71-7.68 (3H, m), δ 7.49 (1H, d, J= 2.8 Hz), δ 7.47-7.42 (2H, m), δ 7.36 (1H, bs), δ 7.27 (1H, bs), δ 7.24-7.22 (1H, m), δ 5.26 (2H, s), δ 5.21 (OH,), δ 3.91 (3H, s).

Methyl 2-(1,7-dihydroxynaphthalen-2-yl)benzo[*d*]oxazole-4-carboxylate (65). Pd/C (10%, 0.06g) was added to a solution of **1** (0.175 g, 0.394 mmol) in ethanol (15 mL) in a Parr shaker. The flask was sealed, charged with H_2 (60 PSI) and shaken for 48 hours. The slurry was vacuum filtered through celite. The filtrate with concentrated under reduced pressure to give 0.132 g of the desired product (71% yield). ^{1}H NMR (400 MHz, d6-DMSO) δ 8.15 (1H, dd, J= 8.4 Hz, J= 0.8 Hz), δ 8.01 (1H,dd, J= 7.6 Hz, J= 0.8 Hz), δ 7.82 (1H, d, J= 8.8 Hz), δ 7.77 (1H, d, J= 8.8 Hz), δ 7.61 (1H, d, J= 2.4 Hz), δ 7.57 (1H, t, J= 8.4 Hz), δ 7.48 (1H, d, J= 8.4 Hz), δ 7.23 (1H, dd, J= 8.8 Hz, J= 2.4), δ 3.97 (3H, s). ^{13}C NMR (100 MHz, *d6*-DMSO) δ 165.3, 165.0, 156.5, 156.2, 149.9, 139.2, 130.8, 130.1, 127.5, 126.0, 125.6, 121.9, 120.4, 120.1, 118.9, 116.2, 105.3, 103.2, 52.8.

Successful Preparation of **Methyl 2-(1-hydroxy-7-((3-(3-trifluoromethyl)-3*H*-diazirin-3-yl)benzyl)oxy)naphthalen-2-yl)benzo[*d*]oxazole-4-carboxylate (64)**. Anhydrous DMF (0.5 mL) and anhydrous acetone (1 mL) were added to a flame dried round bottom flask containing **65** (0.135 g, 0.401 mmol) under inert atmosphere. Anhydrous acetone (0.50 mL) was added to a flask containing bromide **60** (0.112 g, 0.401 mmol) and the solution was cannulated into the reaction vessel. K_2CO_3 (0.111 g, 0.802 mmol) was added to the solution and the reaction was stirred at 60°C overnight. The slurry was transferred to a separatory funnel, diluted with CH_2Cl_2 (50 mL), washed with NH_4Cl (30 mL), H_2O (4 x 30 mL), and brine (30 mL), dried over $MgSO_4$, filtered, and concentrated under reduced pressure to give a brown oily solid (0.194 g). Crude

product was purified *via* flash chromatography (50% ether in hexane, R_f 0.29) to give 0.032 g of the desired compound as a white flakey solid (14% yield). ^{1}H NMR (400 MHz, $CDCl_3$) δ 8.18 (1H, d, J= 8.8 Hz), δ 8.07 (1H,dd, J= 8.0 Hz, J= 1.2 Hz), δ 7.83 (1H, d, J= 8.8 Hz), δ 7.71-7.68 (3H, m), δ 7.49 (1H, m), δ 7.47-7.42 (2H, m), δ 7.36 (1H, bs), δ 7.27 (1H, bs), δ 7.24-7.22 (1H, m), δ 5.26 (2H, s), δ 3.91 (3H, s). ^{19}F NMR (376 MHz, $CDCl_3$, δ 0.00 for CF_3CO_2H) δ 10.4. ^{13}C NMR (100 MHz, $CDCl_3$) δ 165.9, 163.3, 154.9, 154.1, 151.3, 141.4, 138.4, 131.9, 130.1, 129.9, 129.3, 129.2, 129.1, 127.2, 126.3, 125.6, 124.62, 124.60, 123.9, 12.1, 120.5, 116.4, 114.8, 105.3, 76.0, 52.3. ^{13}C NMR (100 MHz, *d6*-benzene) δ 165.4, 162.8, 155.3, 154.2, 151.2, 141.7, 139.2, 131.7, 130.3, 129.9, 129.0, 128.9, 127.0, 125.9, 124.4, 124.2, 123.7, 122.7, 120.4, 116.7, 114.2, 105.2, 75.3, 51.4.

C. Biochemical Methods

i. NS3 Helicase Assays

Expression and purification of HCV NTPase/helicase. The NTPase/helicase domain was expressed in *E.coli* BL21 harboring the pET21b::*HCVH* plasmid encoding 461 aa from the COOH terminus of the NS3 protein. The bacterial culture was grown at 37°C until OD600 = 0.6-0.8. Isopropyl-β-d-thiogalactopyranoside (IPTG) was added to a final concentration of 0.3 mM to overexpress the protein for about 4 h at 37°C. The bacteria were collected by centrifugation at 5000 x g and the pellet was stored at –80°C. Cells were suspended in Tris/glycerol/Triton X-100 (TGT) buffer (20 mM Tris-HCl pH 7.5, 10 % glycerol, 0.05 % Triton X-100, 200 mM NaCl), mechanically homogenized and disrupted by sonication. The soluble proteins were separated by centrifugation at 12000 x g for 20 min from the insoluble cell components.

After centrifugation the supernatant was mixed overnight with 3 mL nickel-charged resin equilibrated with TGT buffer. The mixture was transferred onto a column. The column was washed and bound proteins were eluted in an imidazole gradient (0-250 mM).

To improve the purity of the fractions containing HCV NTPase/helicase those fractions were combined and rechromatographed on nickel-charged resin. The fractions obtained after elution showed high purity of the enzyme. Samples containing the protein were concentrated by ultrafiltration with a 50 kDa membrane (Amicon Ultra Centrifugal Filter Devices, Millipore).

Production of substrate for helicase assays. The substrate for the helicase assays was obtained by annealing two partially complementary oligonucleotides with a sequence corresponding to that described previously by Gallinari *et al*.[34] The release strand was 5´-end labeled with [γ-^{32}P]ATP using T4 polynucleotide kinase (MBI, Fermentas) as recommended by the manufacturer (MBI, Fermentas). For the annealing reaction, the labeled oligonucleotide was combined at molar ratio of 1:10 with the template strand, denatured for 5 min at 96°C and slowly renatured by bringing it to room temperature. The resulting duplex substrate was mixed with 25% (v/v) glycerol and bromphenol blue, electrophoresed on a 15% native Tris/borate/EDTA (TBE) polyacrylamide gel, visualized by autoradiography.

ATPase activity assay. The reaction mixture (final volume 20 μL) containing 20 mM Tris-HCl pH 7.5, 10% glycerol, 0.05% Triton X-100, 2 mM $MgCl_2$, 100 μM [γ-^{32}P]ATP (0.5 μCi) and HCV NTPase/helicase. The reaction proceeded for 30 min, at 37°C and

was terminated by addition of 20 mM EDTA. Afterwards, 1 μL of each sample were separated by thin layer chromatography (TLC) in 0.4 M KH_2PO_4 pH 3.4. The plate was dried and exposed to a Kodak X-ray film at – 80 °C. Parts of the plates corresponding to the non-hydrolyzed ATP and the P_i were cut out and Cerenkov radiation was measured.

Helicase activity assay. The helicase activity was tested with 0.5 pmol of HCV NTPase/helicase incubated in the following reaction mixture: 20 mM Tris-HCl pH 7.5, 10% glycerol, 0.05% Triton X-100, 2 mM $MgCl_2$, 100 μM ATP and dsDNA or dsRNA as substrate. The reaction was conducted for 30 min at 37°C and stopped by addition of 5 μL of termination buffer (100 mM Tris-HCl pH 7.5, 20 mM EDTA, 0.5% SDS, 0.1% Triton X-100, 25% glycerol, 0.1% bromophenol blue). The samples were separated on a 15% TBE polyacrylamide gel containing 0.1% SDS. The gels were dried and exposed to Kodak X-ray films at -70°C. Subsequently, the parts of the gels corresponding to the released strand, and to the duplex substrate, were cut out and ^{32}P radioactivity was measured.

Gel Mobility Assay. The compounds were studied in regard to their nucleic acid intercalatory or binding properties using the dsNA migration retardation assay. dsDNA and dsRNA (both 20 nM) were incubated for 60 min at room temperature with 20, 100 and 500 μM compounds in 20 mM Tris pH 7.5, and then submitted to electrophoresis in 1% agarose gel in 1× TAE. The gel was subsequently stained with EtBr.

ii. HCV Replicon Assays

Compounds were dissolved in dimethyl sulfoxide, stored at -20ºC protected from light, and further diluted in culture medium prior to use.

The Huh 5-2 and Huh 9-13 HCV subgenomic replicon-containing cells were provided by Prof R Bartenschlager (University of Heidelberg, Heidelberg, Germany). Huh 5.2 cells, containing the hepatitis C virus genotype 1b I389luc-ubi-neo/NS3-3'/5.1 replicon were sub-cultured in DMEM supplemented with 10% FCS, 1% non-essential amino acids, 1% penicillin/streptomycin and 2% Geneticin at a ratio of 1:3 to 1:4, and grown for 3-4 days in 75 cm^2 tissue culture flasks. One day before addition of the compound, cells were harvested and seeded in assay medium (DMEM, 10% FCS, 1% non-essential amino acids, 1% penicillin/streptomycin) at a density of 6 500 cells/well (100 µL/well) in 96-well tissue culture microtiter plates for evaluation of anti-metabolic effect and CulturPlate (Perkin Elmer) for evaluation of the antiviral effect. The microtiter plates were incubated overnight (37 °C, 5% CO2, 95-99% relative humidity), yielding a non-confluent cell monolayer.

The evaluation of the anti-metabolic as well as antiviral effect of each compound was performed in parallel. Four-step, 1-to-5 compound dilution series were prepared for the first screen, to collect data for a more detailed dose-response curve, an eight-step, 1-to-2 dilution series was used. Following assay setup, the microtiter plates were incubated for 72 hours (37 °C, 5% CO2, 95-99% relative humidity). For the evaluation of anti-metabolic effects, the assay medium was aspirated, replaced with 75 µL of a 5% MTS solution in phenol red-free medium and incubated for 1.5 hours (37 °C, 5% CO2, 95-99% relative humidity). Absorbance was measured at a wavelength of 498 nm and optical densities were converted to percentage of untreated controls. For the evaluation of

antiviral effects, assay medium was aspirated and the cell monolayers were washed with PBS. The wash buffer was aspirated, and 25 µL of Glo Lysis Buffer (Promega) was added allowing for cell lysis to proceed for 5 min at room temperature. Subsequently, 50 µL of Luciferase Assay System (Promega) was added, and the luciferase luminescence signal was quantified immediately (1000 ms integration time/well, Safire, Tecan). Relative luminescence units were converted into percentage of untreated controls.

The EC50 and EC90 (values calculated from the dose-response curve) represent the concentrations at which 50% and 90% inhibition, respectively, of viral replication is achieved. The CC50 (value calculated from the dose-response curve) represents the concentration at which the metabolic activity of the cells is reduced by 50 % as compared to untreated cells.

A concentration of compound is considered to elicit a genuine antiviral effect in the HCV replicon system when the anti-replicon effect is well above the 70% threshold at concentrations where no significant anti-metabolic activity is observed.

Compounds that reproducibly matched the above-outlined selection criteria were evaluated for selective antiviral activity in the Huh 9-13 replicon system. A similar assay setup was used as described above; the antiviral and anti-metabolic effect of the compounds was evaluated in parallel. The anti-metabolic activity of the compounds was quantified as outlined above. For the evaluation of the antiviral effect, assay medium was aspirated and the plates with dry monolayer were stored at -80 °C awaiting extraction. Following thawing of the plates at room temperature, the cell monolayer was lysed with 100 µL of cell-to-cDNA lysis buffer (Invitrogen). Lysis of the cells was allowed to proceed for 10 min at room temperature after which all liquid was transferred to a PCR

plate (Axygen). The PCR plate was incubated for 15min at 75 °C (T3, Biometra). The lysate was diluted 1:2 with RNase/DNase-free water, after which 5 µL was transferred to a real-time PCR plate (Applied Biosystems). Replicon RNA content was quantified using a real-time quantitative one-step RT-PCR method (RT-qPCR). Per sample, 20 µL master mix was added containing 12.5 µL 2x RT-qPCR mix (Low Rox One-Step RT-qPCR master mix, Abgene), 0.125 µL of a 60 µM forward primer solution (5'-CCA GAT CAT CCT GAT CGA CCA G-3', final [ ] of 300 nM), 0.125 µL of a 60 µM reversed primer solution (5'-CCG GCT ACC TGC CCA TTC-3', final [ ] of 300 nM), 0.3µL of a 5 µM probe solution (5'-ACA TCG CAT CGA GCG AGC ACG TAC-3', final [ ] of 60 nM) and 6.825 µL of DNase/RNase-free water (ACROS). The samples were analyzed using a SDS7500F (Applied Biosystems, standard thermocycling profile: 30 min at 48 °C, 10 min at 95 °C, 40 cycles of 15 sec at 95 °C and 1 min at 60 °C). Replicon RNA quantities were converted to percentage of untreated controls, allowing to calculate EC50 and EC90 values. Similar as for the Huh 5-2 assay, a compound is only considered to be a selective inhibitor of HCV replication when clear inhibition of virus replication is observed at concentrations that do not elicit a significant anti-metabolic effect on the host cells.

Vital Stains to assess pleiotropic effects on the host cell: Nile Red was obtained from Sigma, Monodansylcadaverine and LipiTOX Red Neutral lipid stain was obtained from life technologies. Huh 9-13 cells were seeded in glass bottom 35 mm culture dishes (Mattek) at a density of 25.000 cells/dish in complete DMEM without G418 at 37°C and 5% CO2. The next day medium was replaced by complete DMEM containing either the proper dilution of the compound tested or DMSO. The cells were further incubated for 3 days at 37°C and 5% CO2 after which the medium was replaced with complete medium

without neutral red and either Nile Red (2 µg/ml), Monodansylcadaverine (50 µM) or LipiTOX Red Neutral lipid stain (diluted 1/1000). Next, the cells were incubated for an additional 30 minutes at 37°C and 5% CO2 after which the cells were imaged using a laser-scanning SP5 confocal microscope (Leica Microsystems) equipped with a DMI 6000 microscope and an Acousto optical beam splitter. For nile red the yellow-gold fluorescence was monitored at an excitation wavelength (λex) of 552 nm and an emission wavelength (λem) of 636 nm; the red fluorescence was monitored at λex of 485 nm and λem of 525 nm. Monodansylcadaverine was imaged at λex of 340 nm and λem 530 nm of and LipiTOX Red Neutral lipid stain was assessed at λex of 577 nm and λem 609 nm.

D. Photoaffinity Labeling

Resuspension of NS3 helicase: Purified and lyophilized NS3h was received from Dr. Andrea Baier at the John Paul II Catholic University of Lublin. Protein of unknown mass was reconstituted in protein buffer (20mM Tris HCl pH= 7.5, 30 mM NaCl) until a final concentration of ~40 µM was reached, as determined by measuring the absorbance at 280 nm on a Thermofisher Nanodrop 1000 UV-VIS spectrophotometer using an extinction coefficient of 51760 $cm^{-1}M^{-1}$. Insoluble matter was removed *via* centrifugation at 10xg at 2°C. Resuspended protein was aliquoted and stored at -80°C until further use.

Denaturation and digestion of NS3 helicase: Methodology adapted from that suggested by Promega®, as listed on Trypsin Gold® protocol. NS3h in protein buffer (19 uL of ~40 µM) was added to a microcentrifuge tube. Guanidine HCl (29 mgs), H_2O (10

μL, ultrapure), and DTT (10 μL of 100 mM, final concentration 20 mM) were added and the solution was heated at 95°C for 20 minutes in a dry heat bath. The solution was then cooled to RT, iodoacetamide (5 μL of 440 mM, final concentration of 40 mM) was added, and then mixture was incubated for 30 minutes at RT in the dark. The solution was then diluted with 50 mM NH_4HCO_3 (305 μL, pH=7.8) such that the final concentration of guanidine HCl was < 1M. Trypsin (42.6 μL, 50 μg/mL in AcOH) or chymotrypsin (8.52 μL, 0.25 μg/mL in 1 mM HCl) was added such that NS3h:enzyme was (20:1 w/w) and the solution was heated to 37°C (trypsin) or 25°C (chymotrypsin) for 24 hours. The solution was then lyophilized and resuspended in H_2O (20-50 μL, ultrapure) such that a suitable concentration for HPLC MS/MS was achieved. The solution was stored at 0°C until analysis.

Photoaffinity labeling of NS3 helicase: A solution of photoactivatable analog in DMSO (1 μL) was added to NS3h in protein buffer (19 μL, ~40 μM) to a final inhibitor concentration ranging from 0.5-500 μM. The mixture was gently agitated and then incubated for 30 minutes at temperature ranging from 3°C-37°C. The inhibitor-protein complex was then irradiated with a Hg lamp, at a distance of ~6 inches, using a 320 nm cutoff filter in an ice bath for 60 minutes. The protein was then denatured and digested with either trypsin or chymotrypsin. The solution was then lyophilized and resuspended in H_2O (20-50 μL, ultrapure) such that a suitable concentration for HPLC MS/MS was achieved. The solution was stored at 0°C until analysis. The solution was then injected (10 μL) into a nanoflow HPLC using ACN:H_2O gradient elution and subsequently analyzed *via* MS/MS on a Bruker 12T Apex IV Fourier Transform ICR equipped with a nano-electrospray. The data were then analyzed using Peaks® 7.0.

References

1. World Health Organization. Hepatitis C Factsheet No. 164. April 2014. http://www.who.int/mediacentre/factsheets/fs164/en/; World Health Organization. Global Alert and Response: Hepatitis C. http://www.who.int/csr/disease/hepatitis/whocdscsrlyo2003/en/index3.html.
2. Lavanchy, D. The Global Burden of Hepatitis C. *Liver Int*. **2009**, *29*, 74-81.
3. Food and Drug Administration. FDA Approves First Combination Pill to Treat Hepatitis C. October 2014. http://www.who.int/mediacentre/factsheets/fs164/en/.
4. Alter, J.; Mast, E. The Epidemiology of Hepatitis C in the United States. *Gastroenterol. Clin. North Am.* **1994**, *23*, 437-455.
5. Lauer, M.; Walker, D. Hepatitis C Virus Infection. *N. Engl. J. Med.* **2001**, *345*, 41-52.
6. Brown, S.; Gaglio, J. Scope of World-Wide Hepatitis C Problem. *Liver Transpl.* **2003**, *9*, S10-S13.
7. L. Choo, H. Richman, H. Han, K. Berger, C. Lee, C. Dong, C. Gallegos, D. Coit, A. Medina-Selby, J. Barr, J. Weiner, W. Bradley, G. Kuo, M. Houghton. Genetic Organization and Diversity of the Hepatitis C Virus. *Proc. Natl. Acad. Sci*. **1991**, *88*, 2451-2455.
8. Tan, S.; He, Y. *Hepatitis C: Antiviral Drug Discovery and Development*; Caister Academic Press: UK, **2011**.
9. Grakoui, A.; McCourt, W.; Wychowski, C.; Feinstone, M.; Rice, C. A Second Hepatitis C Virus-Encoded Proteinase. *Proc. Natl. Acad. Sci. U.S.A.* **1993**, *90*, 10583-10587.
10. Hijikata, M.; Mizushima, H.; Akagi, T.; Mori, S.; Kakiuchi, N.; Kato, N.; Tanaka, T.; Kimura, K.; Shimotohno, K. Two Distinct Proteinase Activities Required for the Processing of a Putative Nonstructural Precursor Protein of Hepatitis C Virus. *J. Virol*. **1993**, *67*, 4665-4675.
11. Lorenz, I.; Marcotrigiano, J.; Dentzer, T; Rice, C. Structure of the Catalytic Domain of the Hepatitis C Virus NS2-3 Protease. *Nature*. **2006**, *442*, 831-835.

12. Failla, C.; Tomei, L.; De Francesco, R. Both NS3 and NS4A Are Required for Proteolytic Processing of Hepatitis C Virus Nonstructural Proteins. *J. Virol.* **1994**, *68*, 3753-3760.
13. Bartenschlager, R.; Ahlborn-Laake, L.; Mous, J.; Jacobson, H. Nonstructural Protein 3 of the Hepatitis C Virus Encodes a Serine-Type Proteinase Required for Cleavage at the NS3/4 and NS4/5 Junctions. *J. Virol.* **1993**, *67*, 3835-3844.
14. Malcolm, A.; Liu. R.; Lahser, F.; Agrawal, S.; Belanger, B.; Butkiewicz, N.; Chase, R.; Gheyas, F.; Hart, A.; Heck, D. SCH 503034, A Mechanism-Based Inhibitor of Hepatitis C Virus NS3 Protease, Suppresses Polyprotein Maturation and Enhances the Antiviral Activity of Alpha Interferon in Replicon Cells. *Antimicrob. Agents Chemother.* **2006**, *50*, 1013-1020.
15. Cheng, W.; Dumont, S.; Tinoco, I.; Bustamante, C. NS3 Helicase Actively Separates RNA Strands and Senses Sequence Barriers Ahead of the Opening Fork. *Proc. Natl. Acad. Sci. U.S.A.* **2007**, *104*, 13954-13959.
16. Lam, M.; Frick, N. Hepatitis C Virus Subgenomic Replicon Replication Requires an Active NS3 RNA Helicase. *J. Virol.* **2006**, *80*, 404-411.
17. Kolykhalov, A.; Mihalik, K.; Feinstone, M.; Rice, M. Hepatitis C Virus-Encoded Enzymatic Activities and Conserved RNA Elements in the 3′ Nontranslated Region Are Essential for Virus Replication In Vivo. *J. Virol.* **2000**, *74*, 2046-2051.
18. Rajkowitsch, L.; Chen, D.; Stampfl, S.; Semrad, K.; Waldsich, C.; Mayer, O.; Jantsch, F.; Konrat, R.; Schroeder, R. RNA chaperones, RNA annealers and RNA helicases. *RNA Biol.* **2007**, *4*, 118-130.
19. Jarvis, C.; Newport, W.; von Hippel, H. Stimulation of the Processivity of the DNA Polymerase of Bacteriophage T4 by the Polymerase Accessory Proteins: The Role of ATP Hydrolysis. *J. Biol. Chem.* **1991**, *266*, 1830-1840.
20. Sun, S.; Rao, B.; Rossmann, G. Genome Packaging in Viruses. *Curr. Opin. Struct. Biol.* **2010**, *20*, 114-120.
21. Selby, J.; Choo, L.; Berger, K.; Kuo, G.; Glazer, E.; Eckart, M.; Lee, C.; Chien, D.; Kuo, C.; Houghton, M. Expression, Identification and Subcellular

Localization of the Proteins Encoded by the Hepatitis C Viral Genome. *J. Gen. Virol.* **1993**, *74*, 1103-1113.

22. Einav, S.; Gerber, D.; Bryson, D.; Sklan, H.; Elazar, M.; Maerkl, J.; Glenn, S.; Quake, R. Discovery of a Hepatitis C Target and its Pharmacological Inhibitors by Microfluidic Affinity Analysis. *Nat. Biotechnol.* **2008**, *26*, 1019-1027.
23. Egger, D.; Wolk, B.; Gosert, R.; Bianchi, L.; Blum, E.; Moradpour, D.; Bienz, K. Expression of Hepatitis C Virus Proteins Induces Distinct Membrane Alterations Including a Candidate Viral Replication Complex. *J. Virol.* **2002**, *76*, 5974-5984.
24. Elazar, M.; Liu, P.; Rice, M.; Glenn, S.; Cheong, H. Amphipathic Helix-Dependent Localization of NS5A Mediates Hepatitis C Virus RNA Replication. *J. Virol.* **2003**, *77*, 6055-6061.
25. Macdonald, A.; Harris, M. Hepatitis C Virus NS5A: Tales of a Promiscuous Protein. *J. Gen. Virol.* **2004**, *85*, 2485-2502.
26. Tellinghuisen, T.; Marcotrigiano, J.; Gorbalenya, A.; Rice, C. The NS5A Protein of Hepatitis C Virus is a Zinc Metalloprotein. *J. Biol. Chem.* **2004**, *279*, 48576-48587.
27. Hughes, M.; Gretton, S.; Shelton, H.; Brown, D.; McCormick, J.; Angus, G.; Patel, H.; Griffin, S.; Harris, M. A Conserved Proline Between Domains II and III of Hepatitis C Virus NS5A Influences Both RNA Replication and Virus Assembly. *J. Virol.* **2009**, *83*, 10788-10796.
28. Blight, J.; Kolykhalov, A.; Rice, M. Efficient Initiation of HCV RNA Replication in Cell Culture. *Science.* **2000**, *290*, 1972-1974.
29. Gale Jr., M.; Blakely, M.; Kwieciszewski, B.; Tan, L.; Dossett, M.; Tang, M.; Korth, J.; Polyak, J.; Gretch, R.; Katze, G. Control of PKR Protein Kinase by Hepatitis C Virus Nonstructural 5A Protein: Molecular Mechanisms of Kinase Regulation. *Mol. Cell Biol.* **1998**, *18*, 5208-5218.
30. Le Pogam, S.; Seshaadri, A.; Kosaka, A.; Chiu, S.; Kang, H.; Hu, S.; Rajyaguru, S.; Symons, J.; Cammack, N.; Najera, I. Existence of Hepatitis C Virus NS5B Variants Naturally Resistant to Non-Nucleoside, But Not to Nucleoside, Polymerase Inhibitors Among Untreated Patients. *J. Antimicrob. Chemother.* **2008**, *61*, 1205-1216.

31. Liang, J.; Ghany, M. Current and Future Therapies for Hepatitis C Virus Infection. *N. Engl. J. Med.* **2013**, *368*, 1907-1919.
32. Heathcote, J.; Shiffman, L.; Cooksley, G.; Dusheiko, M.; Lee, S.; Balart, L.; Reindollar, R.; Reddy, K.; Wright, L.; Lin, A.; Hoffman, J.; DePamphilis, J. Peginterferon Alfa-2a in Patients with Chronic Hepatitis C and Cirrhosis *N. Engl. J. Med.* **2000**, *343*, 1673-1680.
33. Lemon, S.; McKeating, J.; Pietschmann, T.; Frick, D.; Glenn, J.; Tellinghuisen, T.; Symons, J.; Furman, P. Development of Novel Therapies for Hepatitis C. *Antiviral Res.* **2010**, *86*, 79-92.
34. Bartenschlager, R.; Frese, M.; Pietschmann, T. Novel Insights into Hepatitis C Virus Replication and Persistence. *Adv. Virus Res.* **2004**, *63*, 71-180.
35. Moradpour, D.; Penin, F.; Rice, M.; Replication of Hepatitis C Virus. *Nat. Rev. Microbiol.* **2007**, *5*, 453-463.
36. Sarazin, C.; Kieffer, TL; Bartels, D. Dynamic Hepatitis C Virus Genotypic and Phenotypic Changes in Patients Treated with the Protease Inhibitor Telaprevir. *Gastroenterology*, **2007**, *132*, 1767-1777.
37. Susser, S.; Welsch, C.; Wang, Y.; et al. Characterization of Resistance to the Protease Inhibitor Boceprevir in Hepatitis C Virus-Infected Patients. *Hepatology*, **2009**, *50*, 1709-1718.
38. Bacon, R.; Gordon, C.; Lawitz, E. Boceprevir for Previously Treated Chronic HCV Genotype 1 Infection. *N. Engl. J. Med.* **2011**, *364*, 1207-1217.
39. Jacobson, M.; McHutchinson, G.; Dusheiko, G. Telaprevir for Previously Untreated Chronic Hepatitis C Virus Infection. *N. Engl. J. Med*. **2011**, *364*, 2405-2416.
40. Soriano, V.; Labarga, P.; Fernandez-Montero, J.; Benito, J.; Poveda, E.; Rallon, N.; Sanchez, C.; Vispo, E.; Barreiro, P. The Changing Face of Hepatitis C in the New Era of Direct-Acting Antivirals. *Antiviral Res*. **2013**, *97*, 36-40.
41. Hepatitis C New Drug Research And Liver Health: Approved Treatments for Hepatitis C. January 2016. http://hepatitiscnewdrugresearch.com/approved-treatments-for-hepatitis-c.html.

42. Food and Drug Administration: Hepatitis B and C Treatments. April 2015. http://www.fda.gov/forpatients/illness/hepatitisbc/ucm408658.htm
43. Food and Drug Administration. Faster, Easier Cures for Hepatitis C. July 2014. http://www.fda.gov/forconsumers/consumerupdates/ucm405642.htm.
44. Food and Drug Administration. FDA Approves First Combination Pill to Treat Hepatitis C. October 2014. http://www.fda.gov/newsevents/newsroom/pressannouncements/ucm418365.htm.
45. Gritsenko, D.; Hughes, G. Ledipasvir/Sofosbuvir (Harvoni): Improving Options for Hepatitis C Infection. Pharmacy and Therapeutics: Drug Forcast. **2015**, *40*, 256-276.
46. Hagan, M.; Sulkowski, S.; Schinazi, F.; Cost Analysis of Sofosbuvir/Ribavirin versus Sofosbuvir/Simeprevir for Genotype 1 Hepatitis C Virus in Interferon-Ineligible/Intolerant Individuals. *Hepatology*. **2014**, *60*, 37-45.
47. Gao, M.; Antiviral Activity and Resistance of HCV NS5A Replication Complex Inhibitors. *Curr. Opin. Virol*. **2013**, *3*, 514-520.
48. Vermehren, J.; Sarrazin, C. The Role of Resistance in HCV Treatment. *Best Pract. Res. Cl.. Ga*. **2012**, *26*, 487-503.
49. Prescribing Information: Harvoni (Ledipasvir/Sofosbuvir). Gilead Sciences Inc. October 2014.
50. Issur, M.; Gotte, M.; Resistance Patterns Associated with HCV NS5A Inhibitors Provide Limited Insight into Drug Binding. *Viruses*. **2014**, *6*, 4227-4241.
51. Poveda, E.; Wyles, D.; Mena, A.; Pedreira, J.; Castro-Iglesias, A.; Cachay, E. Update on Hepatitis C Virus Resistance to Direct-Acting Antiviral Agents. *Antiviral Res*. **2014**, *108*, 181-191.
52. Shibata, K.; Kashiwada, M.; Ueki, M.; Taniguchi, M. UK-1, A Novel Cytotoxic Metabolite From *Streptomyces* sp. 517-02. *J. Antibiotic*. **1993**, *46*, 1095-1100.
53. Reynolds, M.; DeLuca, M.;Kerwin, S. M. The Novel Bis(benzoxazole) Cytotoxic Natural Product UK-1 is a Magnesium Ion-Dependent DNA Binding Agent and Inhibitor of Human Topoisomerase II *Bioorg. Chem.* **1999,** *27*, 326-337.

54. Kumar, D.; Jacob, M. R.; Reynolds, M. B; Kerwin, S. M. Synthesis and Evaluation of Anticancer Benzoxazoles and Benzimidazoles related to UK-1 *Bioorg. Med. Chem. Lett.* **2002,** *10*, 3997-4004.
55. McKee, M.; Kerwin, S. Synthesis, Metal Ion Binding, and Biological Evaluation of New Anticancer 2-(2'-Hydroxyphenyl)benzoxazole Analogs of UK-1. *Bioorg. Med. Chem*. **2008**, *16*, 1775-1783.
56. Goldgur, Y. et al. Three new structures of the core domain of HIV-1 integrase: An active site that binds magnesium. *Proc. Natl. Acad. Sci.USA*. **1998**, *95*, 9150-9154.
57. Marchand, C.; Johnson, A.; Semenova, E.; Pommier, Y. Mechanisms and Inhibition of HIV Integration. *Curr. Top. Med. Chem.* **2004**, *4*, 1059-1077.
58. Pluymers, W.; Pais, G.; Maele, B.; Pannecouque, C.; Fikkert, V.; Burke, T.; Clercq, E.; Witvrouw, M.; Neamati, N.; Debyser, Z. *Antimicrob. Agents.* Inhibition of Human Immunodeficiency Virus Type 1 Integration by Diketo Derivatives. *Chemother*. **2002**, *46*, 3292-3297.
59. Ward, D.; Talley, D.; Tavag, M.; Menji, S.; Schaughency, P.; Smith, P. UK-2 and Structural Analogs are Potent Inhibitors of Hepatitis C Virus Replication. *Bioorg. Med. Chem. Lett*. **2014**, *24*, 609-612.
60. Talley, D.; Leen, Delang.; Neyts, J.; Leyssen, P.; Smith, P. Exploring the Importance of Zinc Binding and Steric/Hydrophobic Factors in Novel HCV Replication Inhibitors. *Bioorg. Med. Chem. Lett*. **2016**. *In Press*: doi:10.1016/j.bmcl.2016.01.035
61. Schregel, V.; Jacobi, S.; Penin, F.; Tautz, N. Hepatits C Virus NS2 is a Protease Stimulated by Cofactor Domains in NS3. *Proc. Natl. Acad. Sci. USA*. **2009**, *106*, 5342-5347.
62. Tedbury, P.; Harris, M. Characterization of the Role of Zinc in the Hepatitis C Virus NS2/3 Auto-Cleavage and NS3 Protease Activities. *J. Mol. Biol***. 2007**, *366*, 1652-1660.
63. Stempniak, M.; Hostomska, Z.; Nodes, B.; Hostomsky, Z. The NS3 Proteinase Domain of Hepatitis C Virus is a Zinc-Containing Enzyme. *J. Virol*. **1997**, *71*, 2881-2886.

64. Love, R.; Parge, H.; Wickersham, J.; Hostomsky, Z.; Habuka, N.; Moomaw, E.; Adachi, T.; Hostomsky, Z. The Crystal Structure of Hepatitis C Virus NS3 Proteinase Reveals a Trypsin-Like Fold and a Structural Zinc Binding Site. *Cell*. **1996**, *87*, 331-342.
65. Tellinghuisen, T.; Marcotrigiano, J.; Rice, C. Structure of the Zinc-Binding Domain of an Essential Component of the Hepatitis C Virus Replicase. *Nature*. **2005**, *435*, 374-379.
66. Kim, J.; Morgenstern, K.; Lin, C.; Fox, T.; Dwyer, M.; Landro, J.; Chambers, S.; Markland, W.; Lepre, C.; O'Mailey, E.; Harbeson, S.; Rice, C.; Murcko, M.; Caron, P.; Thompson, J. Crystal Structure of the Hepatitis C Virus NS3 Protease Domain Complexed with a Synthetic NS4A Cofactor Peptide. *Cell*, **1996**, 87, 343-355.
67. De Francesco, R.; Urbani, A.; Nardi, C.; Tomei, L.; Steinkuhler, C.; Tramontano, A. A Zinc Binding Site in Viral Serine Proteinases. *Biochemistry*. **1996**, *35*, 13282-13287.
68. Reddy, M.; Reddy, V.; Satyanarayana, B. Equilibrium Studies on Ternary Chelates of Trivalent Metal Ions with 2-(2-Hydroxyphenyl)benzimidazole, 2-(2-Hydroxyphenyl)benzoxazole and Other Ligands in Solution. *J. Indian Chem. Soc*. **2006**, *83*, 722-724.
69. Henary, M.; Fahrni, C.; Excited State Intermolecular Proton Transfer and Metal Ion Complexation of 2-(2'-hydroxyphenyl)benzazoles in Aqueous Solution. *J. Phys. Chem. A*. **2002**, *106*, 5210-5220.
70. Andreini, C.; Banci, L.; Bertini, I.; Rosato, A. Counting the Zinc Proteins Encoded in the Human Genome. *J. Proteome Res*. **2006**, *5*, 196.
71. Maret, Wolfgang. Zinc and Sulfur: A Critical Biological Partnership. *Biochemistry*. **2004**, *43*, 3301-3309.
72. Azumaya, I.; Okamoto, T.; Imabeppu, F.; Takayanagi, H. Simple and Convenient Synthesis of Tertiary Benzanilides Using Dichlorotriphenylphosphorane. *Tetrahedron*. **2003**, *59*, 2325-2331.

73. Huang, S.-T.; Hsei, I.-J.; Chen, C. Synthesis and Anticancer Evaluation of Bis(benzimidazoles), Bis(benzoxazoles), and Benzothiazoles. *Bioorg. Med. Chem*. **2006**, *14*, 6106-6119.
74. Overman, L.; Petty, S. Nucleophilic Cleavage of the Sulfur-Sulfur Bond by Phosphorus Nucleophiles. III. Kinetic Study of the Reduction of a Series of Ethyl Aryl Disulfides with Triphenylphosphine and Water. *J. Org. Chem*. **1975**, *40*, 2779-2781.
75. Kaminski, Z. 2-Chloro-4,6-Disubstituted-1,3,5-Triazines A Novel Group of Condensing Reagents. *Tett. Lett*. **1985**, *26*, 2901-2904.
76. Milen, Matyas.; Grun, A.; Balint, E.; Dancso, A.; Keglevich, G. Solid-Liquid Phase Alkylation of *N*-Heterocycles: Microwave-Assisted Synthesis as an Environmentally Friendly Alternative. *Syn. Comm*. **2010**, *40*, 2291-2301.
77. Blight, K.; Norgard, E. In *Hepatitis C Viruses: Genomes and Molecular Biology*. Tan, S-L. Ed.; Norfolk (UK): Horizon Bioscience, **2006**, Chapter 11, pp 311-351.
78. Tai, L.; Chi, K.; Chen, S.; Hwang, H. The Helicase Activity Associated with the Hepatitis C Virus Non-Structural Protein 3 (NS3). *J. Virol*. **1996**, *70*, 8477-8484.
79. Caruthers, J.; McKay, D.; Helicase Structure and Function. *Curr. Opin. Struct. Biol*, **2002**, *12*, 123-133.
80. Walker, E.; Saraste, M.; Runswick, J.; Gay, J. Distantly Related Sequences in the Alpha- and Beta- subunits of ATP Synthase, Myosin, Kinases, and Othe ATP-Requiring Enzymes and a Common Nucleotide Binding Fold. *EMVO. J*. **1982**, *1*, 945-951.
81. Mackintosh, G.; Lu, Z.; Jordan, B.; Harrison, K.; Sakon, B.; Sharma, D.; Cameron, E.; Raney, D.; Sakon, J. Structural and Biological Identification of Residues on the Surface of NS3 Helicase Required for Optimal Replication of the Hepatitis C Virus. *J. Biol. Chem*. **2006**, *281*, 3528-3535.
82. Kim, J.; Morgenstern, K.; Griffith, J.; Dwyer, M.; Thomson, J.; Murcko, M.; Lin, C.; Caron, P.; Hepatitis C virus NS3 RNA helicase domain with a bound oligonucleotide: the crystal structure provides insights into the mode of unwinding. *Structure*. **1998**, 6, 89–100.

83. Gu, M.; Rice, M. Three Conformational Snapshots of the Hepatitis C Virus NS3 Helicase Reveal a Ratchet Translocation Mechanism. *Proc. Natl. Acad*. **2010**, *107*, 521-528.
84. Yao, N.; Hesson, T.; Cable, M.; Hong, Z.; Kwong, D. Le, V.; Weber, C. Structure of the Hepatitis C Virus RNA Helicase Domain. *Nat. Struct. Biol*, **1997**, *4*, 463-467.
85. Cho, S.; Ha, C.; Kang, W.; Chung, M.; Back, H.; Jang, K.; Oh, H. Crystal Structure Uof the RNA Helicase from Genotype 1b Hepatitis C Virus. A feasible Mechanism of Unwinding Duplex RNA. *J. Biol. Chem*. **1998**, *273*, 15045-15052.
86. Yao, N.; Reichert, P.; Taremi, S.; Prosise, W.; Weber, C. Molecular Views of Viral Polyprotein Processing Revealed by the Crystal Structure of the Hepatitis C Virus Bifunctional Protease-Helicase. *Structure*, **1999**, *7*, 1353-1363.
87. Kyono, K.; Miyashiro, M.; Taguchi, I. Detection of Hepatitis C Virus Helicase Activity Using the Scintillation Proximity Assay System. *Anal. Biochem*. **1998**, *257*, 120-126.
88. Boguszewska-Chachulska, M.; Krawczyk, M.; Stankiewicz, A.; Gozdek, A.; Haenni, A.; Strokovskaya, L. Direct Fluorometric Measurement of Hepatitis C Virus Helicase Activity. *FEBS. Lett*, **2004**, *567*, 253-258.
89. Rypma, R.; Lam, A.; Frick, D. *Bacterial DNA, DNA Polymerase and DNA Helicases*. Effect of Substrate Traps on Hepatitis C Virus NS3 Helicase Catalyzed DNA Unwinding: Evidence for Enzyme Catalyzed Strand Exchange. **2009**, W.D. Knudsen, S.S. Bruns, eds. Nova Sciences Publishers Inc: New York, 389-407.
90. Handson, A.; Hernandez, J.; Shadrick, W.; Frick, D. *Methods in Enzymology*. Identification and Analysis of Inhibitors Targeting the Hepatitis C Virus NS3 Helicase. **2012**, *511*, 463-483.
91. Heck, A.; Lam, M,; Narayanan, N.; Frick, D. Effects of Mutagenic and Chain Terminating Nucleotide Analogs on Enzymes Isolated from Various Hepatitis C Virus Genotypes. *Antimicrob. Agents. Chemother*. **2008**, *52*, 1901–1991.

92. Borowski, P.; Deinert, J.; Schalinski, S. Halogenated Benzimidazoles and Benzotriazoles as Inhibitors of the NTPase/Helicase Activities of Hepatitis C and Related Viruses. *Eur. J.Biochem*. **2003**, *270*, 1645–1653.
93. Zhang, N.; Chen, M.; Koch, V.; Schmitz, H.; Liao, C.; Bretner, M.; Bhadti, V.; Fattom, A.; Naso, R.; Hosmane, R.; Borowski, O. Ring-Expanded ("fat") Nucleoside and Nucleotide Analogues Exhibit Potent in vitro Activity Against Flaviviridae NTPases/ Helicases, Including Those of the West Nile Virus, Hepatitis C Virus, and Japanese Encephalitis Virus. *J. Med. Chem*. **2003**, *46*, 4149–4164.
94. Zhang, N.; Chen, H.; Koch, V. Potent inhibition of NTPase/helicase of the West Nile Virus by ring-expanded ("fat") nucleoside analogues. *J. Med. Chem.* **2003**, *46*, 4776–4789.
95. Ujjinamatada, K.; Baier, A.; Borowski, P.; Hosmane, S. An Analog of AICAR with Dual Inhibitory Against WNV and HCV NTPase/Helicase: Synthesis and in vitro Screening. *Bioorg. Med. Chem. Lett*. **2007**, *17*, 2285-2288.
96. Chen, S.; Chiou, T.; Chen, S.; Chen, C.; Hu, Y.; Chi, K.; Chu, D.; Hwang, H.; Chen, J.; Chen, S.; Liaw, H.; Chern, W. Structure-Based Discovery of Triphenylmethane Derivatives as Inhibitors of Hepatitis C Virus Helicase. *J. Med. Chem*. **2009**, *52*, 2716-2723.
97. Maga, G.; Gemma, S.; Fattorusso, C.; Specific targeting of hepatitis C virus NS3 RNA helicase. Discovery of the potent and selective competitive nucleotide-mimicking inhibitor QU663. *Biochemistry*, **2005**, *44*, 9637–9644.
98. Boguszewska-Chachulska, A.; Krawczyk, M.; Najda, A. Searching for a new anti-HCV therapy: synthesis and properties of tropolone derivatives. *Biochem. Biophys. Res. Commun*. **2006**, *341*, 641–647.
99. Funk, C.; Davis, A.; Hopkins, J.; Middleton, K. Development of high-throughput screens for discovery of kinesin adenosine triphosphatase modulators. *Anal. Biochem*. **2004**, *329*, 68–76.
100. Stankiewicz-Drogo, A.; Palchykovska, G.; Kostina, G.; Alexeeva, V.; Shved, D.; Boguszewska-Chachulska, M. New Acridone-4-Carboxylic Acid Derivatives as

Potential Inhibitors of Hepatitis C Infection. *Bioorg. Med. Chem*. **2008**, *16*, 8846-8852.

101. Cate, L. A. An Efficient Carboxylation of 1-Naphthols Using Magnesium Methyl Carbonate. *Synthesis* **1983**, 385-386.
102. Singh, A.; Thornton, R.; Westheimer, H. The Photolysis of Diazoacetylchymotrypsin. *J. Biol. Chem*. **1962**, *237*, 3006.
103. Dubinsky, L.; Krom, B.; Meijler, M. Diazirine Based Photoaffinity Labeling. *Bioorg. Med. Chem. Lett*. **2012**, *20*, 554-570.
104. Dorman, G.; Prestwich, D. Using Photolabile Ligands in Drug Discovery and Development. *Trends. Biotechnol*. **2000**, *18*, 64-77.
105. Das, J.; Aliphatic Diazirines a Photoaffinity Probes for Proteins: Recent Developments. *Chem. Rev*. **2011**, *111*, 4405-4417.
106. Vodovozova, E.; Photoaffinity Labeling and its Application in Structural Biology. *Biochemistry-Moscow*, **2007**, *72*, 1-20.
107. Sumranjit, J.; Chung, S.; Recent Advances in Target Characterization and Identification by Photoaffinity Probes. *Molecules*, **2013**, *18*, 10425-10451.
108. Prestwich, G.; Dorman, G.; Elliot, J.; Marecak, D.; Chaudhary, A. Benzophenone Photoprobes for Phosphoinositides, Peptides, and Drugs. *Photochem. Photobiol*, **1997**, *65*, 222.
109. Ford, F.; Yuzawa, T.; Platz, M.; Matzinger, S.; Fulscher, M. Rearrangement of Dimethylcarbene to Propene: Study by Laser Flash Photolysis and Ab Initio Molecular Orbital Theory. *J. Am. Chem. Soc*. **1998**, *120*, 4430.
110. Toscano, J. P.; Platz, M. S.; Nikolaev, V. Lifetimes of Simple Ketocarbenes. *J. Am. Chem. Soc*. **1995**, *117*, 4712.
111. Brunner, J.; Senn, H.; Richards, F. 3-Trifluormethyl-3-phenyldiazirine. *J. Biol. Chem*. **1980**, *255*, 3313-3318.
112. Nassal, M. 4-(1-Azi-2,2,2-trifluoroethyl)benzoic Acid, a Highly Photolabile Carbene Generating Label Readily Fixable to Biochemical Agents. *Liebig. Ann. Chem*. **1983**, 1510-1523.